Signals from the FOMC: The profitability of currency carry trades*

Maximilian Boeck[1], Alina Steshkova[2], and Thomas O. Zörner[3]

[1] Vienna University of Economics and Business
[2] Vienna University of Economics and Business, Research Institute for Capital Markets
[3] Oesterreichische Nationalbank (OeNB)

First Version: March, 2023
This Version: August, 2026

Abstract

This paper studies how monetary policy announcements from the Federal Open Market Committee (FOMC) affect foreign currency excess returns against the U.S. dollar. In a sample of advanced-economy currencies, we show that a contractionary monetary policy shock and a central bank information shock have opposing effects on exchange rates and currency excess returns. The monetary policy shock favors short positions in foreign currencies on FOMC days, whereas the central bank information shock favors short positions in the U.S. dollar. The resulting cross-sectional heterogeneity in currency excess returns gives rise to profitable carry trade opportunities. Conditioning currency positions on signals extracted from FOMC announcements generates positive abnormal returns that are not captured by the conventional carry factor. Expected excess returns implied by a multivariate time-series model corroborate the evidence from realized excess returns and point to a downward-sloping term structure of currency risk premia. We find little evidence that these responses systematically vary with within-currency speculative carry trade activity.

Keywords: Exchange rates, carry trade, countercyclical currency risk premia, monetary policy

JEL Codes: C24, C32, E52, F31, F41

*Maximilian Boeck, Vienna University of Economics and Business, Welthandelsplatz 1, 1020 Vienna, Austria. E-mail: maximilian.boeck@wu.ac.at. Alina Steshkova, Research Institute for Capital Markets, Vienna University of Economics and Business, Welthandelsplatz 1, 1020 Vienna. E-mail: alina.steshkova@wu.ac.at. Thomas O. Zörner, Monetary Policy Section, Oesterreichische Nationalbank. Otto-Wagner-Platz 3, 1090 Vienna, Austria. E-mail: thomas.zoerner@oenb.at.
We thank Paolo Cavallino, Georg Cejnek, Thomas Dangl, Gerardo Ferrara, Pia Heckl, Florian Huber, Zhengyang Jiang, Ingrid Kubin, Philip Lane, Hanno Lustig, Stefan Pichler, Daria Prem, Otto Randl, Ákos Török, Andrea Vedolin, Annette Vissing-Jorgensen, Clinton Watkins, Josef Zechner, and Irina Zviadadze, and participants in various seminars and conferences for helpful comments. Frane Gudelj provided excellent research assistance.
Disclaimer: The views expressed in this paper do not necessarily reflect those of the Oesterreichische Nationalbank or the Eurosystem.

1. Introduction

The currency carry trade is a prominent strategy in foreign exchange markets. It involves borrowing in low-interest-rate currencies and investing in high-interest-rate currencies. Under uncovered interest parity (UIP), the expected excess return from such a strategy is zero because expected exchange-rate movements offset interest rate differentials. However, high-interest-rate currencies have historically failed to depreciate sufficiently to offset their interest rate advantage and have often even appreciated. This pattern is consistent both with the forward premium puzzle and the persistent profitability of the carry trade (Fama, 1984; Burnside et al., 2011). Beyond pure hedging motives, the carry trade is a popular strategy among speculative investors and amplifies volatility and crash risk in foreign exchange markets (Brunnermeier et al., 2008; Menkhoff et al., 2012; Zviadadze, 2017). While monetary policy announcements are known to drive currency risk premia and carry trade profitability (Mueller et al., 2017), the role of different signals contained in FOMC announcements remains largely unexplored. Understanding how these signals shape currency excess returns is therefore central to understanding the profitability of the currency carry trade.

This paper studies how different signals contained in FOMC announcements—contractionary monetary policy shocks and central bank information shocks—affect realized currency excess returns and currency risk premia. We identify these shocks using high-frequency surprises around scheduled FOMC announcements. To isolate the underlying transmission channels, we decompose realized and ex ante currency excess returns into the interest rate differential and (expected) exchange-rate movements. We are then interested in the heterogeneous responses across currencies with different interest rate differentials and whether this heterogeneity can be exploited to improve the profitability of a currency carry trade strategy. We explore two extensions. First, we study whether these effects vary across holding horizons, thereby shaping the term structure of currency risk premia. Second, we explore whether risk premia depend on within-currency variation in speculative carry trade activity.

Monetary policy and central bank information shocks affect realized and expected currency excess returns through different transmission channels. Monetary policy shocks affect realized excess returns mainly through revaluations of the exchange rate, while the central bank information shock operates more strongly through the interest-rate-differential channel. We find that both realized and expected excess returns increase in response to signals about monetary policy, while they decline in response to signals about central bank information. The responses of currency risk premia vary systematically along the interest rate differential. High-interest-rate currencies exhibit larger increases following monetary policy shocks, but larger declines following central bank information shocks. Accordingly, contractionary monetary policy shocks favor long U.S. dollar positions, whereas contractionary central bank information shocks favor short U.S. dollar positions, implying that the type of FOMC signal is crucial for carry trade profitability. Conditioning currency positions on these announcement signals yields significantly higher risk-adjusted returns than a conventional carry trade strategy. Additionally, we show that currency risk premia have a downward-sloping term structure. While we document pronounced cross-sectional heterogeneity across currencies, we find little evidence that these responses vary systematically with within-currency speculative carry trade activity.

We empirically investigate currency excess returns from two complementary perspectives. The cross-sectional analysis focuses on realized excess returns, which we decompose into the interest rate differential and the future revaluation of the currencies. In the time series analysis, we use a multivariate vector autoregressive (VAR) model to provide evidence on expected excess returns by investigating model-implied revaluations of currencies based on an impulse response analysis. We use monthly data for seven advanced economies spanning 1995 to 2024, including central bank policy rates, government bond yields with different maturities, and bilateral exchange and forward rates vis-à-vis the U.S. dollar. Regarding the release of information from the central bank, we rely on the identification of the monetary policy shock and the central bank information shock following Jarociński and Karadi (2020). The identification strategy builds upon high-frequency surprises in interest rate derivatives and the S&P 500 stock market index around scheduled FOMC announcements. Monetary policy shocks are identified through a negative comovement of these surprises, and central bank information shocks through a positive one. We focus on contractionary shocks, which increase the U.S. short-term rate.[1] By now, the nature of this type of information is well understood. Non-monetary news dominates a large part of the communication from the central bank, which, according to Cieslak and Schrimpf (2019), can be further differentiated between economic growth and risk premium news. As we focus on surprises in stock prices and short-term yields, we interpret the central bank information shock mainly as a release of information about positive changes to fundamentals. To integrate the U.S. dollar's role as a safe and highly liquid asset into the framework, we account for the convenience yield of U.S. Treasuries (Jiang et al., 2021).

Both shocks affect realized and expected currency excess returns. The cross-sectional analysis shows that realized excess returns respond positively to monetary policy shocks but negatively to central bank information shocks. The sensitivity varies systematically along the average interest rate differential, reflecting the attractiveness of the carry trade. In line with Brunnermeier et al. (2008), we show that currencies with larger interest rate differentials also exhibit stronger speculative positioning. A decomposition of realized excess returns reveals that monetary policy shocks primarily operate through an appreciation of the U.S. dollar, generating deviations from UIP. While this appreciation is subsequently reversed, the reversal is stronger for low-interest-rate currencies. Consequently, the level of realized excess returns is highest for these currencies, although changes exhibit much less cross-sectional heterogeneity. The VAR complements this evidence by studying changes in expected currency excess returns rather than realized outcomes. It shows that expected excess returns increase most for high-interest-rate currencies and remain elevated for several years because the decline in the interest rate differential is insufficient to offset the expected depreciation of the U.S. dollar. From an investor's perspective, this implies that, following a contractionary monetary policy shock, expected returns to taking future short-dollar positions against high-interest-rate currencies increase. This provides the economic rationale for conditioning carry trade positions on the information revealed by FOMC announcements. For central bank information shocks, the picture reverses. Positive news about fundamentals leads to a depreciation of the U.S. dollar, in line with Pinchetti and Szczepaniak

[1] Note that we treat these shocks as being symmetric. Hence, the interpretation of the results flips for expansionary shocks. We do not specifically examine differences between contractionary and expansionary shocks.

(2023). Although realized excess returns decline as the interest rate differential declines, *expected* currency excess returns also fall because the expected appreciation of foreign currencies reinforces the effect of the interest rate differential.

This sheds light on how the market interprets monetary and non-monetary news released by the central bank. Our results are in line with the interpretation of countercyclical currency risk premia of Lustig et al. (2014), but using two cleanly identified signals allows us to examine distinct shocks. A contractionary monetary policy shock induces a "risk-off" episode: the dollar appreciates as investors demand safe dollar assets, while expected foreign-currency excess returns rise as compensation for bearing currency risk. In contrast, central bank information shocks reveal positive news about economic growth and induce a "risk-on" episode. The dollar depreciates as investors shift toward risky foreign currencies and reduce their demand for the U.S. dollar, thus compressing investors' expected excess returns.

The tight relationship between FOMC signals, interest rate differentials, and currency excess returns suggests that trading strategies incorporating these signals should outperform simpler alternatives. We leverage these findings to construct trading strategies that improve upon both the conventional High-minus-Low (HML) carry strategy (Lustig and Verdelhan, 2007) and the announcement-day strategy (Mueller et al., 2017). Investors adjust their carry trade exposure based on the different signals from the FOMC announcements. On announcement days, we implement a strategy that tilts toward a long dollar position when the high-frequency surprises are dominated by news about interest rate derivatives and toward the standard carry trade when the surprise reflects news about the stock market. The resulting strategy outperforms the conventional carry trade in both average returns and on a risk-adjusted basis, delivering a statistically significant weekly alpha of 19 basis points (bps) relative to the standard carry factor and 16 bps relative to the strategy trading on announcement days.

Finally, we examine whether realized and ex ante currency excess returns exhibit a term structure and depend on speculative carry trade activity. While realized excess returns decline with the holding horizon, the estimates are not statistically significant. By contrast, currency risk premia display a clear downward-sloping term structure that gradually flattens over time. We measure speculative carry trade intensity using the net open interest, adjusted for whether the U.S. dollar serves as the funding or investment currency, and compare its role with that of the convenience yield, measured by the Treasury basis (Jiang et al., 2021). Overall, we find little evidence of state dependence. Higher speculative activity slightly amplifies realized excess returns following monetary policy shocks, although the effect is insignificant. For central bank information shocks, higher carry trade intensity attenuates the decline in realized excess returns. Similar patterns emerge for expected currency excess returns. The convenience yield appears more relevant in the low carry trade intensity regime, whereas speculative motives play a larger role in the high regime. Overall, however, currency risk premia differ little across regimes.

The remainder of the paper is structured as follows. Section 2 describes the data and introduces the definition of excess returns. In Section 3, we show the cross-sectional evidence, consisting of the regression-based analysis and the trading exercise, before presenting the multivariate time series evidence in Section 4. Finally, Section 5 concludes.

Related literature. We contribute to several strands of the literature. First, we contribute to the literature on currency carry trades and currency risk premia. A large literature documents the persistent profitability of carry trade strategies and relates them to compensation for crash risk, volatility risk, and other systematic sources of currency risk (Lustig and Verdelhan, 2007; Brunnermeier et al., 2008; Lustig et al., 2011; Menkhoff et al., 2012). Existing work further shows that a substantial share of currency risk premia is earned on FOMC announcement days and that monetary policy surprises affect the profitability of carry trades (Mueller et al., 2017; Brusa et al., 2020; Falconio, 2023). We contribute to this literature by showing that decomposing FOMC announcements into different components, namely monetary and non-monetary news, fundamentally changes the interpretation of announcement-day currency returns. The two signals have opposing effects on exchange rates, interest rate differentials, and currency excess returns, implying opposite optimal carry trade positions and substantially different announcement-day profitability.

Second, a large monetary policy literature has documented that a contractionary monetary policy shock leads to an appreciation of the domestic currency (Kim and Roubini, 2000; Stavrakeva and Tang, 2015; Boeck and Mori, 2025). However, FOMC announcements convey information beyond monetary policy, as documented by Cieslak and Schrimpf (2019). For currency markets, Franz (2020), Gürkaynak et al. (2021), Pinchetti and Szczepaniak (2023), and Antolin-Diaz et al. (2023) trace the implications of central bank information shocks and their effects on the term structure of currency returns. Building on Zviadadze (2017), we connect the announcement-day behavior of realized currency excess returns to the dynamic evolution of expected currency risk premia. We show that monetary policy and central bank information shocks generate distinct cross-sectional responses across currencies sorted by interest rate differentials and propagate differently across holding horizons. Using model-implied expected excess returns allows us to characterize how signals from FOMC announcements shape the term structure of currency risk premia.

Third, we contribute to the literature on time-varying currency risk premia (Verdelhan, 2010; Lustig et al., 2014; Colacito et al., 2020), which documents that expected excess returns are countercyclical, elevated in bad times and compressed in good times. We extend this literature by identifying one mechanism underlying these fluctuations: the two signals contained in FOMC announcements capture distinct macroeconomic states in currency markets. Contractionary monetary policy shocks raise expected foreign-currency risk premia across maturities, consistent with a deterioration in macroeconomic conditions ("risk-off"), whereas central bank information shocks compress risk premia, consistent with an improvement in the growth outlook ("risk-on").

2. Data and definitions

Data. We collect daily, weekly, and monthly nominal spot exchange rates against the U.S. dollar, central bank policy rates, forward exchange rates, and government bond yields from January 1995 to December 2024 for seven major developed markets among G10 currencies. We gather data on interest rates, government bond yields, and forward rates at 1-week, 1-month, 3-month, 6-month, and 12-month maturities, which allows us to study the term structure of currency risk premia. The following currencies constitute our baseline sample: Australian dollar (AUD), Canadian dollar (CAD), Swiss franc (CHF), euro (EUR), British pound (GBP), Japanese yen (JPY), and New Zealand dollar (NZD).[2] We focus on these currencies because they represent the most liquid currency markets, ranked highest by daily turnover of currency pairs against the U.S. dollar (Bank for International Settlements, 2025), while consistent data availability for all variables used in the empirical analysis is ensured. We collect the corresponding U.S. data whenever required. We denote the logarithm of the nominal exchange rate by s_t and the logarithm of the forward exchange rate with m-month maturity by f_t^m. Both spot and forward exchange rates are expressed in units of foreign currency per U.S. dollar. An increase in the spot exchange rate corresponds to an appreciation of the U.S. dollar. The domestic U.S. interest rate with m-month maturity at time t is denoted by $i_t^{\$,m}$, and the foreign one by $i_t^{*,m}$. An overview of the data sources and the sample is provided in Appendix A.

We measure unanticipated U.S. monetary policy surprises via high-frequency proxies. These high-frequency proxies are changes in the prices of interest rate derivatives and in the S&P 500 stock market index in a narrow window surrounding FOMC monetary policy announcements and are labeled as surprises.[3] This window is defined as 10 minutes before and 20 minutes after the announcement and rules out potential confounding factors. These changes then reflect the exogenous changes in expectations due solely to the announcement of the new and unanticipated monetary policy stance. We exploit the comovement between those surprises to differentiate between a monetary policy shock and a central bank information shock. A conventional monetary policy shock, MP_t, is defined as a negative comovement between the interest-rate-derivative and asset-price surprises, while a positive comovement implies a central bank information shock, CBI_t.[4] Note that we use only surprises originating from scheduled meetings to avoid potential confounding effects stemming from unexpected or emergency policy announcements (Lucca and Moench, 2015; Mueller et al., 2017; Cieslak et al., 2019). Thereby, we ensure that the high-frequency surprises predominantly reflect monetary policy news rather than contemporaneous macroeconomic or financial stress. To this end, we construct monthly shock measures by aggregating the underlying intraday surprises within each month. If more than one FOMC announcement occurs in month t, we sum the corresponding intraday surprises. If no announcement takes place, both shock measures are set to zero.

As a proxy for carry trade activity, we use the futures position data from the U.S. Commodity Futures Trading Commission (CFTC) provided by Brunnermeier et al. (2008) and Fong (2013). Higher net open

[2] For the period before the introduction of the euro on January 1, 1999, we splice the euro series together with the exchange rate of the German mark to the U.S. dollar, and we use German interbank rates in place of euro interbank rates.

[3] We follow the methodology in Jarociński and Karadi (2020) to construct the surprises in the interest rate derivatives. These are constructed as the first principal component of five high-frequency surprises: the current-month Fed funds future, the 3-month Fed funds future, and the eurodollar futures with horizons of two, three, and four quarters, respectively. The advantage of this procedure is that it partly captures unconventional monetary measures, like forward guidance. We obtained the data via `https://marekjarocinski.github.io/jkshocks/jkshocks.html`.

[4] This method is robust to the critique of Bauer and Swanson (2023a), who show that alternative estimates of the information effect may be contaminated by differences in the perceived and actual reaction functions of the central bank to economic news. They posit a "Fed response to news" channel, which originates from imperfect understanding by financial market participants of the reaction function of the central bank to economic news. As a substantial fraction of the variation around this window moves interest rates and stock prices in the same direction, it provides evidence of the presence of non-monetary news unrelated to the "Fed response to news" channel by Bauer and Swanson (2023b). While other sources (such as changes in risk premia) can be behind this non-monetary news, we follow the majority of the literature and label it a "central bank information shock".

interest reflects stronger speculative demand for a currency and, therefore, provides a direct proxy for the intensity of carry trade activity. The *net open interest*

$$noi_t = \frac{\text{long}_t - \text{short}_t}{\text{total open interest}_t} \tag{2.1}$$

is the difference between the long and short futures positions of non-commercial traders in foreign currency, expressed as a fraction of the total open interest of all traders. Non-commercial traders are classified as market participants who use futures contracts for purposes other than hedging and are therefore considered speculative investors. We note, however, that futures positions data are subject to limitations arising from the imperfect classification of commercial and non-commercial traders and, more importantly, from the fact that much of the liquidity is in the over-the-counter forward market. Nevertheless, they remain the best publicly available measure of speculative positioning in the market. A positive value of the net open interest is economically equivalent to a currency trade in which the foreign currency is the investment currency and the U.S. dollar is the funding currency. However, for a currency trade in which the foreign currency is the funding currency and the U.S. dollar is the investment currency, a negative value of the net open interest is economically equivalent to an increase in speculative activity. To capture these different directions of the trade in a common measure, we construct a carry trade intensity indicator for each currency as follows

$$CTI_t = noi_t \times \text{sign}(\overline{pird}), \tag{2.2}$$

where $\overline{pird} = \bar{i}^* - \bar{i}^\$$ is the average policy interest rate differential, which we use to classify currencies as investment or funding currencies against the U.S. dollar. We interpret an increase in the CTI_t measure as an increase in speculative activity because it takes into account the direction of the carry trade through the policy interest rate differential, similar to Brunnermeier et al. (2008). As speculative positioning varies substantially across currencies and over time, our indicator constitutes a natural state variable for examining whether monetary policy transmission depends on the intensity of carry trade activity.

Definitions. The carry trade strategy consists of borrowing in low-interest-rate currencies and investing in high-interest-rate currencies. We denote the annualized realized excess return on an investment in foreign currency financed by borrowing in domestic currency, holding it over an m-month horizon as

$$rx_{t+m} = ird_t^m - (12/m)\Delta s_{t+m}, \tag{2.3}$$

where $ird_t^m = i_t^{*,m} - i_t^{\$,m}$ denotes the annualized interest rate differential, and $\Delta s_{t+m} = s_{t+m} - s_t$ is the revaluation of the foreign currency. We annualize the change in the spot rate with the factor $(12/m)$, taking the holding horizon into account. The currency excess return is a measure of the exchange-rate return in excess of the prediction implied by UIP. Accordingly, rx_{t+m} should not be forecastable: $\mathbb{E}_t[rx_{t+m}] = 0$. We define currency risk premia as ex ante currency excess returns, $\mathbb{E}_t[rx_{t+m}]$. This is the abnormal return to a carry trade strategy where the foreign currency is the investment currency and the U.S. dollar is the funding currency. In most of our analysis, and in line with most of the literature on UIP, we look at interest rate differentials and currency excess returns expressed relative to the U.S. dollar. In reality, carry traders do not necessarily take positions relative to the U.S. dollar but exploit, for instance, high interest rates in AUD for investment and low interest rates in JPY for borrowing. Nevertheless, our analysis sheds light on the profitability of such a strategy, as a revaluation of the U.S. dollar also changes the relative valuation of the AUD to the JPY. Hence, while we do not directly form the carry trade strategies that investors might engage in, our framework nevertheless captures their expected profitability because movements in the U.S. dollar simultaneously affect bilateral exchange rates among foreign currencies.

An alternative way to implement the carry trade is to sell forward currencies that are at a forward premium and buy forward currencies that are at a forward discount. We define the m-month forward discount as

$$fd_{t+m} = f_t^m - s_t, \tag{2.4}$$

where a foreign currency is said to be at a forward discount if $fd_{t+m} > 0$, and at a forward premium if $fd_{t+m} < 0$ relative to the U.S. dollar. Under the assumption of covered interest rate parity, the forward discount is equal to the interest rate differential $fd_{t+m} \approx i_t^{*,m} - i_t^{\$,m}$. Hence, the annualized currency excess return can also be stated as the forward discount minus the change in the spot rate,

$$rx_{t+m} \approx (12/m)(fd_{t+m} - \Delta s_{t+m}). \tag{2.5}$$

This expression can be simplified to $rx_{t+m} \approx (12/m)(f_t^m - s_{t+m})$. Again, under the UIP, excess returns should not be forecastable as $f_t^m = \mathbb{E}_t[s_{t+m}]$, and thus $\mathbb{E}_t[rx_{t+m}] = (12/m)(f_t^m - \mathbb{E}_t[s_{t+m}]) = 0$.

As the analysis is conducted relative to the U.S. dollar, we account for the special role of the United States as the world's largest supplier of safe assets, which investors are willing to hold at lower returns. This is dubbed the convenience yield (Krishnamurthy and Vissing-Jorgensen, 2012; Jiang et al., 2021). We use the U.S. Treasury basis as our key measure for the demand for dollar safe assets, which is proportional to the convenience yield. The Treasury basis is defined as the difference between the yield on U.S. Treasuries, $i_t^{\$,12m}$, and a synthetic dollar yield of a foreign government bond, which earns a yield $i_t^{*,12m}$ in foreign currency and is then hedged back into dollars,

$$x_t^{Treas} \equiv (i_t^{\$,12m} - i_t^{*,12m}) + (f_t^{12m} - s_t). \tag{2.6}$$

A negative Treasury basis implies that U.S. Treasuries are more expensive compared to foreign counterparts, mainly because foreign government bonds are not as safe and liquid as U.S. Treasuries, so investors accept a lower yield to hold the latter. Jiang et al. (2021) provide the link to the convenience yield, $\lambda_t^{\$,*} - \lambda_t^{*,*}$, via $x_t^{Treas} = -(1-\beta^*)(\lambda_t^{\$,*} - \lambda_t^{*,*})$, where the proportionality factor depends on a constant $0 < \beta^* < 1$, which they estimate to be $\beta^* \approx 0.9$. Hence, the Treasury basis is strongly linked to the convenience yield. For our sample, the average Treasury basis is negative for all currencies except the AUD (see Table 1).

Summary statistics. Table 1 reports summary statistics for monthly annualized realized currency excess returns, including their mean, standard deviation, skewness, and kurtosis, together with the average interest rate differential and the average change in the spot rate for different holding horizons and across all currencies in our sample. Additionally, we report the average policy interest rate differential, net open interest, and Treasury basis. The sample ranges from 1995 to 2024 for the 3-month and 12-month holding horizons. However, the sample periods are considerably shorter for

Table 1: Summary statistics of realized currency excess returns and their components.

	JPY	CHF	EUR	CAD	GBP	AUD	NZD
Holding horizon: 1-month							
Mean	−2.360	0.294	0.459	0.512	−2.638	2.675	−0.193
Standard deviation	9.489	9.793	9.248	8.779	8.979	12.203	13.415
Skewness	−0.104	0.164	−0.147	−0.500	−0.317	−0.480	−0.209
Kurtosis	3.421	5.830	4.480	5.764	4.325	4.873	4.275
Interest rate differential	−1.383	−1.365	−0.254	0.238	0.096	1.848	1.832
FX revaluation	0.977	−1.659	−0.712	−0.274	2.735	−0.828	2.025
Holding horizon: 3-month							
Mean	−3.854	−0.605	−1.063	0.140	−0.083	1.109	1.874
Standard deviation	6.464	5.442	5.392	4.488	4.904	6.858	6.921
Skewness	0.347	0.105	−0.144	−0.040	−0.538	−0.584	−0.114
Kurtosis	3.966	2.980	3.461	5.304	5.577	6.537	4.121
Interest rate differential	−2.241	−1.697	−0.439	0.157	0.674	1.584	2.181
FX revaluation	1.631	−1.072	0.634	0.028	0.761	0.489	0.327
Holding horizon: 6-month							
Mean	−2.998	0.660	−0.729	0.194	−2.552	1.153	0.236
Standard deviation	4.345	3.336	3.962	3.157	4.076	4.962	5.156
Skewness	0.043	0.327	−0.220	−0.122	−1.038	−0.303	−0.277
Kurtosis	2.925	3.659	2.801	4.819	5.259	5.399	6.126
Interest rate differential	−2.143	−1.255	−0.636	0.202	0.057	1.508	1.847
FX revaluation	0.854	−1.915	0.092	0.007	2.609	0.355	1.612
Holding horizon: 12-month							
Mean	−4.004	−0.701	−1.470	0.184	−0.334	0.796	1.753
Standard deviation	3.130	2.604	2.813	2.197	2.484	3.673	3.744
Skewness	−0.129	0.138	0.168	−0.033	−0.688	0.217	−0.075
Kurtosis	2.259	3.759	2.639	3.655	3.963	2.957	3.139
Interest rate differential	−2.415	−1.750	−0.866	0.170	0.385	1.328	1.988
FX revaluation	1.658	−0.982	0.636	0.013	0.735	0.408	0.297
Policy interest differential	−2.377	−1.815	−0.330	0.081	0.548	1.461	1.991
Net open interest	−13.117	−10.332	2.226	−0.264	−1.982	4.967	14.222
Treasury basis	−0.448	−0.428	−0.374	−0.197	−0.005	0.011	−0.032

Notes: This table reports summary statistics for annualized realized currency excess returns $rx_{t+m} = ird_t^m - (12/m)\Delta s_{t+m}$, including the mean, standard deviation, skewness, and kurtosis, and the mean for the annualized interest rate differential, $ird_t^m = i_t^{*,m} - i_t^{\$,m}$ and for annualized foreign exchange (FX) revaluations, $(12/m)\Delta s_{t+m}$ across different holding horizons $m \in \{1, 3, 6, 12\}$ and across all currencies in our sample (AUD, CAD, CHF, EUR, GBP, JPY, NZD). The last three rows of the table report the mean of the policy interest rate differential, the net open interest, and the Treasury basis across all currencies in our sample. Currencies are ordered in ascending order by their policy interest rate differential.

the 1-month and 6-month holding horizons, as reported in Table A2 in Appendix A. The currencies in the table are ordered in ascending order by their policy interest rate differential.

Three stylized facts emerge from the data. First, average excess returns are strongly increasing in the policy interest rate differential (or, equivalently, the forward discount) across 3- and 12-month horizons, confirming the well-known profitability of investing in high-interest-rate currencies. For 1- and 6-month horizons, only GBP and NZD, respectively, deviate from this pattern. In Table C1 in Appendix C, we report the summary statistics with the forward discount. There is a close correspondence between forward discounts and interest rate differentials (correlation coefficient of $\rho = 0.97$ with a p-value ≈ 0), which is consistent with covered interest rate parity holding closely in our sample.

Figure 1: Currency excess returns, net open interest, and the policy interest rate differential.

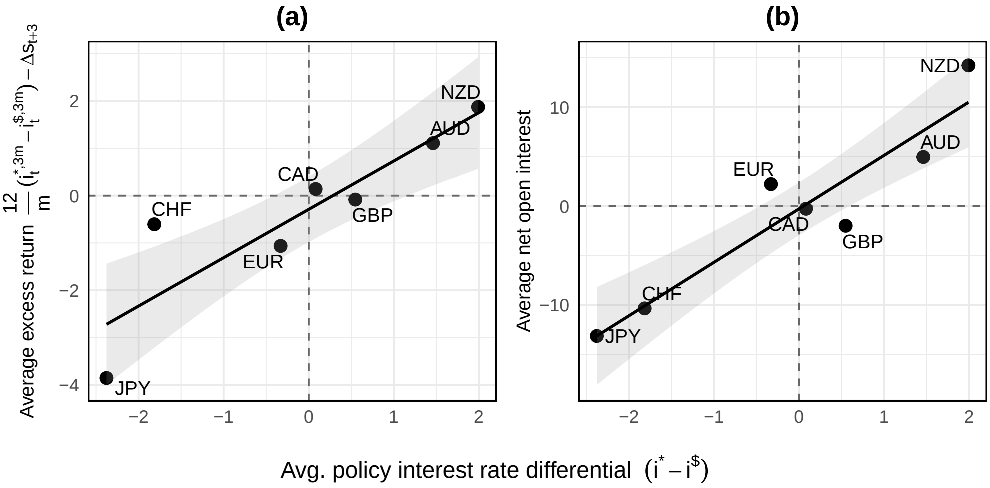

Notes: Panel (a) plots average annualized excess returns against the average policy interest rate differential ($\overline{pird} = \bar{i}^* - \bar{i}^\$$) relative to the U.S., while panel (b) plots average net open interest against the same differential across currencies. Net open interest is calculated as the difference between the long and short futures positions of non-commercial traders divided by the total open interest (data retrieved from CFTC). Shaded areas denote the 90% confidence intervals.

Second, speculative positioning closely mirrors these interest rate differentials. High-interest-rate currencies, such as the AUD and NZD, exhibit positive average net open interest, whereas low-interest-rate currencies, such as the JPY and CHF, display negative net open interest, consistent with their respective roles as investment and funding currencies. Third, return distributions exhibit pronounced asymmetries and fat tails. High-interest-rate currencies tend to display stronger negative skewness and elevated kurtosis, indicating greater exposure to downside and crash risk. Higher-order moments decrease for longer holding horizons. Skewness is more pronounced at shorter horizons than at longer horizons. Similarly, kurtosis is much more elevated at short holding horizons, while at longer horizons, it is lower and closer to 3 (the level of kurtosis for a normal distribution). There are also currencies that do not perfectly fit these facts: EUR and GBP. Their excess returns vary in size across holding horizons and do not fit as well into the cross-sectional picture.

Before turning to the formal analysis, we illustrate these relationships graphically. In Figure 1, we show the relationship between the average policy interest rate differential and the average currency excess returns with a 3-month holding horizon and the net open interest. There is a clear positive relationship between these variables, which is statistically significant. We report the regression coefficients and standard errors in Table C2 in Appendix C. In panel (a), we report the relationship with the currency excess returns. As the interest rate differential increases, the carry trade becomes increasingly attractive. High-interest-rate currencies with positive differentials, such as AUD and NZD, are associated with higher average excess returns, whereas low-interest-rate currencies with negative differentials, such as JPY and CHF, tend to exhibit lower or negative excess returns. Panel (b) shows that the same relationship also holds for the net open interest. High-interest-rate currencies tend to display a positive net open interest, consistent with stronger speculative demand for investment currencies. By contrast, currencies with a negative interest rate differential show a negative net open interest, which indicates that the respective currency is predominantly used as a funding currency. Thus, the figure suggests that larger interest rate differentials make carry trades more attractive and are associated with both higher excess returns and more pronounced speculative positioning.

Together, these stylized facts raise the question of how different signals from FOMC announcements affect these relationships, both in the cross-section and in a time series analysis. We first examine whether monetary policy and central bank information shocks generate heterogeneous responses across currencies before studying the underlying transmission channels and the role of speculative positioning in a multivariate framework.

3. Cross-sectional evidence on realized currency excess returns

This section investigates how spot exchange rates, interest rate differentials, and excess returns are related to monetary policy and central bank information shocks in the cross-section. We relate the estimated elasticities for each currency to the currencies' average interest rate differentials. This allows us to understand how the underlying components contribute quantitatively to the realized currency excess returns across currencies. Given the documented heterogeneity in currencies' responses to the shocks, we construct a trading exercise to check whether monetary policy announcements can be exploited profitably.

3.1 Regression-based analysis

We start the analysis by examining how realized currency excess returns and their components are affected by monetary policy and central bank information shocks. First, we regress the spot rate, the revaluation of the spot rate, the interest rate differential, and realized currency excess returns on the two shocks for each currency separately

$$y_t = \beta_0 + \beta_{MP} MP_t + \beta_{CBI} CBI_t + u_t, \tag{3.1}$$

where $y_t \in \{s_t, \Delta s_t, \Delta s_{t+3}, ird_t^{3m}, rx_{t+3}\}$. Estimation is done using ordinary least squares. The coefficients β_j ($j \in \{MP, CBI\}$) measure how strongly the respective outcome variable reacts to a one-standard-deviation change in either the monetary policy or central bank information shock. As we are not estimating the first-stage regression of the shocks on the short-term interest rates, the interpretation of the shock size is not straightforward economically. Hence, we standardize the shock measures such that a unit change represents a one-standard-deviation increase in the Eurodollar futures. Sample periods differ across currencies and regressions due to data availability and the construction of forward-looking outcomes. The respective sample periods are reported in Table A2.

In Figure 2, we report the cross-sectional variation of the estimated effect sizes (together with their 90% confidence intervals) in relation to the average policy interest rate differential. Additionally, we show a fitted regression line together with its 90% confidence band for this relationship. We report the regression coefficients and standard errors in Table C2 in Appendix C. The scatter plots illustrate the relationship separately for the monetary policy shock (left panel, blue color) and the central bank

Figure 2: Cross-sectional variation of the reaction to the monetary policy and central bank information shocks.

(a) Dependent variable: spot rates.

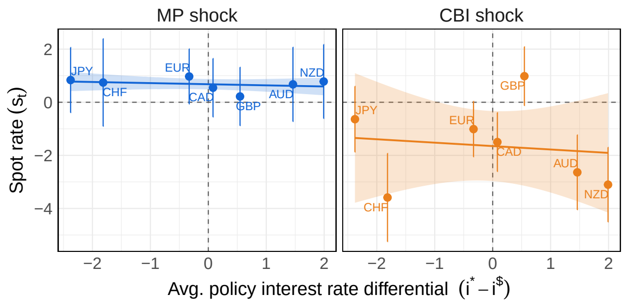

(b) Dependent variable: change in spot rates.

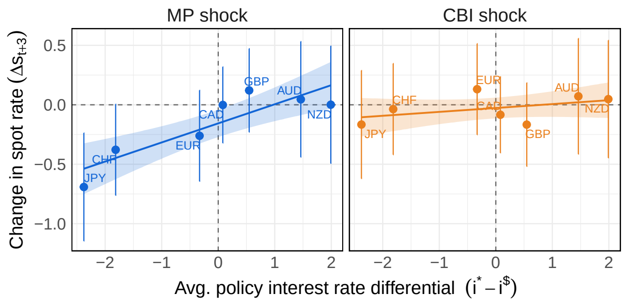

(c) Dependent variable: interest rate differentials.

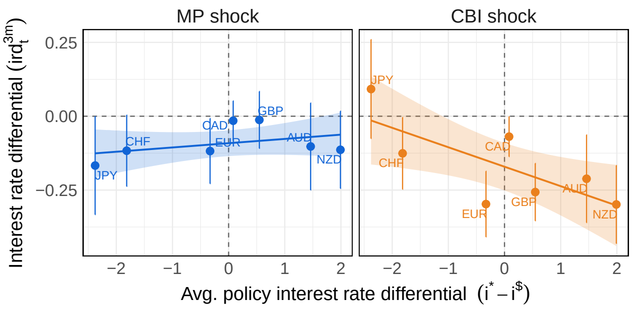

(d) Dependent variable: currency excess returns.

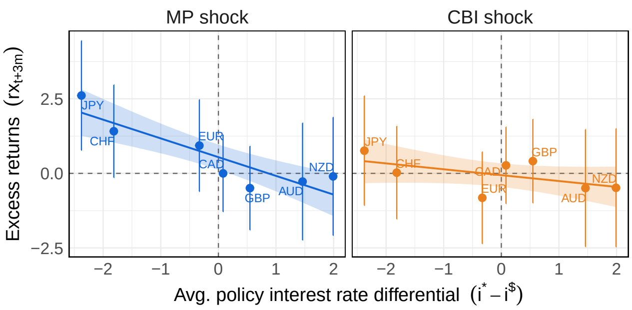

Notes: This figure shows the cross-sectional relationship between the average policy interest rate differential ($\overline{pird} = \overline{i}^* - \overline{i}^\$$) and the effect sizes of the spot rates (panel a), changes in spot rates (panel b), interest rate differentials (panel c), and currency excess returns (panel d) associated with the monetary policy shock (left panel, blue color) and with the central bank information shock (right panel, orange color) for each currency. The shocks are standardized. Definitions of the change in the spot rate, $\Delta s_{t+3} = s_{t+3} - s_t$, the interest rate differential, $ird_t^{3m} = i_t^{*,3m} - i_t^{\$,3m}$, and the currency excess returns, $rx_{t+3} = ird_t^{3m} - 4\Delta s_{t+3}$. The vertical bars denote 90% confidence intervals around the estimated coefficient. The solid line in each panel represents the fitted cross-sectional regression, and the shaded area its 90% confidence interval.

information shock (right panel, orange color) for the spot rate (panel a), the change in the spot rate (panel b), the interest rate differential for 3-month holding horizons (panel c), and realized currency excess returns for 3-month holding horizons (panel d).

The relationship differs markedly by shock type. A monetary policy (central bank information) shock leads to an appreciation (depreciation) of the U.S. dollar. This first finding corroborates the results of Pinchetti and Szczepaniak (2023) documenting the same pattern in response to both monetary policy and central bank information shocks. The reaction of the spot rate does not change with the interest rate differential. For currency excess returns, the future change in the spot rate is more relevant, as it reacts heterogeneously along the interest rate differential. We observe that following a monetary policy shock, currencies with lower interest rate differentials tend to depreciate less strongly against the U.S. dollar. In contrast, currencies appreciate more strongly following the depreciation of the U.S. dollar in response to the central bank information shock. This is consistent with the overshooting hypothesis of Dornbusch (1976).

The response of the interest rate differential is similar across shocks. The interest rate differential declines in response to both shocks. For the monetary policy shock, most effect sizes are relatively small, with JPY showing the strongest response. In the cross-section, we do not find a strong pattern. For the central bank information shock, we find a statistically significant negative relationship in the cross-section. Hence, the interest rate differential declines for currencies with a larger policy interest differential on average. In the last panel, we observe the effects on the realized currency excess returns, which are positive for the monetary policy shock and negative for the central bank information shock. For both shocks, this cross-sectional relationship is downward sloping. This implies that realized currency excess returns (in absolute terms) are smaller for the monetary policy shock and larger for the central bank information shock for high-interest-rate currencies.

The opposing responses to monetary policy and central bank information shocks are not merely differences in statistical significance but are statistically distinguishable from each other. Table C3 in Appendix C reports Wald tests of the null hypothesis that the responses to both shocks are equal for each currency and outcome variable. The null hypothesis is rejected for many specifications involving spot rates and interest rate differentials, whereas the evidence is weaker for the change in the spot rate and the level of excess returns, consistent with the visual evidence in Figure 2.

Taken together, these results imply that, following a monetary policy shock, currencies with a lower average interest rate differential show stronger future U.S. dollar depreciations with a small decline in the interest rate differential, resulting in higher realized currency excess returns. We observe higher realized currency excess returns for low-interest-rate currencies.[5] By contrast, we find the opposite for the central bank information shock. The larger decline in realized currency excess returns for currencies with a higher interest rate differential is then a combination of stronger future appreciation and a larger decline in the interest rate differential. These results suggest that the effects of monetary

[5] However, when we inspect the *change* in the realized excess returns in Figure C1, we observe that the realized excess returns turn clearly positive for both low- and high-interest-rate currencies. The stronger relationship for the level of realized excess returns reflects both the announcement-induced change and pre-existing cross-sectional differences in the average level of excess returns across currencies. Focusing on changes isolates the revision attributable to the announcement, resulting in a considerably flatter cross-sectional relationship.

Table 2: Impact of monetary policy and central bank information shocks on spot rates, interest rate differentials, and realized currency excess returns.

Panel A: Average effects	$s_{i,t}$	$\Delta s_{i,t}$	$\Delta s_{i,t+3}$	$ird^{3m}_{i,t}$	$\Delta ird^{3m}_{i,t}$	$rx_{i,t+3}$	$\Delta rx_{i,t+3}$
	(1)	(2)	(3)	(4)	(5)	(6)	(7)
MP_t	0.681	0.463***	−0.166	−0.092	0.000	0.583	1.571**
	(0.628)	(0.105)	(0.197)	(0.064)	(0.017)	(0.790)	(0.614)
CBI_t	−1.643**	−0.072	−0.029	−0.167***	−0.018	−0.048	−0.131
	(0.728)	(0.134)	(0.215)	(0.058)	(0.011)	(0.873)	(0.502)
δ_i	YES	YES	YES	YES	YES	YES	YES
Adj. R^2	0.991	0.028	0.000	0.499	0.003	0.005	0.008
Observations	2,520	2,513	2,499	2,520	2,513	2,499	2,492

Panel B: Transmission mechanisms	$\Delta s_{i,t}$		$\Delta s_{i,t+3}$		$\Delta ird^{3m}_{i,t}$		$\Delta rx_{i,t+3}$	
	(8)	(9)	(10)	(11)	(12)	(13)	(14)	(15)
MP_t	0.452***	0.478***	−0.234	−0.171	−0.016	−0.000	1.587**	1.784***
	(0.120)	(0.107)	(0.206)	(0.210)	(0.017)	(0.016)	(0.715)	(0.609)
CBI_t	−0.085	−0.103	0.050	−0.091	−0.017*	−0.017	−0.084	−0.152
	(0.109)	(0.137)	(0.216)	(0.217)	(0.010)	(0.011)	(0.532)	(0.499)
$x^{Treas}_{i,t-1}$	−0.048		0.114		0.015		0.186	
	(0.193)		(0.225)		(0.011)		(0.0736)	
$CTI_{i,t-1}$		0.003		−0.001		0.000		0.013
		(0.003)		(0.005)		(0.000)		(0.016)
$MP_t \times x^{Treas}_{i,t-1}$	−0.033		−0.194		−0.064*		0.085	
	(0.256)		(0.337)		(0.036)		(1.179)	
$MP_t \times CTI_{i,t-1}$		0.004		−0.004		−0.000*		0.012
		(0.002)		(0.004)		(0.000)		(0.014)
$CBI_t \times x^{Treas}_{i,t-1}$	−0.047		0.414		0.001		0.252	
	(0.357)		(0.387)		(0.021)		(1.319)	
$CBI_t \times CTI_{i,t-1}$		0.007**		0.003		−0.000		0.031*
		(0.003)		(0.005)		(0.000)		(0.014)
δ_i	YES	YES	YES	YES	YES	YES	YES	YES
Adj. R^2	0.026	0.035	0.000	0.000	0.016	0.008	0.007	0.013
Observations	2,494	2,333	2,479	2,312	2,494	2,333	2,473	2,312

Notes: This table presents panel regression results in which the dependent variables are the spot rate (s_t), the change in the spot rate (Δs_t), the future revaluation of the spot rate ($\Delta s_{i,t+3}$), the interest rate differential ($ird^{3m}_{i,t}$), the change in the interest rate differential ($\Delta ird^{3m}_{i,t}$), the realized excess returns ($rx_{i,t+3}$), and the change in the realized excess returns ($\Delta rx_{i,t+3}$) for a currency i. The independent variables are the monetary policy shock (MP_t) and the central bank information shock (CBI_t) and interactions with the lagged Treasury basis ($x^{Treas}_{i,t-1}$) and the lagged carry trade intensity indicator ($CTI_{i,t-1}$). The data are monthly. The models are estimated by fixed-effects OLS, with time-clustered standard errors reported in parentheses. *, **, and *** indicate statistical significance at the 10%, 5%, and 1% levels, respectively.

policy are transmitted strongly through future revaluations of the currency, while the central bank information shock shows a combination of both channels. These results thus document asymmetric responses of excess returns to monetary policy and central bank information shocks. Furthermore, these results are robust to excluding the Global Financial Crisis (GFC) and the COVID period. We show these robustness exercises in Figures C2 and C3 in Appendix C.

So far, we have examined the response of the realized currency excess returns and their components in the cross-section. We now move to a panel analysis in which we examine how currency excess returns change in response to the signals and whether these changes are stronger for higher speculative carry trade activity. We also investigate whether the demand for safe assets acts as a possible transmission mechanism. To do so, we estimate a panel regression that pools information across currencies and time. This approach allows us to quantify the average transmission of monetary policy and central bank information shocks while accounting for persistent differences across currencies through fixed effects. Specifically, we estimate the following panel regression for currency i and time t:

$$\begin{aligned} y_{i,t} &= \delta_i + \delta_{MP} MP_t + \delta_{CBI} CBI_t \\ &\quad + \delta_{MP,TB} MP_t \times x^{Treas}_{i,t-1} + \delta_{CBI,TB} CBI_t \times x^{Treas}_{i,t-1} \\ &\quad + \delta_{MP,CTI} MP_t \times CTI_{i,t-1} + \delta_{CBI,CTI} CBI_t \times CTI_{i,t-1} + u_{i,t} \end{aligned} \tag{3.2}$$

with $y_{i,t} \in \{s_{i,t}, \Delta s_{i,t}, \Delta s_{i,t+3}, ird^{3m}_{i,t}, \Delta ird^{3m}_{i,t}, rx_{i,t+3}, \Delta rx_{i,t+3}\}$ and where $i = 1,\dots,N$ and $t = 1,\dots,T$. All estimated specifications contain currency (δ_i) fixed effects. We estimate several specifications, which are nested in Eq. (3.2), by setting combinations of $\delta_{s,v}$ ($s \in \{MP, CBI\}$ and $v \in \{TB, CTI\}$) to zero. The interaction terms allow the effects of the two shocks to differ across transmission mechanisms, enabling us to examine the conditional transmission of both shocks on the Treasury basis (TB) and speculative carry trade intensity (CTI). Since both shocks vary only over time, identification comes exclusively from the time-series variation in the announcement shocks, while the panel dimension increases estimation precision. Standard errors are clustered by month, allowing for arbitrary dependence across currencies exposed to the same shock.

Table 2 reports the estimation results. In Panel A, we regress all outcome variables on both shocks before starting with the interactions in Panel B. There, we focus on the response to the changes in realized excess returns (and interest rate differentials), rather than their levels, to isolate the announcement-induced revision in profitability. We observe that monetary policy shocks cause an appreciation of the U.S. dollar before it starts to depreciate in the future due to overshooting. The appreciation is reflected in both the positive coefficient in column (1), which captures the level response, and the significantly positive coefficient in column (2), which captures the appreciation during the announcement month. The negative coefficient in column (3) points to a subsequent depreciation three months in the future. The response of the interest rate differential is mildly negative. Together, this generates sizable realized excess return changes. For the central bank information shock, we observe a depreciation of the U.S. dollar, followed by a mild additional appreciation. The interest rate differential declines significantly, creating negative excess returns. The coefficients on these variables are similar in the models with interactions, but their marginal effects differ. For the Treasury basis, we mostly find non-significant coefficients. Its association with the future U.S. dollar revaluations is statistically insignificant, while the interaction points to a further decline in the interest rate differential in the case of monetary policy shocks. Speculative carry trade intensity attenuates the depreciation of the U.S. dollar and the negative currency excess returns to central bank information shocks. Economically, it does not affect the transmission of monetary policy shocks too strongly.

By extending the panel setup to include the holding horizon as well, we can interact the shocks with maturity indicators. This allows us to examine whether the effects vary systematically across the term structure of currency excess returns. Specifically, we estimate the following panel regression for currency i, maturity m, and time t

$$\Delta y_{i,t,m} = \delta_i + \delta_m + \delta_{MP} MP_t + \delta_{CBI} CBI_t + \sum_{\mu \in \mathcal{M}} \left(\delta_{MP,m} MP_t \times \mathbb{1}(m=\mu) + \delta_{CBI,m} CBI_t \times \mathbb{1}(m=\mu) \right) + u_{i,t,m} \tag{3.3}$$

with $y_{i,t,m} \in \{\Delta s_{i,t+m}, \Delta ird^m_{i,t}, \Delta rx_{i,t+m}\}$ and where $i = 1,\ldots,N$, $t = 1,\ldots,T$, and $m \in \mathcal{M} = \{1m, 3m, 6m, 12m\}$. All estimated specifications contain currency (δ_i) and maturity (δ_m) fixed effects. The interaction terms allow the effects of the two shocks to differ across holding horizons.

Table 3 reports the estimation results. The first specification (columns 1, 3, 5) for each dependent variable estimates the average effect of monetary policy and central bank information shocks across maturities, while the second specification (columns 2, 4, 6) allows these effects to vary with the holding horizon through the interaction terms. We use the 1-month holding horizon as the reference maturity. The results broadly confirm the individual-currency regression-based analysis. The effects of contractionary monetary policy shocks gradually weaken, with varying degrees of statistical precision across holding horizons and outcome variables. The weaker pass-through to future revaluations of the U.S. dollar translates into lower realized currency excess returns. For central bank information shocks, we observe that they significantly compress the interest rate differential at short maturities, while this effect becomes weaker at longer horizons.

Taken together, the panel analysis corroborates that contractionary monetary policy shocks primarily affect currency excess returns through the exchange-rate channel. They induce a significant appreciation of the U.S. dollar, a future depreciation of the U.S. dollar, and an increase in foreign-currency excess returns. In contrast, central bank information shocks operate through both channels. Consequently, their impact on currency excess returns is considerably smaller and generally statistically insignificant. Overall, the panel evidence confirms that signals around FOMC announcements propagate through distinct transmission mechanisms. The systematic variation in currency excess returns is consistent with the view that currency risk premia are time-varying and countercyclical (Lustig and Verdelhan, 2007; Lustig et al., 2014). Because these differences align closely with carry trade characteristics, speculative positioning, and average excess returns, they suggest that the nature of the shock may contain economically relevant information for return predictability. This information helps to explain why currencies earn systematically higher average excess returns on scheduled FOMC announcement days (Mueller et al., 2017).

3.2 Analysis based on a trading strategy

This section investigates whether the information contained in high-frequency interest-rate and equity surprises around FOMC announcements can be exploited to construct a profitable trading strategy. Changes in interest-rate derivatives and the S&P 500 index within a narrow window around FOMC announcements capture the market response to FOMC announcement information and can therefore serve as signals. As the effects on excess returns strengthen with the interest rate differential and depend on the respective shock, we examine whether conditioning on the composition of the announcement-day surprise delivers risk-adjusted outperformance beyond the standard carry factor.

Table 3: Impact of monetary policy and central bank information shocks on spot rates, interest rate differentials, and realized currency excess returns along the term structure.

	$\Delta s_{i,t+m}$		$\Delta ird^{m}_{i,t}$		$\Delta rx_{i,t+m}$	
	(1)	(2)	(3)	(4)	(5)	(6)
MP_t	0.088	−0.114	−0.006	0.011	0.502***	0.693***
	(0.195)	(0.145)	(0.0133)	(0.020)	(0.149)	(0.262)
CBI_t	0.201	−0.068	−0.025***	−0.041**	−0.116	0.092
	(0.239)	(0.137)	(0.009)	(0.016)	(0.144)	(0.234)
$MP_t \times$						
$\mathbb{1}(m=3m)$		−0.052		−0.011		−0.300
		(0.152)		(0.013)		(0.283)
$\mathbb{1}(m=6m)$		0.416		−0.023		−0.218
		(0.279)		(0.014)		(0.225)
$\mathbb{1}(m=12m)$		0.459		−0.032*		−0.188
		(0.469)		(0.019)		(0.242)
$CBI_t \times$						
$\mathbb{1}(m=3m)$		0.039		0.023*		−0.125
		(0.148)		(0.014)		(0.228)
$\mathbb{1}(m=6m)$		0.320		0.017		−0.335
		(0.281)		(0.013)		(0.207)
$\mathbb{1}(m=12m)$		0.729		0.021		−0.325
		(0.433)		(0.016)		(0.220)
δ_i	YES	YES	YES	YES	YES	YES
δ_m	YES	YES	YES	YES	YES	YES
Adj. R^2	0.001	0.019	0.011	0.014	0.017	0.018
Observations	9,926	9,926	8,768	8,768	8,614	8,614

Notes: This table presents panel regression results in which the dependent variables are the future revaluation of the spot rate ($\Delta s_{i,t+m}$), the change in the interest rate differential ($\Delta ird^{m}_{i,t}$), and the change in the realized excess returns ($\Delta rx_{i,t+m}$) for a currency i and maturity m. The independent variables are the monetary policy shock (MP_t) and the central bank information shock (CBI_t) and interactions with the maturity horizon. The data are monthly. The models are estimated by fixed-effects OLS, with time-clustered standard errors reported in parentheses. *, **, and *** indicate statistical significance at the 10%, 5%, and 1% levels, respectively.

In this analysis, we focus on the surprises in interest rate derivatives and the S&P 500 stock market index, not on the two identified shocks (monetary policy and central bank information shocks). We argue that the surprises are observable from an investor's perspective, whereas the decomposition into the two identified shocks is not performed by investors in real time. We discuss robustness to this choice further below. Building on Lustig and Verdelhan (2007) and Mueller et al. (2017), we construct a U.S.-dollar-funded carry trade strategy in which we sort currencies into three portfolios according to their interest rate differentials relative to the United States. The standard carry trade strategy is constructed as a portfolio that is long the high-interest-rate currencies and short the low-interest-rate currencies (High-minus-Low). We then condition the portfolio formation on the surprises underlying monetary policy and central bank information shocks to test whether these contain additional information beyond the standard carry factor.

We construct currency carry trade portfolios by sorting currencies based on their forward discounts. Under covered interest parity, the one-week currency excess return from investing in the foreign currency i is equal to $rx_{i,t+1w} = f^{1w}_{i,t} - s_{i,t+1w}$, where $f^{1w}_{i,t}$ is the log one-week forward rate and $s_{i,t+1w}$ is the log spot rate for foreign currency i at maturity $t+1w$ against the U.S. dollar. The one-week tenor is preferred here, given that it is the shortest maturity with sufficient liquidity in major currency pairs and incorporates the near-term interest rate differential. According to Table 2 of Bank for International

Settlements (2025), outright forwards with maturities of up to seven days account for 34% of total outright forward turnover, equivalent to approximately $633 billion per day in April 2025. Furthermore, to isolate the currency market response to FOMC announcements from confounding macroeconomic variation, we prefer to use a one-week holding period.

In each time period, all available currencies are ranked in ascending order according to their forward discounts and are assigned to three portfolios. Portfolio 1 contains currencies with the lowest forward discounts (low-interest-rate currencies), whereas Portfolio 3 contains currencies with the highest forward discounts (high-interest-rate currencies). Portfolio 2 comprises the remaining currencies and is not traded. Currencies within each portfolio are equally weighted. The carry trade factor, denoted HML (High-minus-Low), is the excess return on a zero-cost portfolio that is long the high-interest-rate portfolio and short the low-interest-rate portfolio: $\text{HML}_t = \bar{R}_t^{P3} - \bar{R}_t^{P1}$, where $\bar{R}_t^{P1}$ and $\bar{R}_t^{P3}$ denote the average excess return of Portfolio 1 and Portfolio 3, respectively.

We examine three different implementations of this strategy that differ in the timing of portfolio formation and the information set used for sorting. The benchmark strategy, $\text{HML}^{\texttt{eom}}$, forms portfolios at the end of the calendar months containing a scheduled FOMC announcement. Restricting the formation dates in this way ensures a common sample across strategies and renders their comparison directly meaningful. The second strategy, $\text{HML}^{\texttt{fomc}}$, applies the same sorting rule but moves the formation date to the FOMC announcement day and therefore isolates the component of carry returns that specifically accrues around the release of new information. The third and new strategy, $\text{HML}^{\texttt{surprises}}$, conditions the portfolio formation on the sign and composition of the announcement-day surprises. Although surprises are measured within a narrow intraday window around the announcement, portfolio formation and trade execution occur at the end of the announcement day because forward exchange rate data are not available at an intraday frequency, which requires the use of daily spot and forward exchange rate data. In addition to the carry factor, we consider a dollar factor that captures the return on a long position in the U.S. dollar against a basket of foreign currencies. Specifically, we define $\text{Dollar}_{t+1w} = -\frac{1}{N}\sum_{i=1}^{N} rx_{i,t+1w}$, where $rx_{i,t+1w}$ denotes the excess return from investing in foreign currency i funded in U.S. dollars.

The relative importance and the sign of the two surprises jointly determine the allocation between the dollar and carry strategies. Let $m_t^{\texttt{fff}}$ denote the high-frequency interest rate derivative surprise and $m_t^{\texttt{sp500}}$ the high-frequency S&P 500 surprise. We define the weight governing the exposure to the dollar factor as

$$w_t^{\text{Dollar}} = \frac{\max(m_t^{\texttt{fff}}, 0)^2 + \max(-m_t^{\texttt{sp500}}, 0)^2}{(m_t^{\texttt{fff}})^2 + (m_t^{\texttt{sp500}})^2}, \tag{3.4}$$

where $w_t^{\text{Dollar}} \in [0,1]$, such that the portfolio is fully allocated across the two factors. This weighting scheme ensures that an increase in the interest rate derivative surprise favors an appreciation of the U.S. dollar, while a decrease favors the carry trade. In the remaining cases, where the surprises share the same sign, it is a priori not clear whether an investor should favor the dollar or the carry factor. Hence, the allocation is determined proportionally by the relative magnitude of the two surprises. In

Table 4: Currency portfolio returns (1-week holding period) with risk-adjusted alphas.

	$\text{HML}^{\texttt{eom}}$	$\text{HML}^{\texttt{fomc}}$	$\text{HML}^{\texttt{surprises}}$
Panel A: Summary statistics			
Mean (bps)	14.430	13.277	21.681
SD (%)	1.653	1.356	1.096
Skewness	−1.601	−0.588	−0.626
Excess Kurtosis	12.554	5.759	5.361
Sharpe ratio	0.087	0.098	0.198
N	240	240	240
Panel B: Alpha relative to HML^{eom}			
$\alpha^{\text{HML}^{\texttt{eom}}}$ (bps)		10.823	19.182***
$\alpha^{\text{HML}^{\texttt{eom}}}$ SE		(8.274)	(6.975)
Panel C: Alpha relative to HML^{fomc}			
$\alpha^{\text{HML}^{\texttt{fomc}}}$ (bps)			16.179**
$\alpha^{\text{HML}^{\texttt{fomc}}}$ SE			(6.433)

Notes: This table reports the performance of three currency strategies constructed from one-week forward exchange rates for the period from January 1995 to December 2024. The currency universe comprises seven developed market currencies against the U.S. dollar. The sample is restricted to months containing scheduled FOMC announcements. $HML^{\texttt{eom}}$ sorts currencies by forward discounts at the end of the month. $\text{HML}^{\texttt{fomc}}$ applies sorting on the FOMC announcement day. $\text{HML}^{\texttt{surprises}}$ conditions portfolio allocation on both surprises. Mean returns are weekly and expressed in basis points. Standard deviation is in percent. The Sharpe ratio is the mean excess return divided by its standard deviation. The risk-adjusted alpha is obtained from time-series regressions in Eq. (3.6) relative to $\text{HML}^{\texttt{eom}}$ and $\text{HML}^{\texttt{fomc}}$, with Newey-West standard errors (four lags) in parentheses. *, **, and *** indicate statistical significance at the 10%, 5%, and 1% levels, respectively.

the absence of both surprises, i.e., when $m_t^{\texttt{fff}} = m_t^{\texttt{sp500}} = 0$, we set $w_t^{\text{Dollar}} = 0.5$, corresponding to a neutral allocation. The resulting strategy payoff is given by

$$\text{HML}_{t+1w}^{\texttt{surprises}} = w_t^{\text{Dollar}} \times (\text{Dollar}_{t+1w}) + \left(1 - w_t^{\text{Dollar}}\right) \times \text{HML}_{t+1w}^{\texttt{fomc}}. \tag{3.5}$$

To assess whether alternative strategies generate returns beyond the standard end-of-month carry factor or the FOMC announcement day carry factor ($\texttt{j} \in \{\texttt{eom}, \texttt{fomc}\}$), we estimate their risk-adjusted alphas in spanning regressions (Jensen, 1968). Specifically, for each strategy $\texttt{k} \in \{\texttt{fomc}, \texttt{surprises}\}$, we run

$$r_{\texttt{k},t+1w} = \alpha_{\texttt{k}} + \beta_{\texttt{k}} \, \text{HML}_{t+1w}^{\texttt{j}} + \varepsilon_{\texttt{k},t+1w}, \tag{3.6}$$

where $r_{\texttt{k},t+1w}$ denotes the one-week currency excess return on strategy $\texttt{k}$, while $\text{HML}_{t+1w}^{\texttt{j}}$ denotes the benchmark carry-factor return of strategy $\texttt{j}$. The intercept $\alpha_{\texttt{k}}$ measures the component of average returns that is not captured by exposure to the benchmark carry factor. A positive and statistically significant intercept indicates that the corresponding strategy delivers abnormal returns relative to $\text{HML}^{\texttt{eom}}$ or to $\text{HML}^{\texttt{fomc}}$, meaning that its payoffs go beyond the standard carry trade. Eq. (3.6) is estimated by OLS with Newey–West standard errors (Newey and West, 1987).

Table 4, Panel A, reports the performance of the three strategies. The benchmark strategy, $\text{HML}^{\texttt{eom}}$, delivers a mean return of 14.43 bps per week with a weekly standard deviation of 1.65%, yielding a weekly Sharpe ratio of 0.09. The distribution is highly non-normal, exhibiting pronounced negative skewness of −1.60 and excess kurtosis of 12.55, consistent with the well-documented crash risk of the carry trade (Brunnermeier et al., 2008). Restricting portfolio formation to FOMC announcement days, $\text{HML}^{\texttt{fomc}}$ lowers the mean return to 13.28 bps and reduces volatility to 1.36%, leaving the Sharpe ratio equal to 0.10. The risk-adjusted alpha of $\text{HML}^{\texttt{fomc}}$ with respect to $\text{HML}^{\texttt{eom}}$ is 10.82 bps but is statistically indistinguishable from zero, indicating that announcement-window carry returns do not generate significant excess performance beyond the conventional carry trade, $\text{HML}^{\texttt{eom}}$. The surprise-conditioned strategy, $\text{HML}^{\texttt{surprises}}$, exhibits markedly different return properties. It delivers the highest average excess return among the three strategies, 21.68 bps per week, while at the same time displaying the lowest volatility, 1.10%. As a result, its Sharpe ratio is 0.20. The higher-order moments also differ substantially. The skewness of $\text{HML}^{\texttt{surprises}}$ remains moderately negative (-0.63), but it is considerably less pronounced than for the benchmark strategy (-1.60). At the same time, excess kurtosis declines markedly from 12.55 for $\text{HML}^{\texttt{eom}}$ to 5.36 for the surprise-conditioned strategy.

In Panels B and C, we report the results from the regressions specified in Eq. (3.6) for Jensen's alpha. When we regress $\text{HML}^{\texttt{surprises}}$ on $\text{HML}^{\texttt{eom}}$, the intercept is 19.18 bps per week and is highly statistically significant. This positive and significant Jensen's alpha indicates that the surprise-conditioned strategy delivers abnormal returns that are not spanned by the conventional carry factor. Similarly, we find that the intercept of the same strategy relative to $\text{HML}^{\texttt{fomc}}$ is 16.18 bps per week and statistically significant as well. These results indicate that conditioning on the composition of FOMC announcement surprises substantially reduces the asymmetry and tail risk that are characteristic of conventional carry trade returns. Furthermore, strategies incorporating information from FOMC announcements outperform conventional carry trade strategies.

These results are robust to using strategies based on the individual surprises, which we report in Table C5. We further show that the results are robust to using the identified monetary policy and central bank information shocks, either individually or jointly, in Table C6. This suggests that the strategy is also profitable when either surprise is considered individually or when the portfolio allocation is based on the monetary policy shock or both identified shocks jointly. Lastly, we show robustness to excluding the GFC and the COVID period, as shown in Tables C7 and C8.

4. Time series evidence on expected currency excess returns

The previous section established that the response of *realized* currency excess returns to FOMC announcement signals differs systematically with the average interest rate differential across currencies. We now turn to a multivariate time-series framework to examine whether these signals also shape *expected* currency risk premia. The VAR allows us to decompose ex ante currency excess returns into their two fundamental components—the interest rate differential and expected exchange-rate movements—while controlling for broader macro-financial conditions, including the demand for safe dollar assets and speculative carry trade activity. This framework, therefore, links the realized cross-sectional evidence to the evolution of expected currency risk premia over time. Finally, we extend the analysis to the term structure of expected excess returns and investigate whether these transmission channels depend on the intensity of speculative carry trade activity.

4.1 Effects of monetary policy and central bank information shocks

Econometric framework. We use exogenous high-frequency instruments to identify both monetary policy and central bank information shocks. Let $\{\boldsymbol{Y}_t\}_{t=1}^{T}$ denote an $n \times 1$ vector collecting high-frequency instruments and endogenous macroeconomic and financial variables for a currency pair at a monthly frequency. The vector $\boldsymbol{Y}_t = (\boldsymbol{m}_t', \boldsymbol{y}_t')'$ consists of an $n_y \times 1$ vector $\boldsymbol{y}_t$ of endogenous macroeconomic and financial variables and an $n_m \times 1$ vector $\boldsymbol{m}_t$ of high-frequency instruments aggregated to a monthly frequency (Jarociński and Karadi, 2020). The macro-financial variable set includes $n_y = 5$ variables, $\boldsymbol{y}_t = (i_t^{\$,3m}, i_t^{*,3m}, x_t^{Treas}, s_t, noi_t)'$, which denote the 3-month U.S. and foreign interest rates, the Treasury basis, the exchange rate, and the net open interest. We use $n_m = 2$ proxies, $\boldsymbol{m}_t = (m_t^{\text{fff}}, m_t^{\text{SP500}})'$, denoting high-frequency movements in policy-relevant interest rate derivatives and in the S&P 500 stock market index, respectively. Then, the vector autoregressive (VAR) equation reads as

$$\underbrace{\begin{pmatrix} \boldsymbol{m}_t \\ \boldsymbol{y}_t \end{pmatrix}}_{=\boldsymbol{Y}_t} = \underbrace{\begin{pmatrix} \boldsymbol{0} \\ \boldsymbol{c}^y \end{pmatrix}}_{=\boldsymbol{c}} + \sum_{j=1}^{p} \underbrace{\begin{pmatrix} \boldsymbol{0} & \boldsymbol{0} \\ \boldsymbol{A}_j^{my} & \boldsymbol{A}_j^{yy} \end{pmatrix}}_{=\boldsymbol{A}_j} \underbrace{\begin{pmatrix} \boldsymbol{m}_{t-j} \\ \boldsymbol{y}_{t-j} \end{pmatrix}}_{=\boldsymbol{Y}_{t-j}} + \underbrace{\begin{pmatrix} \boldsymbol{\varepsilon}_t^m \\ \boldsymbol{\varepsilon}_t^y \end{pmatrix}}_{=\boldsymbol{\varepsilon}_t}, \qquad \boldsymbol{\varepsilon}_t \sim \mathcal{N}(\boldsymbol{0}, \boldsymbol{\Sigma}), \tag{4.1}$$

where $\boldsymbol{c}^y$ denotes the $n_y \times 1$ vector of constants, $\boldsymbol{A}_j^{yy}$ is the $n_y \times n_y$ matrix of coefficients for lag j, $\boldsymbol{A}_j^{my}$ denotes an $n_y \times n_m$ matrix of coefficients, and $\boldsymbol{\Sigma}$ is an $n \times n$ variance-covariance matrix. In the empirical application, we set $p = 2$ based on the BIC.

This reduced-form model is estimated for each currency pair separately using Bayesian methods. For the VAR coefficients, we use the horseshoe shrinkage prior introduced by Carvalho et al. (2010). It is a global-local Bayesian shrinkage prior and specifies a hierarchical prior distribution that allows the degree of shrinkage to vary stochastically across individual coefficients. This is in contrast to a deterministic shrinkage profile introduced via the well-known Minnesota prior (Doan et al., 1984). We follow the suggestion of Litterman (1986) and impose a unit-root prior on non-stationary variables to mitigate the small-sample bias. The advantage of the horseshoe prior is that we do not have to specify prior hyperparameters, and sampling can be done efficiently within a Gibbs sampler (Makalic and Schmidt, 2015). For the covariance matrix, we use an inverse-Wishart prior distribution (Karlsson, 2013). We approximate the full posterior distribution through Markov chain Monte Carlo integration. For more details on the prior specification, we refer to Appendix B. We sample 45,000 draws from the posterior distribution, discarding the first 10,000 and using a thinning factor of two on the remaining draws. This leaves us with 17,500 draws for the posterior analysis.

This specification assumes that the surprises in $\boldsymbol{m}_t$ have a zero mean and do not depend on any lags of endogenous variables. These assumptions are reasonable insofar as financial market surprises are not predictable. Identification of the causal effects is achieved through sign restrictions. Specifically, for the monetary policy shock, we require a negative comovement between high-frequency surprises in interest rate derivatives and stock market prices, whereas for the central bank information shock, we impose a positive comovement between these variables. In addition, we impose a positive sign on the U.S. interest rate so that all currency-specific models feature an increase in the U.S. interest rate on impact. The sign restrictions are implemented using the algorithm of Rubio-Ramírez et al. (2010).

For that, we assume a uniform prior on the space of rotations, conditionally on satisfying the imposed sign restrictions. The resulting framework is a set-identified, semi-structural, and linear model.

We estimate the model for each currency pair separately: AUD, CAD, CHF, EUR, GBP, JPY, and NZD. The sample ranges from January 1995 to December 2024.[6] We also report the results in an aggregate manner across all currencies. To achieve this, we construct the average impulse response function as follows. First, we average the coefficients before computing the objects of interest. To obtain the average coefficient vector, we compute $\overline{\boldsymbol{\theta}} = \sum_{i=1}^{N} w_i \boldsymbol{\theta}_i$ for $i = 1, \ldots, N$, where $\boldsymbol{\theta}_i$ denotes the vector of all coefficients of the model of the currency pair i, and $N = 7$ denotes the number of currencies. In the baseline, we focus on equally weighted coefficients, which implies that $w_i = 1/N$, but in a robustness check, we use trade weights. For each posterior draw, we compute the cross-sectional average of the currency-specific coefficients, yielding a posterior distribution for the group-mean object, which we use to compute objects of interest, such as impulse response functions. Nonlinear objects, such as impulse response functions, are subsequently evaluated at this group-mean parameter vector. This procedure yields the same regression coefficients as averaging currency-by-currency estimates, as proposed by Pesaran and Smith (1995).

Results. While the cross-sectional analysis has examined realized excess returns, the VAR allows us to decompose ex ante currency risk premia into their two fundamental components: the interest rate differential and expected exchange-rate movements. This decomposition is also central to understanding the profitability of currency carry trades. Carry traders borrow in low-interest-rate currencies and invest in high-interest-rate currencies, such that expected excess returns are determined jointly by the interest rate differential earned on the position and the expected exchange-rate revaluation. Monetary policy can therefore affect carry trade profitability through two distinct channels: by changing the interest rate differential between the investment and funding currencies or by altering expectations about future exchange-rate movements. The VAR framework allows us to quantify the relative importance of these two channels over time and across maturities. Therefore, we compute the implied interest rate differential as the difference between the foreign and U.S. interest rates, $ird_t^m = i_t^{*,m} - i_t^{\$,m}$, and the annualized ex ante excess returns $rx_{t+m} = ird_t^m - \frac{12}{m}\mathbb{E}_t[\Delta s_{t+m}]$ based on VAR expectations of the exchange rate.[7]

Figure 3 summarizes the average transmission of monetary policy and central bank information shocks across currencies. The impulse responses reveal how monetary policy and central bank information shocks affect the two components of currency excess returns and thus the evolution of currency risk premia. We show the impulse responses to a contractionary monetary policy (upper panel) and a central bank information (lower panel) shock using the equally weighted group-mean estimator of the single-currency VAR models. Both shocks are normalized such that the U.S. short-term interest rate increases by 25 bps. We emphasize that our analysis focuses on a contractionary monetary policy

[6] We have two exceptions: AUD starts only at September 1996 due to the unavailability of 12-month government bond yields for constructing the Treasury basis, and NZD starts only in December 2005 due to the unavailability of the net open interest before that. When moving to the term structure models, the samples are considerably shorter for the 1-month and 6-month holding horizons for specific currencies. An exact overview is provided in Table A2 in Appendix A.

[7] Since the interest rate with maturity m is expressed in annualized terms, we use the expected spot-rate revaluation over the same horizon and annualize it accordingly.

Figure 3: Impulse responses of the baseline model.

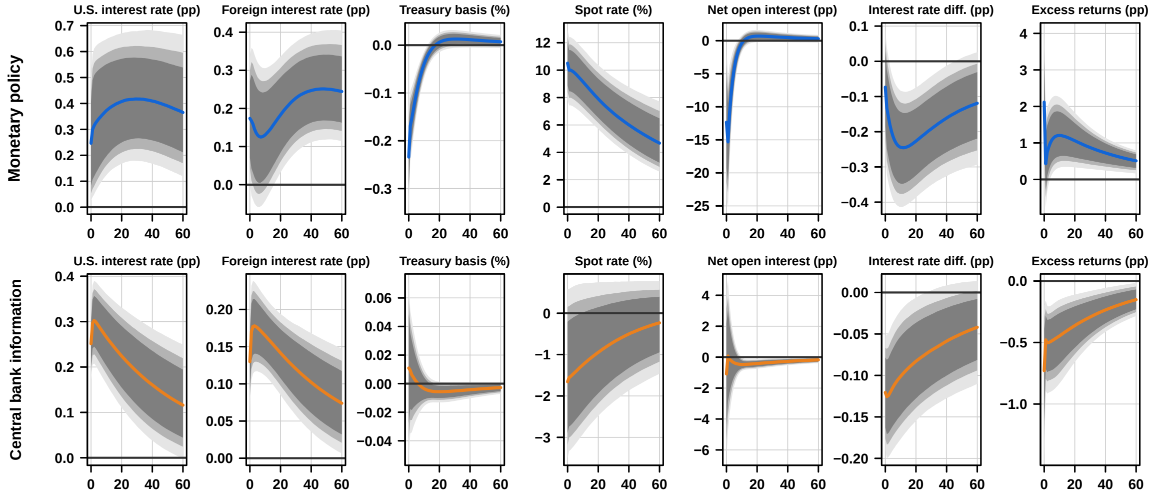

Notes: The figure shows the impulse responses to the U.S. monetary policy shock (upper panel, blue color) and to the central bank information shock (lower panel, orange color). Estimation is based on the group-mean estimator of the linear VAR model. Definitions of the constructed responses for the interest rate differential, $ird_t^m = i_t^{*,m} - i_t^{\$,m}$, and the currency excess returns, $rx_{t+m} = ird_t^m - \frac{12}{m}\mathbb{E}_t[\Delta s_{t+m}]$. Solid lines represent posterior median estimates and shaded areas indicate the 68%, 80%, and 90% credible sets. The horizontal axes measure time in months. The vertical axes measure deviations from the pre-shock level in percent (%) or percentage points (pp).

shock, which raises U.S. interest rates relative to foreign rates and—conditional on the U.S. dollar being used as the funding currency—reduces the attractiveness of borrowing in U.S. dollars to invest abroad. By symmetry, an expansionary monetary policy shock would increase the attractiveness of this carry trade. The solid line shows the median estimates, while the shaded areas indicate the 68%, 80%, and 90% credible sets. The horizontal axes measure the impulse response horizon in months. The vertical axes measure deviations from the pre-shock level, either in percentage points (interest rates, net open interest, interest rate differential, excess returns) or in percent (Treasury basis, spot rate).

We first consider the monetary policy shock. It elicits an increase in both the U.S. interest rate and the foreign interest rate. The foreign interest rate reacts more sluggishly and overall less strongly than the U.S. interest rate, which leads to a decline in the implied interest rate differential. The increase in the U.S. interest rate leads to a strong appreciation of the U.S. dollar vis-à-vis the foreign currency before the U.S. dollar starts returning to the pre-shock level. The dollar appreciates strongly before starting to depreciate, reaching an overall appreciation of 4% in the long run.[8] This is in line with the overshooting hypothesis of Dornbusch (1976), although we do not find evidence of delayed overshooting behavior.[9] The model-implied depreciation following the initial appreciation of the U.S. dollar is sizable, affecting currency risk premia. The Treasury basis strongly declines on impact before

[8] The effects on the spot rate are rather large and are driven by the choice of our variables. We use end-of-month spot rates instead of averages within the month. We use end-of-month values to avoid contamination of the shock, but those exhibit much higher variability. When using averages, the quantitative effects are smaller (around 3-4% appreciation for the monetary policy shock), but qualitatively the same. We show this in a robustness check in Figure D7 in Appendix D.

[9] The pattern of delayed overshooting refers to the empirical tendency for the domestic currency to appreciate over a protracted period before it starts to depreciate (Eichenbaum and Evans, 1995; Scholl and Uhlig, 2008). As pointed out by

turning positive after about one year. This finding squares with Jiang et al. (2021), as we find evidence for an increase in the convenience yield, meaning that investors demand more safe U.S. dollar assets, which supports the sharp appreciation of the U.S. dollar. Furthermore, the reaction of the net open interest provides additional evidence on the behavior of speculative carry-trade positions. A decline in noi_t following a contractionary monetary policy shock suggests that investors reduce leveraged dollar carry exposures, consistent with a partial unwinding of speculative positions and an increase in risk aversion (Brunnermeier et al., 2008). The strong appreciation of the dollar generates ex ante excess returns, indicating strong deviations from UIP and sizable currency risk premia. In Figure D1 in Appendix D, we examine possible transmission mechanisms. We find that the monetary policy shock induces a strong rise in measures of uncertainty and risk aversion, while the global financial cycle contracts. Effectively, the contractionary monetary policy shock induces a "risk-off" episode. This is in line with Forbes and Warnock (2012), who show that these risk measures are strongly associated with capital flows and that increases in global risk lead to retrenchment and sudden stops in capital flows.

Turning to the central bank information shock, it elicits a jump in both U.S. and foreign interest rates. The foreign interest rate shows a hump-shaped response but generally reacts less strongly than the U.S. rate, which again leads to a decline in the implied interest rate differential. However, neither the Treasury basis nor the net open interest reacts significantly to this shock. In line with the findings of Pinchetti and Szczepaniak (2023), the information shock leads to a dollar depreciation instead of an appreciation. The depreciation and subsequent appreciation are strong enough to generate a fall in the ex ante foreign-currency excess returns, indicating deviations from UIP. When examining the possible transmission mechanisms in Figure D1, we find a clear increase in economic activity and a decrease in uncertainty across different measures. This lends support to a "risk-on" interpretation and corroborates the interpretation that this shock mainly contains signals about economic growth (Cieslak and Schrimpf, 2019).

In the next step, we exploit the cross-sectional dimension of our results. In Figure 4, we show the responses of the spot rate, the interest rate differential, and currency excess returns for selected horizons ($h \in \{0, 12, 24, 60\}$) for each individual currency. We relate the size of the effect to the average policy interest rate differential, which allows us to compare the estimated effects on the model-implied currency risk premia to the realized excess returns in Figure 2. A contractionary monetary policy shock induces stronger appreciations for high-interest-rate currencies, which are followed by larger depreciations due to overshooting. Hence, we observe a positive relationship in the cross-section for the spot rate reaction, which flattens out over the horizon. This contrasts with earlier findings using realized revaluations of the currency. This indicates a mismatch between realized spot reactions and expectations. As the monetary policy shock induces a "risk-off" episode, the demand for the U.S. dollar increases, as indicated by an increase in the convenience yield. Investors expect a stronger appreciation of the U.S. dollar on impact, followed by a larger subsequent depreciation. This translates into higher currency risk premia for high-interest-rate currencies, as indicated by the positive cross-sectional relationship. The reaction of the interest rate differentials in the VAR system to the average

Kim et al. (2017), delayed overshooting is primarily a phenomenon of the 1980s. This is in line with our evidence, given that the sample period of each currency model starts only in the post-Volcker period.

Figure 4: Cross-sectional results in the baseline model.

(a) Spot rates.

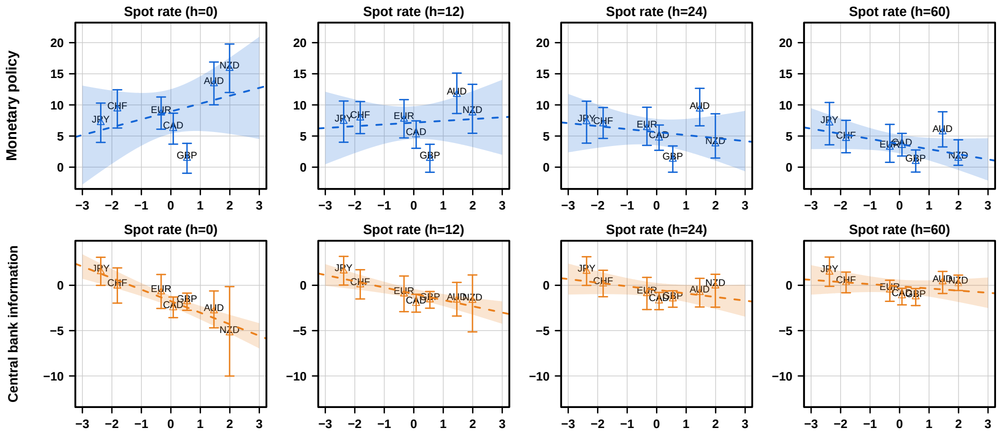

(b) Interest rate differentials.

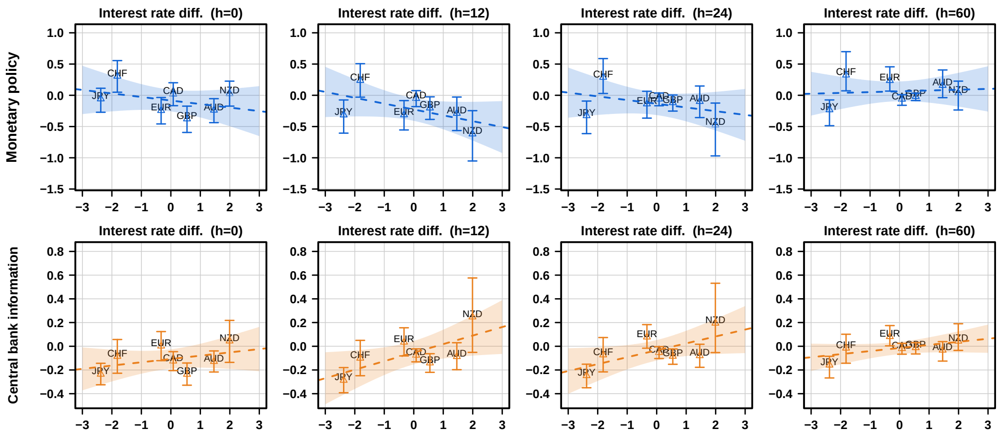

(c) Currency excess returns.

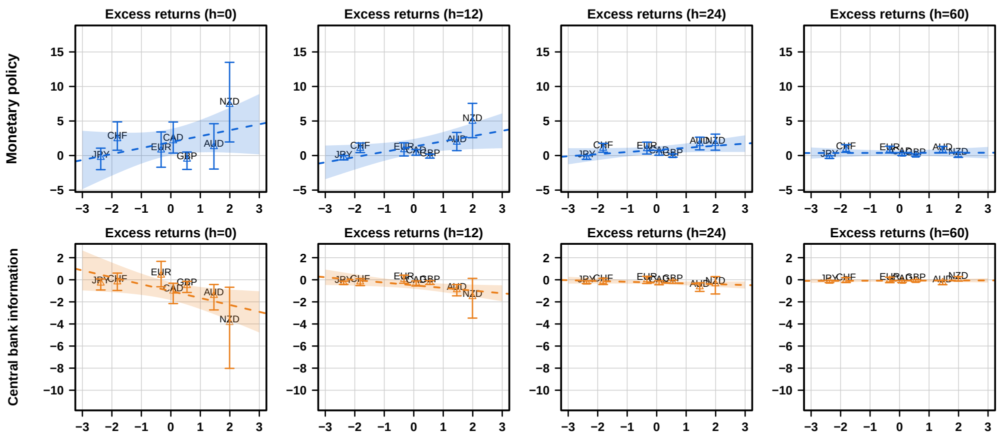

Notes: This figure shows the relationship between the average policy interest rate differential ($\overline{pird} = \overline{i}_t^* - \overline{ir}^{\$}$) and the cross-sectional reaction of the spot rates (panel a), interest rate differentials (panel b), and currency excess returns (panel c) for selected horizons ($h \in \{0, 12, 24, 60\}$) to the monetary policy shock (upper panel, blue) and central bank information shock (lower panel, orange) for each currency. Definitions of the constructed responses for the interest rate differential, $ird_t^m = i_t^{*,m} - i_t^{\$,m}$, and the currency excess returns, $rx_{t+m} = ird_t^m - \frac{12}{m}\mathbb{E}_t[\Delta s_{t+m}]$. The vertical bars denote 68% credible sets around the estimated reaction. The dashed line in each panel represents the fitted cross-sectional regression, and the shaded area its 90% confidence band.

Figure 5: Term structure effects.

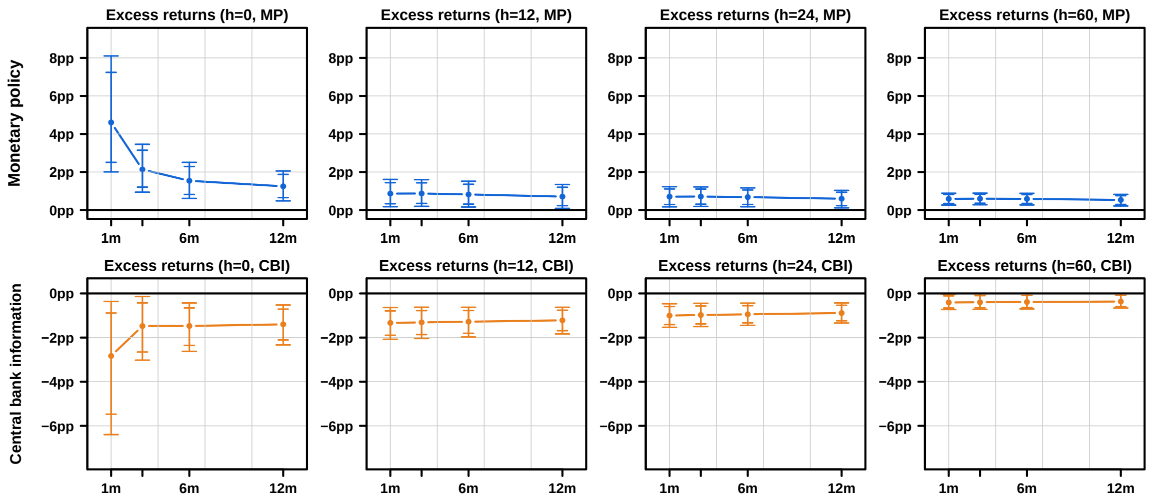

Notes: This figure shows the effects on the term structure for the U.S. monetary policy shock (upper panel, blue color) and for the central bank information shock (lower panel, orange color). Estimation is based on the group-mean estimator of the linear VAR model. Definitions of the constructed responses for the currency excess returns, $rx_{t+m} = (i_t^{*,m} - i_t^{\$,m}) - \frac{12}{m}\mathbb{E}_t[\Delta s_{t+m}]$. Points represent posterior median estimates and the whiskers indicate the 68% and 80% credible sets. The horizontal axes measure maturity in months. The vertical axes measure deviations from the pre-shock level in percentage points (pp).

policy interest rate differential is slightly negative, ruling it out as a possible explanation for the apparent mismatch. These effects are most pronounced on impact and are clearly visible after one year ($h = 12$), but they tend to flatten out from two years onward. The effects on the currency risk premia lack strong statistical support.

A contractionary central bank information shock constitutes a signal from the FOMC that is associated with positive news about economic growth or a decrease in the risk premium (Cieslak and Schrimpf, 2019). In line with earlier findings, the shock causes a depreciation of the U.S. dollar, which is stronger for high-interest-rate currencies. For those currencies, the model-implied appreciation is also stronger. The effects are fairly persistent but flatten out after two years. Again, the relationship between the dynamic response of the interest rate differential and the long-run interest rate differential lacks strong statistical support; if anything, the effects show a slight positive relationship. In terms of ex ante currency excess returns, we find evidence that there is a strong negative relationship for the impact effects; however, it flattens out relatively quickly afterward. The "risk-on" nature of the shock depresses currency risk premia for U.S. investors and favors long positions in the foreign currency.

Finally, we use the model to investigate the effects along the term structure. In the baseline model, we use both the U.S. and foreign interest rates with a 3-month maturity. We extend the model by including interest rates (U.S. and foreign) with 1-, 6-, and 12-month maturities. Hence, the number of endogenous variables increases to $n_y = 11$.[10]

[10] In the appendix, we show robustness with two alternative specifications. In the first specification, we replace the 3-month U.S. and foreign interest rates with each alternative maturity one at a time to keep the number of endogenous variables at $n_y = 5$. In the second specification, we add either the 1-, 6-, or 12-month maturity to the 3-month rates, increasing the

From the perspective of a carry trader, the term structure of currency excess returns describes how the expected profitability of borrowing in low-yield currencies and investing in high-yield currencies evolves over different holding horizons. We report the results in Figure 5, where we show the dynamic effects on the term structure at horizons $h \in \{0, 12, 24, 60\}$. We find that the term structure of ex ante excess returns is strongly downward-sloping for both shocks. The strongest excess returns arise when using interest rates with a 1-month maturity, while the lowest occur for higher maturities. In terms of dynamics, the effects dissipate relatively quickly. Beyond the one-year horizon, the excess returns are relatively small and start to become insignificant across both shocks.

Robustness. In Appendix D, we report several robustness checks to our analysis. We show that using different weights or varying the number of lags does not affect the results. We also show that our results are not affected by the GFC and COVID episode.

4.2 Nonlinear analysis based on the intensity of speculative carry trade activity

Having established the cross-sectional evidence and the implications for trading, we now ask whether these transmission mechanisms depend on market conditions, particularly whether currency risk premia vary with the intensity of speculative activity. We use the carry trade intensity indicator to explore, in a nonlinear time-series model, whether there are within-currency differences. Our main hypothesis is that an increase in speculative carry trade activity may amplify the spot reactions, thereby affecting the risk premia.

Econometric framework. Let $\boldsymbol{Y}_t = (\boldsymbol{m}_t', \boldsymbol{y}_t')'$ denote the $n \times 1$ vector of high-frequency instruments and endogenous macroeconomic and financial variables for a currency pair at a monthly frequency, as introduced in the previous section. Then, we use a threshold vector autoregressive (TVAR) model, which is specified as follows

$$\boldsymbol{Y}_t = \begin{cases} \boldsymbol{c}_1 + \sum_{j=1}^{p} \boldsymbol{A}_{1j} \boldsymbol{Y}_{t-j} + \boldsymbol{\varepsilon}_t, & \boldsymbol{\varepsilon}_t \sim \mathcal{N}(\boldsymbol{0}, \boldsymbol{\Sigma}_1) \quad \text{if } -\infty < CTI_{t-1} \leq \gamma_1, \\ \boldsymbol{c}_2 + \sum_{j=1}^{p} \boldsymbol{A}_{2j} \boldsymbol{Y}_{t-j} + \boldsymbol{\varepsilon}_t, & \boldsymbol{\varepsilon}_t \sim \mathcal{N}(\boldsymbol{0}, \boldsymbol{\Sigma}_2) \quad \text{if } \gamma_1 < CTI_{t-1} \leq \gamma_2, \\ \boldsymbol{c}_3 + \sum_{j=1}^{p} \boldsymbol{A}_{3j} \boldsymbol{Y}_{t-j} + \boldsymbol{\varepsilon}_t, & \boldsymbol{\varepsilon}_t \sim \mathcal{N}(\boldsymbol{0}, \boldsymbol{\Sigma}_3) \quad \text{if } \gamma_2 < CTI_{t-1} < \infty, \end{cases} \tag{4.2}$$

where $\boldsymbol{c}_r$ is an $n \times 1$ regime-specific constant, $\boldsymbol{A}_{rj}$ is an $n \times n$ regime-specific coefficient matrix for lag $j = 1, \ldots, p$, and $\boldsymbol{\Sigma}_r$ is an $n \times n$ regime-specific variance-covariance matrix for regime $r = 1, 2, 3$. The threshold parameters, γ_1 and γ_2, differentiate the regimes through the threshold variable CTI_{t-1}, which is the first lag of the MA(5)-smoothed carry trade intensity indicator. The model is estimated for each currency separately using Bayesian methods developed in Chen and Lee (1995) and Boeck and Zörner (2024). As the model is linear conditional on the threshold parameters, we use the same prior distributions for the VAR coefficients and covariance matrix as in the linear model. For the threshold parameters, we use a truncated Normal prior distribution such that the ordering $\gamma_0 = -\infty < \gamma_1 < \gamma_2 < \gamma_3 = +\infty$ is enforced. For more details on the prior specification, we refer to Appendix B. We sample 45,000 draws from the posterior distribution, discarding the first 10,000 and using a thinning factor of two on the remaining draws. This leaves us with 17,500 draws for the posterior analysis.

number of endogenous variables only to $n_y = 7$. We report the results in Figure D4 in Appendix D. Our results are robust to these alternative specifications.

Table 5: Threshold parameters and regime-wise summary statistics for currency excess returns.

	AUD	CAD	CHF	EUR	GBP	JPY	NZD	*Average*
γ_1	0.138	−0.657	15.32	−4.267	−6.094	15.009	7.788	3.891
$Q(10)$	0.022	−0.761	14.891	−4.33	−6.128	14.862	6.792	
$Q(90)$	0.310	−0.636	15.352	−4.172	−6.063	17.743	9.981	
γ_2	2.015	−0.092	15.919	−3.932	−5.528	18.453	18.458	6.471
$Q(10)$	1.766	−0.199	15.648	−4.052	−5.80	18.451	18.057	
$Q(90)$	2.229	−0.002	16.231	−3.192	−5.359	18.478	18.953	
Regime 1								
Share	0.438	0.508	0.528	0.533	0.458	0.475	0.48	0.489
Mean	−2.873	0.237	−2.418	0.758	0.754	−2.473	1.19	−0.689
Standard deviation	23.118	15.621	19.925	19.088	18.293	21.94	26.64	20.661
Skewness	0.723	0.468	0.174	−0.243	−0.335	−0.268	0.539	0.151
Kurtosis	4.736	4.494	2.994	4.08	4.621	3.662	4.094	4.097
Regime 3								
Share	0.524	0.48	0.453	0.458	0.525	0.483	0.439	0.480
Mean	4.176	−0.146	1.295	−2.074	−1.087	−6.057	3.423	−0.067
Standard deviation	25.317	15.71	17.264	19.278	15.962	21.728	24.187	19.921
Skewness	−1.475	−0.532	0.063	−0.124	−0.821	0.814	−1.277	−0.479
Kurtosis	8.395	6.048	2.872	2.911	6.733	4.845	5.7	5.358

Notes: The table shows the posterior 10th, 50th (median), and 90th quantiles of the threshold parameters, γ_1 and γ_2, and regime-wise summary statistics of the currencies across the regimes. We omit the outcomes of the second regime to enhance readability. The table reports the mean, standard deviation, skewness, and kurtosis for monthly observations of annualized three-month log excess returns, $rx_{t+3} = ird_t^{3m} - (12/3)\Delta s_{t+3}$, which is the difference between the interest rate differential, ird_t^{3m}, and the annualized revaluation of the foreign currency, $(12/3)\Delta s_{i\,t+3}$. The mean and standard deviation are in percentage points.

Results. First, we present in Table 5 the results of the nonlinear threshold analysis by investigating the estimated threshold parameters, which define the regimes. Usually, U.S. investors in the dollar carry strategy are long in foreign currencies and short in the dollar for high-interest-rate currencies, and a large positive value of the net open interest indicates high speculative activity. The opposite holds for low-interest-rate currencies. By taking the sign of the policy interest rate differential into account, speculative carry trade activity is elevated in the third regime. In our estimation, the regime allocation confirms that AUD, CHF, JPY, and NZD are mainly used in the speculative carry trade, as indicated by positive threshold estimates. The remaining currencies (CAD, EUR, GBP) show negative thresholds, pointing to less speculative activity. Furthermore, we examine the summary statistics of realized currency excess returns in the different regimes. For the four currencies mainly used in speculative activity, realized excess returns exhibit a much higher mean in the high-carry-trade-intensity regime (with the exception of JPY). For the remaining currencies, that is not the case. The standard deviations are almost equal across regimes. When looking at the skewness of realized excess returns, we find that the sign switches in most cases, indicating asymmetry. Lastly, the kurtosis is much higher in the high-carry-trade-intensity regime. The evidence on skewness and kurtosis holds particularly for the high-interest-rate currencies in our sample, consisting of AUD and NZD. To summarize, we observe elevated crash risk, as indicated by large negative tail events occurring in the high-carry-trade-intensity regime for typical investment currencies (and, on average).

We also observe that most of the time, the analyzed currencies are allocated either to the first or third regime. The regime shares in Table 5 provide evidence of their involvement in speculative carry trade activity. In Figure D8 in Appendix D, we examine the regime allocation over time. The shares across regimes 1 and 3 are almost equally distributed and range between 42% and 52%. None of the models frequently enter the second regime. Transitions to the third regime tend to coincide with episodes of U.S. dollar depreciation, and currencies typically spend no more than a few months in the second regime. Conversely, the transition from the third back to the first regime shows U.S. dollar appreciation almost immediately. The currencies are thus allocated to different regimes over time and show distinct behavior in the respective regimes. We conclude that speculative investors quickly adjust their positions to changes in the respective exchange rates. This is also confirmed by the regime allocation shown together with the carry trade intensity indicator and the estimated thresholds in Figure D9. Here, we additionally see that all currency pairs experience periods of positive and negative values of the carry-trade-intensity indicator. However, given that we only analyze currencies against the U.S. dollar, we do not take other prominent currency pairs for carry trading into account.

In Figure 6, we report the impulse response functions to a monetary policy shock (panel a) and a central bank information shock (panel b) for the lower (upper row in each panel) and higher (lower row in each panel) carry trade intensity regimes. This allows us to test whether excess returns vary with the intensity of speculative carry trade activity. We conclude that there are no strong differences in excess returns across regimes. Generally, the direction of the variables' reactions is qualitatively similar to that in the linear model, but they differ in their quantitative relevance. However, we find that different mechanisms account for this. For the monetary policy shock, we find that the Treasury basis declines strongly, with a more pronounced response than in the linear model, pointing to the convenience yield as a potential mechanism for the strong spot reaction and ex ante excess returns. The net open interest does not react strongly to the shock in the lower regime. In the upper regime, we find the opposite: the Treasury basis declines only for some periods and is not statistically significant, while the net open interest reacts decisively and points to a change in speculative activity in this regime. For the central bank information shock, the picture does not indicate a transmission via the convenience yield in either regime. The Treasury basis does not react significantly in either regime. Rather, the reaction of the net open interest in the high-carry-trade-intensity regime points to greater speculative activity in this regime. While the reaction of the currency risk premia is similar across regimes, it is statistically significant and negative in the high regime.

In Figure D10 in Appendix D, we also report the outcomes of the nonlinear model, exploiting the full cross-sectional information (similar to Figure 4). We relate the sizes of the effects for the spot rate, the interest rate differential, and currency excess returns for selected horizons to the average policy interest rate differential. The effects and signs are similar to the linear benchmark, particularly for the higher regime of carry trade activity. For the monetary policy shock in the low-carry-trade-activity regime, we find no strong relationship between the average interest rate differential and the responses of the spot rate, interest rate differentials, and excess returns. We note, however, that these estimates are subject to large uncertainty. For the central bank information shock, the evidence across regimes is less clear. Lastly, we also extend the term structure results to the nonlinear model and report the

Figure 6: Impulse responses of the nonlinear baseline model.

(a) Monetary policy shock.

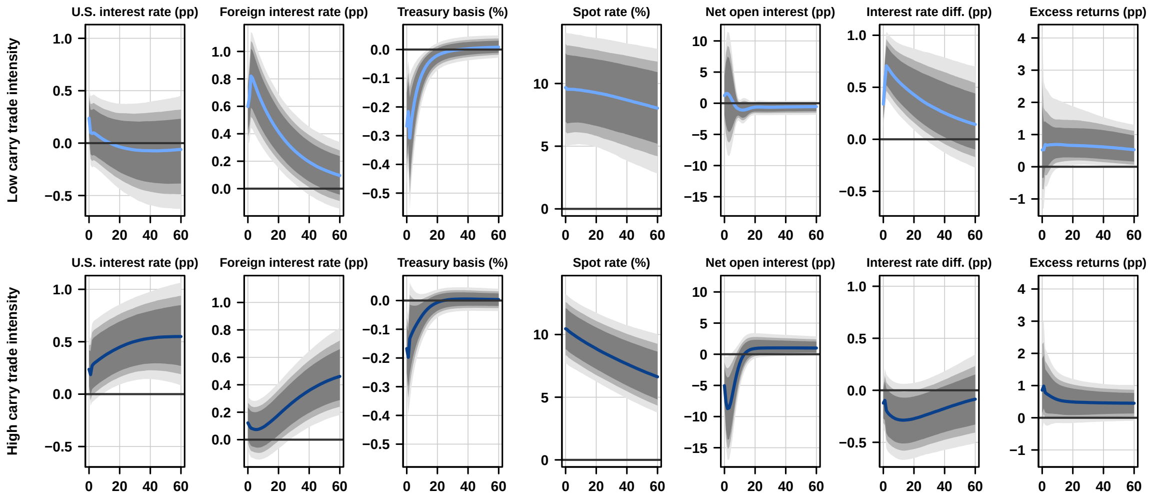

(b) Central bank information shock.

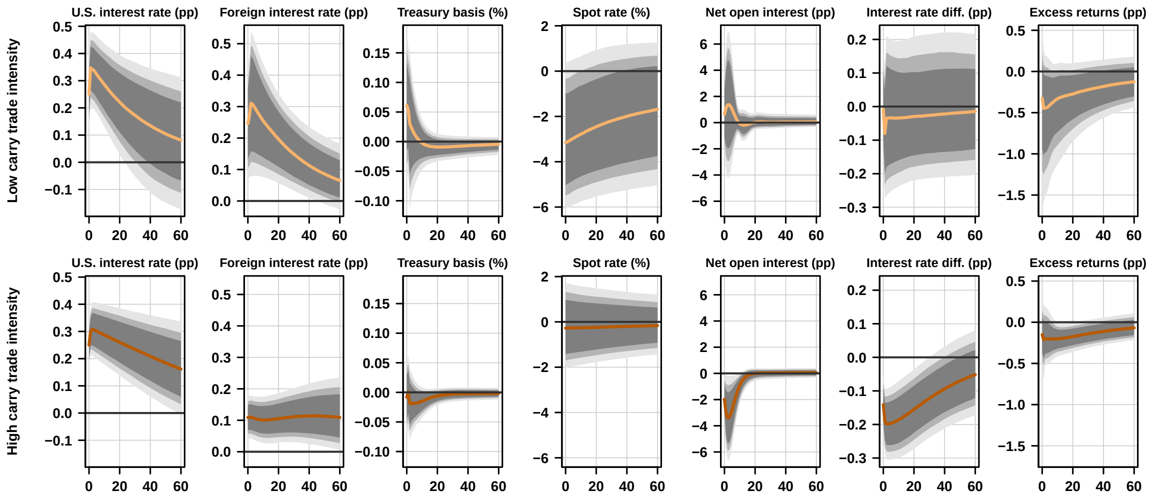

Notes: The figure shows the impulse responses to the U.S. monetary policy shock (panel a, blue colors) and to the central bank information shock (panel b, orange colors) for the high- and low-carry-trade-activity regimes. Estimation is based on the group-mean estimator of the nonlinear threshold VAR model. Definitions of the constructed responses for the interest rate differential, $ird_t^m = i_t^{*,m} - i_t^{\$,m}$, and the currency excess returns, $rx_{t+m} = ird_t^m - \frac{12}{m}\mathbb{E}_t[\Delta s_{t+m}]$. Solid lines represent posterior median estimates and shaded areas indicate the 68%, 80%, and 90% credible sets. The horizontal axes measure time in months. The vertical axes measure deviations from the pre-shock level in percent (%) or in percentage points (pp).

results in Figure D11. Similar to the linear results presented in Figure 5, we find a downward-sloping curve for the term structure, but there are no statistically significant differences across the regimes. This is further evidence supporting the conclusion that excess returns do not vary across different levels of speculative activity.

5. Conclusion

In this study, we examine how currency excess returns are affected by signals surrounding FOMC announcements. We analyze the impact of U.S. monetary policy shocks and central bank information shocks on currency excess returns and their components: the interest rate differential and the exchange-rate revaluation. The analysis uses the U.S. dollar as the base currency, acknowledging its global importance in the international financial landscape. To that end, we use the convenience yield framework to control for the additional demand for U.S. safe assets.

The empirical analysis yields three main conclusions. First, monetary policy and central bank information shocks have fundamentally different implications for currency risk premia because they operate through different transmission channels. While contractionary monetary policy shocks primarily affect currency excess returns through exchange-rate revaluations, the interest-rate-differential channel is comparatively more important for central bank information shocks. Second, these effects differ systematically across currencies, generating substantial cross-sectional heterogeneity that can be exploited to improve the performance of carry trade strategies. Finally, the time-series analysis shows that these effects extend to *expected* currency excess returns and generate a downward-sloping term structure of currency risk premia while providing little evidence that transmission systematically varies with within-currency speculative carry trade activity.

More broadly, our findings highlight that the information content of FOMC announcements is an important determinant of international currency markets. Treating monetary policy announcements as a single source of news masks economically meaningful differences between conventional monetary policy and central bank information shocks. Distinguishing between these signals provides a more complete understanding of the transmission of U.S. monetary policy to exchange rates, currency risk premia, and the profitability of carry trades. More generally, the results suggest that the nature of central bank communication plays an important role in shaping international asset prices and should therefore be incorporated into empirical analyses of currency markets and global monetary transmission.

References

Adrian T. and Shin H S. (2010) "Liquidity and leverage". *Journal of Financial Intermediation*, Vol. 19(3), pp. 418–437.

Alessandri P. and Mumtaz H. (2017) "Financial Conditions and Density Forecasts for US Output and Inflation". *Review of Economic Dynamics*, Vol. 24, pp. 66–78.

Antolin-Diaz J., Cenedese G., Han S., and Sarno L. (2023) *US Interest Rate Surprises and Currency Returns*. Available at SSRN: https://ssrn.com/abstract=4565111.

Bank for International Settlements . (2025) *Triennial Central Bank Survey of foreign exchange and Over-the-counter (OTC) derivatives markets in 2025*. Technical report, Available at https://www.bis.org/statistics/rpfx25.htm.

Bauer M. and Swanson E. (2023a) "An Alternative Explanation for the "Fed Information Effect"". *American Economic Review*, Vol. 113(3), pp. 664–700.

Bauer M D. and Swanson E T. (2023b) "A Reassessment of Monetary Policy Surprises and High-Frequency Identification". *NBER Macroeconomics Annual*, Vol. 37(1), pp. 87–155.

Baumeister C. and Hamilton J D. (2019) "Structural interpretation of vector autoregressions with incomplete identification: Revisiting the role of oil supply and demand shocks". *American Economic Review*, Vol. 109(5), pp. 1873–1910.

Bekaert G., Engstrom E C., and Xu N R. (2022) "The Time Variation in Risk Appetite and Uncertainty". *Management Science*, Vol. 68(6), pp. 3975–4004.

Boeck M. and Mori L. (2025) "Has Globalization Changed the International Transmission of U.S. Monetary Policy?" *Journal of International Economics*, Vol. 157, p. 104139.

Boeck M. and Zörner T O. (2024) "The Impact of Credit Market Sentiment Shocks". *Journal of Money, Credit and Banking*, Vol. 56 (7), pp. 1645–1673.

Brunnermeier M K., Nagel S., and Pedersen L H. (2008) "Carry Trades and Currency Crashes". *NBER Macroeconomics Annual*, Vol. 23(1), pp. 313–348.

Brusa F., Savor P., and Wilson M. (2020) "One Central Bank to Rule Them All". *Review of Finance*, Vol. 24(2), pp. 263–304.

Burnside C., Eichenbaum M., and Rebelo S. (2011) "Carry Trade and Momentum in Currency Markets". *Annual Review of Financial Economics*, Vol. 3(1), pp. 511–535.

Carvalho C M., Polson N G., and Scott J G. (2010) "The Horseshoe Estimator for Sparse Signals". *Biometrika*, Vol. 97(2), pp. 465–480.

Chan J C. (2022) "Asymmetric Conjugate Priors for Large Bayesian VARs". *Quantitative Economics*, Vol. 13(3), pp. 1145–1169.

Chen C W. and Lee J C. (1995) "Bayesian Inference of Threshold Autoregressive Models". *Journal of Time Series Analysis*, Vol. 16(5), pp. 483–492.

Cieslak A., Morse A., and Vissing-Jorgensen A. (2019) "Stock returns over the FOMC cycle". *The Journal of Finance*, Vol. 74(5), pp. 2201–2248.

Cieslak A. and Schrimpf A. (2019) "Non-Monetary News in Central Bank Communication". *Journal of International Economics*, Vol. 118, pp. 293–315.

Colacito R., Riddiough S J., and Sarno L. (2020) "Business cycles and currency returns". *Journal of Financial Economics*, Vol. 137(3), pp. 659–678.

Doan T., Litterman R., and Sims C. (1984) "Forecasting and conditional projection using realistic prior distributions". *Econometric Reviews*, Vol. 3(1), pp. 1–100.

Dornbusch R. (1976) "Expectations and Exchange Rate Dynamics". *Journal of Political Economy*, Vol. 84(6), pp. 1161–1176.

Eichenbaum M. and Evans C L. (1995) "Some Empirical Evidence on the Effects of Shocks to Monetary Policy on Exchange Rates". *The Quarterly Journal of Economics*, Vol. 110(4), pp. 975–1009.

Falconio A. (2023) "Carry Trades and US Monetary Policy". *Review of International Economics*, Vol. 31(1), pp. 237–248.

Fama E F. (1984) "Forward and Spot Exchange Rates". *Journal of Monetary Economics*, Vol. 14(3), pp. 319–338.

Follett L. and Yu C. (2019) "Achieving Parsimony in Bayesian Vector Autoregressions with the Horseshoe Prior". *Econometrics and Statistics*, Vol. 11, pp. 130–144.

Fong W M. (2013) "Footprints in the Market: Hedge Funds and the Carry Trade". *Journal of International Money and Finance*, Vol. 33, pp. 41–59.

Forbes C S., Kalb G R J., and Kofman P. (1999) "Bayesian Arbitrage Threshold Analysis". *Journal of Business & Economic Statistics*, Vol. 17(3), pp. 364–372.

Forbes K J. and Warnock F E. (2012) "Capital flow waves: Surges, stops, flight, and retrenchment". *Journal of International Economics*, Vol. 88(2), pp. 235–251.

Franz T. (2020) "Central Bank Information Shocks and Exchange Rates". *Deutsche Bundesbank Discussion Paper*, Vol. 13/2020.

Gürkaynak R S., Kara A H., Kısacıkoğlu B., and Lee S S. (2021) "Monetary policy surprises and exchange rate behavior". *Journal of International Economics*, Vol. 130, p. 103443.

Haario H., Saksman E., Tamminen J., et al. (2001) "An Adaptive Metropolis Algorithm". *Bernoulli*, Vol. 7(2), pp. 223–242.

Jarociński M. and Karadi P. (2020) "Deconstructing Monetary Policy Surprises – The Role of Information Shocks". *American Economic Journal: Macroeconomics*, Vol. 12(2), pp. 1–43.

Jensen M C. (1968) "The Performance of Mutual Funds in the Period 1945–1964". *Journal of Finance*, Vol. 23(2), pp. 389–416.

Jiang Z., Lustig H., and Krishnamurthy A. (2021) "Foreign safe asset demand and the dollar exchange rate". *The Journal of Finance*, Vol. 76(3), pp. 1049–1089.

Kadiyala K R. and Karlsson S. (1997) "Numerical Methods for Estimation and Inference in Bayesian VAR-Models". *Journal of Applied Econometrics*, Vol. 12(2), pp. 99–132.

Karlsson S. (2013) "Forecasting with Bayesian vector autoregression". *Handbook of Economic Forecasting*, Vol. 2, pp. 791–897.

Kim S.-H., Moon S., and Velasco C. (2017) "Delayed Overshooting: Is It an '80s Puzzle?" *Journal of Political Economy*, Vol. 125(5), pp. 1570–1598.

Kim S. and Roubini N. (2000) "Exchange Rate Anomalies in the Industrial Countries: A Solution with a Structural VAR Approach". *Journal of Monetary Economics*, Vol. 45(3), pp. 561–586.

Krishnamurthy A. and Vissing-Jorgensen A. (2012) "The aggregate demand for treasury debt". *Journal of Political Economy*, Vol. 120(2), pp. 233–267.

Litterman R B. (1986) "Forecasting with Bayesian vector autoregressions—five years of experience". *Journal of Business & Economic Statistics*, Vol. 4(1), pp. 25–38.

Lucca D O. and Moench E. (2015) "The pre-FOMC announcement drift". *The Journal of Finance*, Vol. 70(1), pp. 329–371.

Lustig H., Roussanov N., and Verdelhan A. (2011) "Common Risk Factors in Currency Markets". *The Review of Financial Studies*, Vol. 24(11), pp. 3731–3777.

Lustig H., Roussanov N., and Verdelhan A. (2014) "Countercyclical Currency Risk Premia". *Journal of Financial Economics*, Vol. 111(3), pp. 527–553.

Lustig H. and Verdelhan A. (2007) "The cross section of foreign currency risk premia and consumption growth risk". *American Economic Review*, Vol. 97(1), pp. 89–117.

Makalic E. and Schmidt D F. (2015) "A Simple Sampler for the Horseshoe Estimator". *IEEE Signal Processing Letters*, Vol. 23(1), pp. 179–182.

Menkhoff L., Sarno L., Schmeling M., and Schrimpf A. (2012) "Carry Trades and Global Foreign Exchange Volatility". *The Journal of Finance*, Vol. 67(2), pp. 681–718.

Miranda-Agrippino S. and Rey H. (2020) "US Monetary Policy and the Global Financial Cycle". *The Review of Economic Studies*, Vol. 87(6), pp. 2754–2776.

Mueller P., Tahbaz-Salehi A., and Vedolin A. (2017) "Exchange Rates and Monetary Policy Uncertainty". *The Journal of Finance*, Vol. 72(3), pp. 1213–1252.

Newey W K. and West K D. (1987) "Hypothesis testing with efficient method of moments estimation". *International Economic Review*, Vol. 28(3), pp. 777–787.

Pan J. and Singleton K J. (2008) "Default and recovery implicit in the term structure of sovereign CDS spreads". *The Journal of Finance*, Vol. 63(5), pp. 2345–2384.

Pesaran M H. and Smith R. (1995) "Estimating Long-Run Relationships from Dynamic Heterogeneous Panels". *Journal of Econometrics*, Vol. 68(1), pp. 79–113.

Pinchetti M. and Szczepaniak A. (2023) "Global Spillovers of the Fed Information Effect". *IMF Economic Review*, Vol. 72, pp. 773–819.

Rubio-Ramírez J F., Waggoner D F., and Zha T. (2010) "Structural Vector Autoregressions: Theory of Identification and Algorithms for Inference". *The Review of Economic Studies*, Vol. 77(2), pp. 665–696.

Scholl A. and Uhlig H. (2008) "New Evidence on the Puzzles: Results from Agnostic Identification on Monetary Policy and Exchange Rates". *Journal of International Economics*, Vol. 76(1), pp. 1–13.

Stavrakeva V. and Tang J. (2015) *Exchange rates and monetary policy*. FRB of Boston Working Paper No. 15-16.

Verdelhan A. (2010) "A habit-based explanation of the exchange rate risk premium". *The Journal of Finance*, Vol. 65(1), pp. 123–146.

Zviadadze I. (2017) "Term Structure of Consumption Risk Premia in the Cross Section of Currency Returns". *The Journal of Finance*, Vol. 72(4), pp. 1529–1566.

Online Appendix: Signals from the FOMC: The profitability of currency carry trades

A. Data

The results of this paper are obtained using data from various sources. Table A1 provides details on the data sources, transformations, and final construction. The paper utilizes data from different sources: BIS, Datastream (WM/Reuters Barclays Bank International), Bloomberg, the Federal Reserve Bank of Dallas, the Federal Reserve Economic Data (FRED) database, and individual websites listed below. The macro time series (VIX, global financial cycle, risk aversion, and uncertainty) are seasonally adjusted, either by downloading the already adjusted series from the respective database or by applying a monthly X11 filter.

In Table A2, we provide an overview of the samples used. We provide the sample lengths for the realized currency excess returns rx_{t+m} for $m \in \{1m, 3m, 6m, 12m\}$ and the VAR sample.

Table A1: Data description.

Label	Abbr.	Description	Frequency	Transf.	Source
Policy rate	pir_t	Central bank policy rate	monthly	level	BIS
Spot rate	s_t	Spot exchange rates per unit of U.S. dollar	monthly (eom)	level	Datastream (WM/Reuters and Barclays Bank International)
Net open interest	noi_t	(Long-short)/Total	monthly (eom)	level	U.S. Commodity Futures Trading Commission (CFTC)
Interest rate U.S.	$i_t^{\$,m}$	U.S. 1-week/m-month Treasury bill/government bond yield	monthly (eom)	level	Datastream (WM/Reuters and Barclays Bank International)
Interest rate foreign	$i_t^{*,m}$	Foreign 1-week/m-month Treasury rate/government bond yield	monthly (eom)	level	Datastream (WM/Reuters and Barclays Bank International)
Forward rate	f_t^m	1-week/m-month forward rate	monthly	log	Datastream (WM/Reuters and Barclays Bank International)
Treasury basis	x_t^{Treas}	according to Eq. (2.6) Jiang et al. (2021)	monthly	level	constructed
GIP	gip_t	Industrial Production, World (excl. U.S.)	monthly	log-diff	Database of Global Economic Indicators by the Dallas Fed
WIP	wip_t	World Industrial Production Index	monthly	log-diff	Christiane Baumeister's website
VIX	vix_t	Chicago Board Options Exchange Volatility Index	monthly	log	FRED
Global financial cycle	gfc_t	Global Financial Cycle factor by Miranda-Agrippino and Rey (2020)	monthly	level	Miranda-Agrippino's website
Risk Aversion	ra_t	Risk Aversion Index by Bekaert et al. (2022)	monthly	log	Nancy Xu's website
Uncertainty	unc_t	Uncertainty Index (annual volatility percentage) by Bekaert et al. (2022)	monthly	log	Nancy Xu's website

Notes: Data on the policy rates, spot rates, net open interest, foreign interest rates, the Treasury basis, and forward rates are per currency. (eom) denotes end-of-month. Abbr. denotes abbreviation. Transf. denotes transformation.

Table A2: Sample Overview

Currency	**Symbol**	rx_{t+1m}	rx_{t+3m}	rx_{t+6m}	rx_{t+12m}	**VAR Sample**
Australian dollar	AUD	2001/07-2024/11	1995/01-2024/09	1995/01-2024/06	1996/09-2023/12	1996/09-2024/12
Canadian dollar	CAD	2001/07-2024/11	1995/01-2024/09	1995/01-2024/06	1995/01-2023/12	1995/01-2024/12
Swiss franc	CHF	2006/07-2024/11	1995/01-2024/09	2006/07-2024/06	1995/01-2023/12	1995/01-2024/12
Euro	EUR	2001/07-2024/11	1995/01-2024/09	1997/08-2024/06	1995/01-2023/12	1995/01-2024/12
British pound	GBP	2008/01-2024/11	1995/01-2024/09	2008/01-2024/06	1995/01-2023/12	1995/01-2024/12
Japanese yen	JPY	2001/07-2024/11	1995/01-2024/09	1996/10-2024/06	1995/01-2023/12	1995/01-2024/12
New Zealand dollar	NZD	2008/01-2024/11	1995/01-2024/09	2008/01-2024/06	1995/01-2023/12	2005/12-2024/12

Notes: This table gives an overview of sample construction. Excess returns are constructed via: $rx_{t+m} = (i_t^{*,m} - i_t^{\$,m}) - (12/m)\Delta s_{t+m}$. The baseline VAR sample consists of $\{i_t^{\$,3m}, i_t^{*,3m}, x_t^{Treas}, s_t, noi_t\}$.

B. Estimation Details

The nonlinear version of the model allows for three regimes, which are distinguished by the lagged carry trade intensity indicator, CTI_{t-1}, which serves as the threshold variable. The threshold model with three regimes indicated by $r \in \{1,2,3\}$ for a specific currency i reads as follows

$$\boldsymbol{Y}_t = \begin{cases} \boldsymbol{c}_1 + \sum_{j=1}^{p} \boldsymbol{A}_{1j} \boldsymbol{Y}_{t-j} + \boldsymbol{\varepsilon}_t, & \boldsymbol{\varepsilon}_t \sim \mathcal{N}(\boldsymbol{0}, \boldsymbol{\Sigma}_1) \qquad \text{if } -\infty < CTI_{t-1} \leq \gamma_1, \\ \boldsymbol{c}_2 + \sum_{j=1}^{p} \boldsymbol{A}_{2j} \boldsymbol{Y}_{t-j} + \boldsymbol{\varepsilon}_t, & \boldsymbol{\varepsilon}_t \sim \mathcal{N}(\boldsymbol{0}, \boldsymbol{\Sigma}_2) \qquad \text{if } \gamma_1 < CTI_{t-1} \leq \gamma_2, \\ \boldsymbol{c}_3 + \sum_{j=1}^{p} \boldsymbol{A}_{3j} \boldsymbol{Y}_{t-j} + \boldsymbol{\varepsilon}_t, & \boldsymbol{\varepsilon}_t \sim \mathcal{N}(\boldsymbol{0}, \boldsymbol{\Sigma}_3) \qquad \text{if } \gamma_2 < CTI_{t-1} < \infty, \end{cases} \tag{B.1}$$

where $\boldsymbol{c}_r$ is an $n \times 1$ regime-specific constant, $\boldsymbol{A}_{rj}$ is an $n \times n$ regime-specific coefficient matrix for lag $j = 1, \ldots, p$, and $\boldsymbol{\Sigma}_r$ is an $n \times n$ regime-specific variance-covariance matrix for regime $r = 1,2,3$. The threshold parameters, γ_1 and γ_2, differentiate the regimes through the threshold variable CTI_{t-1}, which is the first lag of the MA(5)-smoothed carry trade intensity indicator. The model is estimated for each currency separately using Bayesian methods. We define the prior distributions and the MCMC algorithm below. For the threshold parameters, we use a truncated Normal prior distribution such that the ordering $\gamma_0 = -\infty < \gamma_1 < \gamma_2 < \gamma_3 = +\infty$ is enforced.

As the model is linear conditional on the threshold parameters, we use the same prior distributions for the VAR coefficients and covariance matrix as in the linear model.

B.1 Prior Specification

In the linear VAR, we have to specify priors only on the VAR coefficients and the covariance matrix, while we need to specify an additional prior distribution for the threshold parameters in the TVAR. In the TVAR, we use the same priors for the VAR coefficients as in the linear model since we estimate a linear VAR conditional on the respective regime allocation. We resort to a relatively standard independent Normal-inverse-Wishart prior setup. We abstain from using the conjugate Normal-inverse-Wishart prior because we want to impose different priors on the own-lag and cross-variable coefficients in the (T)VAR. Thus, we use the Horseshoe (HS) shrinkage prior on the coefficients.[11]

The prior structure of the model can be summarized as follows. Let $\boldsymbol{\alpha}_r = \text{vec}(\boldsymbol{c}_r^{y}, \boldsymbol{A}_{r1}^{my}, \boldsymbol{A}_{r1}^{yy}, \ldots, \boldsymbol{A}_{rp}^{my}, \boldsymbol{A}_{rp}^{yy})$ denote the $k \times 1$ vector of coefficients with $k = n_y(np+1)$ for regime r. Then

$$\alpha_{rj} \,|\, \lambda_{rj}^2, \tau_r \sim \mathcal{N}(\underline{\alpha}_{rj}, \lambda_{rj}^2 \tau_r^2), \qquad \lambda_{rj} \sim C^+(0,1), \qquad \tau_r \sim C^+(0,1), \qquad j = (n_y+1), \ldots, k, \tag{B.2}$$

where $C^+(0,a)$ denotes the half-Cauchy distribution on the positive real numbers with scale parameter a. λ_{rj} denotes the *local* shrinkage parameter that is coefficient specific, and τ_r is a *global* shrinkage term that pulls all elements in $\boldsymbol{\alpha}_r$ toward zero. For the mean hyperparameter, we follow the suggestion by Litterman (1986) and set it to $\underline{\alpha}_{rj} = 0$ for stationary and $\underline{\alpha}_{rj} = 1$ for non-stationary variables. Note that we do not impose a shrinkage prior on the deterministic coefficients (α_{rj} for $j = 1, \ldots, n_y$). Rather, we impose an uninformative Gaussian distribution with zero mean and a large variance

[11] Although Chan (2022) introduces the asymmetric conjugate prior, we abstain from using this prior for three reasons. First, the HS shrinkage prior has proven to have excellent shrinkage properties and works well in VAR settings (Follett and Yu, 2019). Second, the HS prior offers the advantage of being free of user-chosen hyperparameters. Third, in the threshold version of the model, we lose conjugacy anyway.

($\alpha_{rj} \sim \mathcal{N}(0,10)$ for $j = 1,\dots,n_y$) on each element of these coefficients. The variance-covariance matrix $\boldsymbol{\Sigma}_r$ follows

$$\boldsymbol{\Sigma}_r \sim iW(\underline{\nu}, \underline{\boldsymbol{S}}), \qquad r = 1,2,3, \tag{B.3}$$

where $\nu = n+2$ and $\boldsymbol{S} = \text{diag}(s_1^2,\dots,s_n^2)$, where s_l^2 denotes the variance of the residuals of an AR(4) process of variable l ($l = 1,\dots,n$). This is relatively standard according to Kadiyala and Karlsson (1997) and concludes the prior setup for the VAR coefficients and covariance matrix in both models. The linear VAR follows the same prior specification, except that the regime-dependent subscript r is dropped.

In the next step, we specify the prior density on the threshold parameters $\boldsymbol{\gamma} = (\gamma_1, \gamma_2)$. While, in principle, it is sufficient to implement a rejection step in the Gibbs sampler to ensure that the inequality constraints $\gamma_0 < \gamma_1 < \gamma_2 < \gamma_3$ and the boundary conditions $\gamma_0 = -\infty$ and $\gamma_3 = +\infty$ are satisfied, we provide a truncated prior distribution that satisfies the constraints explicitly. Thus, we use the following joint prior distribution specification for the threshold parameters $\boldsymbol{\gamma}$:

$$\begin{aligned} p(\boldsymbol{\gamma}) &= \prod_{j=1}^{2} p(\gamma_j \mid \gamma_{-j}), \\ \gamma_j &\sim \mathcal{TN}\left(\underline{\gamma}_j, \underline{\psi}_j^2, \gamma_{j-1}, \gamma_{j+1}\right), \end{aligned} \tag{B.4}$$

which is a truncated Normal distribution for each threshold value γ_j ($j \in \{1,2\}$) with $\gamma_0 = -\infty$ and $\gamma_3 = +\infty$. Here, γ_{-j} denotes all elements in $\boldsymbol{\gamma}$ except γ_j. This setup roughly corresponds to Forbes et al. (1999), but with the following additional specification. The hyperparameters associated with the mean and the variance are chosen as follows. For the prior mean, we choose $\underline{\gamma}_j = 0$, and the prior variance, $\underline{\psi}_j^2$, is a scaling factor that is set to a rather large value (in our empirical application, we specify $\psi_j^2 = 10^2$ for $j = 1,2$). This allows the threshold parameters to explore the full parameter space, conditional on the constraints $\gamma_{j-1} < \gamma_j$ being satisfied.

B.2 Markov Chain Monte Carlo Sampler

We build a Markov Chain Monte Carlo (MCMC) algorithm to sample from the full posterior distribution. Since the conditional posterior distribution has no standard form, sampling the threshold parameters is a non-trivial task. We sample from the conditional posterior using a random-walk Metropolis-Hastings step (Chen and Lee, 1995; Alessandri and Mumtaz, 2017; Boeck and Zörner, 2024). Our implementation closely follows the sampler in Boeck and Zörner (2024). The MCMC algorithm samples iteratively from the full conditional posterior distributions. We repeat this procedure 45,000 times and discard the first 10,000 draws as burn-in.

We obtain the joint posterior density by multiplying the likelihood by the prior. First, we define $\boldsymbol{Y}$ and $\boldsymbol{S}$ as the full history of $\boldsymbol{Y}_t$ and S_t ($t = 1,\dots,T$). By using Bayes' theorem, we obtain

$$\begin{aligned} p(\boldsymbol{\theta}, \boldsymbol{\gamma} \mid \boldsymbol{Y}) &\propto p(\boldsymbol{Y} \mid \boldsymbol{\theta}, \boldsymbol{\gamma}) p(\boldsymbol{\theta}, \boldsymbol{\gamma}) \\ &\propto \prod_{r=1}^{R} p(\boldsymbol{Y} \mid \boldsymbol{\theta}_r) p(\boldsymbol{\theta}_r \mid \boldsymbol{S}) p(\boldsymbol{S} \mid \boldsymbol{\gamma}) p(\boldsymbol{\gamma}). \end{aligned} \tag{B.5}$$

As we rely on data augmentation, we iterate between the following two steps. First, we classify the observations into one of the regimes, and second, we draw the parameters of the model conditional on the classification. For the classification step, we sample the group indicator $\boldsymbol{S}$ according to

$$p(\boldsymbol{S} \mid \boldsymbol{Y}, \boldsymbol{\theta}, \gamma) \propto p(\boldsymbol{Y} \mid \boldsymbol{S}, \boldsymbol{\theta}, \boldsymbol{\gamma}) p(\boldsymbol{S} \mid \boldsymbol{\gamma}). \tag{B.6}$$

The regime-dependent parameters in $\boldsymbol{\theta}$ are assumed to be fixed, and the indicator depends on the threshold parameter γ. The posterior density of the threshold parameters is given by

$$p(\boldsymbol{\gamma} \mid \boldsymbol{Y}, \boldsymbol{\theta}) \propto p(\boldsymbol{Y} \mid \boldsymbol{\theta}, \boldsymbol{\gamma}) p(\boldsymbol{\gamma}). \tag{B.7}$$

Conditional on the regime indicator $\boldsymbol{S}$, sampling the regime-specific parameters $\boldsymbol{\theta}_r = (\boldsymbol{A}_r, \boldsymbol{\Sigma}_r)$ is particularly easy because we can rely on well-known conditional posterior densities of linear time-series models. Applying Bayes' theorem then yields

$$p(\boldsymbol{\theta}_r \mid \boldsymbol{Y}, \boldsymbol{S}) \propto p(\boldsymbol{Y} \mid \boldsymbol{S}, \boldsymbol{\theta}_r) p(\boldsymbol{\theta}_r \mid \boldsymbol{S}), \quad r = 1, \ldots, 3, \tag{B.8}$$

which gives the posterior distribution of the regime-specific parameters $\boldsymbol{\theta}_r$.

We employ a Gibbs sampler to draw iteratively from the joint posterior density. The resulting Markov chain is then used to inspect and analyze the posterior quantities. We next outline the individual Gibbs steps and how to draw from the conditional posterior distributions.

1. Conditional on the regime indicator $\boldsymbol{S}$, we start by sampling the regime-specific parameters. These consist of three groups of parameters: the VAR coefficients, the associated shrinkage parameters, and the variance-covariance matrix. First, we gather all right-hand-side variables in $\boldsymbol{X}_t = (1, \boldsymbol{m}'_{t-1}, \boldsymbol{y}'_{t-1}, \ldots, \boldsymbol{m}'_{t-p}, \boldsymbol{y}'_{t-p})'$ and stack them into matrix form $\boldsymbol{X} = (\boldsymbol{X}_1, \ldots, \boldsymbol{X}_T)'$. Similarly, we stack $\boldsymbol{m} = (\boldsymbol{m}_1, \ldots, \boldsymbol{m}_T)'$, $\boldsymbol{y} = (\boldsymbol{y}_1, \ldots, \boldsymbol{y}_T)'$, and $\boldsymbol{\varepsilon} = (\boldsymbol{\varepsilon}_1, \ldots, \boldsymbol{\varepsilon}_T)'$. Then, it is convenient to define $\tilde{\boldsymbol{X}}_r = \boldsymbol{D}_r \boldsymbol{X}$, $\tilde{\boldsymbol{y}}_r = \boldsymbol{D}_r \boldsymbol{y}$, $\tilde{\boldsymbol{m}}_r = \boldsymbol{D}_r \boldsymbol{m}$, and $\tilde{\boldsymbol{\varepsilon}}_r = \boldsymbol{D}_r \boldsymbol{\varepsilon}$, where $\boldsymbol{D}_r$ is a selection matrix of size $T_r \times T$ and T_r denotes the number of observations per regime r. Hence, $\tilde{\boldsymbol{X}}_r$, $\tilde{\boldsymbol{y}}_r$, and $\tilde{\boldsymbol{m}}_r$ denote all observations in the respective regime r. The VAR in matrix notation thus reads

$$\begin{pmatrix} \tilde{\boldsymbol{m}}_r & \tilde{\boldsymbol{y}}_r \end{pmatrix} = \tilde{\boldsymbol{X}}_r \begin{pmatrix} \boldsymbol{0} & \boldsymbol{A}_r \end{pmatrix} + \tilde{\boldsymbol{\varepsilon}}_r, \tag{B.9}$$

where $\boldsymbol{A}_r = \left(\boldsymbol{c}_r^y, \boldsymbol{A}_{r1}^{my}, \boldsymbol{A}_{r1}^{yy}, \ldots, \boldsymbol{A}_{rp}^{my}, \boldsymbol{A}_{rp}^{yy}\right)'$ gathers all coefficients, which have to be estimated in the VAR equation. As a last step, we denote with $\boldsymbol{\alpha}_r = \text{vec}(\boldsymbol{A}_r)$ the vectorized version of $\boldsymbol{A}_r$.

   (a) We sample the VAR coefficients following Jarociński and Karadi (2020). First, we construct a diagonal $(n_y(np+1)) \times (n_y(np+1))$ prior covariance matrix $\underline{\boldsymbol{V}_r}$, where we specify the elements in step (b). This yields the following conditional posterior distribution

$$\boldsymbol{\alpha}_r \mid \Sigma_r, \tilde{\boldsymbol{y}}_r, \tilde{\boldsymbol{m}}_r \sim \mathcal{N}\left(\overline{\boldsymbol{\alpha}}_r, \overline{\boldsymbol{V}}_r\right), \tag{B.10}$$

   with the posterior quantities defined as follows:

$$\overline{\boldsymbol{\alpha}_r} = \overline{\boldsymbol{V}_r}\left(\underline{\boldsymbol{V}_r^{-1}\boldsymbol{\alpha}}_r + \left(\left(\boldsymbol{\Sigma}_r^{YY.1}\right)^{-1} \otimes \tilde{\boldsymbol{X}}_r'\right)\left(\tilde{\boldsymbol{y}}_r + \tilde{\boldsymbol{m}}_r\left(\boldsymbol{\Sigma}_r^{MM}\right)^{-1}\boldsymbol{\Sigma}_r^{MY}\right)\right) \tag{B.11}$$

   and

$$\overline{\boldsymbol{V}_r} = \left(\underline{\boldsymbol{V}_r^{-1}} + \left(\boldsymbol{\Sigma}_r^{YY.1}\right)^{-1} \otimes \tilde{\boldsymbol{X}}_r'\tilde{\boldsymbol{X}}_r\right). \tag{B.12}$$

Here, we use the notation $\boldsymbol{\Sigma}_r = \begin{pmatrix} \boldsymbol{\Sigma}_r^{MM} & \boldsymbol{\Sigma}_r^{MY} \\ \boldsymbol{\Sigma}_r^{YM} & \boldsymbol{\Sigma}_r^{YY} \end{pmatrix}$ and $\boldsymbol{\Sigma}_r^{YY.1} = \boldsymbol{\Sigma}_r^{YY} - \boldsymbol{\Sigma}_r^{YM} \left(\boldsymbol{\Sigma}_r^{MM}\right)^{-1} \boldsymbol{\Sigma}_r^{MY}$.

(b) Now we proceed to sample the parameters of the Horseshoe (HS) prior to construct the $k \times k$ prior variance-covariance matrix $\boldsymbol{V}_r = \text{diag}\left(\lambda_{r1}^2 \tau_r^2, \ldots, \lambda_{rk}^2 \tau_r^2\right)$. Makalic and Schmidt (2015) provide a simple and efficient sampling scheme based on auxiliary variables that lead to conjugate conditional posterior distributions of all parameters. Hence, we rewrite the HS prior as follows. We assume that

$$\begin{aligned} \alpha_{rj} \mid \lambda_{rj}^2, \tau_r &\sim \mathcal{N}(\underline{\alpha_{rj}}, \lambda_{rj}^2 \tau_r^2), \\ \lambda_{rj} &\sim C^+(0,1), \\ \tau_r &\sim C^+(0,1), \end{aligned} \tag{B.13}$$

which can be rewritten by making use of the scale mixture representation of the half-Cauchy distribution. We introduce two auxiliary parameters, ν_{rj} $(j = 1, \ldots, k)$ and ξ_r, and write the HS prior with the following hierarchy

$$\begin{aligned} \alpha_{rj} \mid \lambda_{rj}^2, \tau_r &\sim \mathcal{N}(\underline{\alpha_{rj}}, \lambda_{rj}^2 \tau_r^2), \\ \lambda_{rj}^2 \mid \nu_{rj} &\sim \mathcal{IG}(1/2, 1/\nu_{rj}), \\ \tau_r^2 \mid \xi_r &\sim \mathcal{IG}(1/2, 1/\xi_r), \\ \nu_{r1}, \ldots, \nu_{rk}, \xi_r &\sim \mathcal{IG}(1/2, 1). \end{aligned} \tag{B.14}$$

The conditional posterior distributions for the local and global hypervariances are also inverse-Gamma distributed and look as follows

$$\lambda_{rj}^2 \mid \alpha_{rj}, \tau_r^2, \nu_{rj} \sim \mathcal{I}G\left(1, \frac{1}{\nu_{rj}} + \frac{\alpha_{rj}^2}{2\tau_r^2}\right), \qquad j = 1, \ldots, k \tag{B.15}$$

$$\tau_r^2 \mid \boldsymbol{\alpha}_r, \boldsymbol{\lambda}^2, \xi_r \sim \mathcal{I}G\left(\frac{k+1}{2}, \frac{1}{\xi_r} + \frac{1}{2} \sum_{j=1}^{k} \frac{\alpha_{rj}^2}{\lambda_{rj}^2}\right). \tag{B.16}$$

Finally, the conditional posterior distributions for the auxiliary variables are

$$\nu_{rj} \mid \lambda_{rj}^2 \sim \mathcal{IG}\left(1, 1 + \frac{1}{\lambda_{rj}^2}\right), \qquad j = 1, \ldots, k \tag{B.17}$$

$$\xi_r \mid \tau_r^2 \sim \mathcal{IG}\left(1, 1 + \frac{1}{\tau_r^2}\right). \tag{B.18}$$

(c) Draw $\boldsymbol{\Sigma}_r$ from its conditional distribution

$$\boldsymbol{\Sigma}_r \mid \boldsymbol{A}_r, \tilde{\boldsymbol{y}}_r, \tilde{\boldsymbol{m}}_r \sim iW\left(\overline{\nu}_r, \overline{S}_r\right), \tag{B.19}$$

where $\overline{\nu}_r = \nu + T_r$ and $\overline{\boldsymbol{S}}_r = \boldsymbol{S} + \left(\begin{pmatrix}\tilde{\boldsymbol{m}}_r & \tilde{\boldsymbol{y}}_r\end{pmatrix} - \tilde{\boldsymbol{X}}_r \begin{pmatrix}\boldsymbol{0} & \boldsymbol{A}_r\end{pmatrix}\right)' \left(\begin{pmatrix}\tilde{\boldsymbol{m}}_r & \tilde{\boldsymbol{y}}_r\end{pmatrix} - \tilde{\boldsymbol{X}}_r \begin{pmatrix}\boldsymbol{0} & \boldsymbol{A}_r\end{pmatrix}\right)$.

2. We proceed by sampling the threshold parameter vector $\boldsymbol{\gamma}$ according to an adaptive random-walk Metropolis-Hastings step. Here, we follow Chen and Lee (1995) and propose a normally distributed candidate that we draw from a Gaussian, i.e., $\boldsymbol{\gamma}^* \sim \mathcal{N}(\boldsymbol{\gamma}^{(n-1)}, C^{(n-1)})$. $C^{(n-1)}$ is a tuning parameter, and n indexes the MCMC draws. The probability of accepting a candidate

draw $\boldsymbol{\gamma}^*$ depends on the ratio of the posterior densities evaluated at the candidate and current draws. Specifically, we define the acceptance probability as

$$\alpha(\boldsymbol{\gamma}^*, \boldsymbol{\gamma}^{(n-1)}) = \min\left[1, \frac{p(\boldsymbol{\gamma}^* \mid \boldsymbol{Y}, \boldsymbol{\theta})\, q(\boldsymbol{\gamma}^{(n-1)} | \boldsymbol{\gamma}^*)}{p(\boldsymbol{\gamma}^{(n-1)} \mid \boldsymbol{Y}, \boldsymbol{\theta})\, q(\boldsymbol{\gamma}^* | \boldsymbol{\gamma}^{(n-1)})}\right], \tag{B.20}$$

We draw $u \sim U(0,1)$ and set $\boldsymbol{\gamma}^{(n)} = \boldsymbol{\gamma}^*$ if $u \leq \alpha(\boldsymbol{\gamma}^*, \boldsymbol{\gamma}^{(n-1)})$; otherwise, we retain the previous draw $\boldsymbol{\gamma}^{(n)} = \boldsymbol{\gamma}^{(n-1)}$. We follow Haario et al. (2001) to adapt our tuning parameter $C^{(n)}$ by

$$C^{(n)} = \begin{cases} C_0 & \text{if } n \leq N_c, \\ s_d \mathrm{Var}\left(\boldsymbol{\gamma}^{(1)}, \ldots, \boldsymbol{\gamma}^{(n-1)}\right) + s_d \eta & \text{if } n > N_c. \end{cases} \tag{B.21}$$

We assume a constant tuning parameter for the first $N_c = 50$ draws and subsequently use the empirical variance to tune the MH-step. We set η to a small positive constant and use s_d to fine-tune the algorithm to achieve acceptance probabilities between 20% and 40%. Note that this algorithm is indeed non-Markovian, but Haario et al. (2001) show that this tuning algorithm has correct ergodicity properties.

C. Additional results of the cross-sectional analysis

In this appendix, we present additional results from the cross-sectional analysis. We provide additional summary statistics based on the forward discounts. For the regression-based analysis and the trading exercise, we assess robustness by excluding the Global Financial Crisis and the COVID period. To define the respective crisis periods, we follow the NBER recession dates and define the GFC period as December 2007 to June 2009 and the COVID period as March 2020 to May 2020.

C.1 Additional results of the regression-based analysis

Table C1 repeats the descriptive analysis using forward discounts instead of interest rate differentials. The forward discounts broadly preserve the cross-sectional ranking implied by interest rate differentials, while the definition of the FX revaluation remains unchanged. Moreover, the dispersion and higher-moment properties of excess returns remain broadly comparable across the two measures and display the same decline in volatility at longer holding horizons. Although average excess returns differ for some currencies, the forward-discount measure provides a similar characterization of the cross-sectional heterogeneity underlying our analysis.

Figure C1 shows the regression results of Eq. (3.1) with the dependent variable being *changes* in currency excess returns. We note a weaker cross-sectional relationship for changes in realized excess returns than for levels. Still, the estimated relationship differs across monetary policy and central bank information shocks. We report in Table C2 the regression output of the cross-sectional relationships depicted in Figure 1, Figure 2, and Figure C1.

Figure C2 and Figure C3 demonstrate that the main cross-sectional patterns are robust to the exclusion of the GFC and COVID episodes, respectively. We define the GFC episode as occurring from December 2007 to June 2009, aligning with the NBER recession dates. The COVID episode ranges from March 2020 to May 2020. Omitting the GFC slightly increases the precision of the estimates across the regressions. For currency excess returns, the CBI shock becomes statistically significant for currencies with high average interest rate differentials. By contrast, excluding the COVID period leaves the results virtually unchanged relative to the full-sample estimates. Hence, the documented heterogeneity is not driven solely by either crisis episode, although the GFC appears to be particularly informative for the estimated relationships. In Table C4, we report the regression output of the cross-sectional relationships depicted in Figure 2, Figure C2, and Figure C3. This allows a direct comparison of whether the relationships change when excluding either the GFC or the COVID episode. The statistical relationships are robust to these alternative samples.

Table C1: Summary statistics of realized currency excess returns (forward discounts).

	JPY	CHF	EUR	CAD	GBP	AUD	NZD
Holding horizon: 1-month							
Mean	−3.015	−0.232	−0.035	0.348	−2.945	2.496	−0.557
Standard deviation	9.468	9.790	9.261	8.783	9.030	12.21	13.448
Skewness	−0.119	0.141	−0.194	−0.528	−0.359	−0.506	−0.216
Kurtosis	3.401	5.770	4.578	5.915	4.496	5.019	4.263
Forward discount	−2.038	−1.891	−0.747	0.074	−0.210	1.668	1.468
FX revaluation	0.977	−1.659	−0.712	−0.274	2.735	−0.828	2.025
Holding horizon: 3-month							
Mean	−4.348	−1.064	−1.487	−0.095	−0.394	0.872	1.617
Standard deviation	6.444	5.436	5.401	4.491	4.930	6.867	6.939
Skewness	0.329	0.099	−0.136	−0.050	−0.578	−0.595	−0.123
Kurtosis	3.931	2.978	3.472	5.338	5.770	6.601	4.091
Forward discount	−2.717	−2.136	−0.853	−0.068	0.366	1.361	1.944
FX revaluation	1.631	−1.072	0.634	0.028	0.761	0.489	0.327
Holding horizon: 6-month							
Mean	−3.440	0.127	−0.954	−0.050	−2.766	1.007	−0.049
Standard deviation	4.335	3.316	3.968	3.159	4.092	4.966	5.170
Skewness	0.037	0.270	−0.232	−0.145	−1.073	−0.335	−0.338
Kurtosis	2.913	3.656	2.811	4.865	5.355	5.485	6.168
Forward discount	−2.585	−1.788	−0.861	−0.043	−0.157	1.362	1.563
FX revaluation	0.854	−1.915	0.092	0.007	2.609	0.355	1.612
Holding horizon: 12-month							
Mean	−4.401	−1.093	−1.515	−0.017	−0.358	0.983	1.647
Standard deviation	3.113	2.601	2.788	2.193	2.484	3.667	3.736
Skewness	−0.122	0.154	0.146	−0.044	−0.684	0.164	−0.087
Kurtosis	2.251	3.710	2.673	3.668	3.920	3.017	3.098
Forward discount	−2.807	−2.137	−0.906	−0.032	0.363	1.331	1.876
FX revaluation	1.658	−0.982	0.636	0.013	0.735	0.601	0.297
Policy interest differential	−2.377	−1.815	−0.330	0.081	0.548	1.461	1.991
Net open interest	−13.117	−10.332	2.226	−0.264	−1.982	4.967	14.222
Treasury basis	−0.448	−0.428	−0.374	−0.197	−0.005	0.011	−0.032

Notes: This table reports summary statistics for realized currency excess returns $rx_{t+m} = (12/m)(fd_{t+m} - \Delta s_{t+m})$, including the mean, standard deviation, skewness, and kurtosis, and the mean for the annualized forward discount, $(12/m)fd_{t+m} = (12/m)(f_t^m - s_t)$ and for annualized foreign exchange (FX) revaluations, $(12/m)\Delta s_{t+m}$ across different holding horizons $m \in \{1,3,6,12\}$ and across all currencies in our sample (AUD, CAD, CHF, EUR, GBP, JPY, NZD). The last three rows of the table report the mean of the policy interest rate differential, the net open interest, and the Treasury basis across all currencies in our sample. Currencies are ordered in ascending order by their policy interest rate differential.

Figure C1: Cross-sectional variation of the reaction of the change in realized currency excess returns to the monetary policy and central bank information shocks.

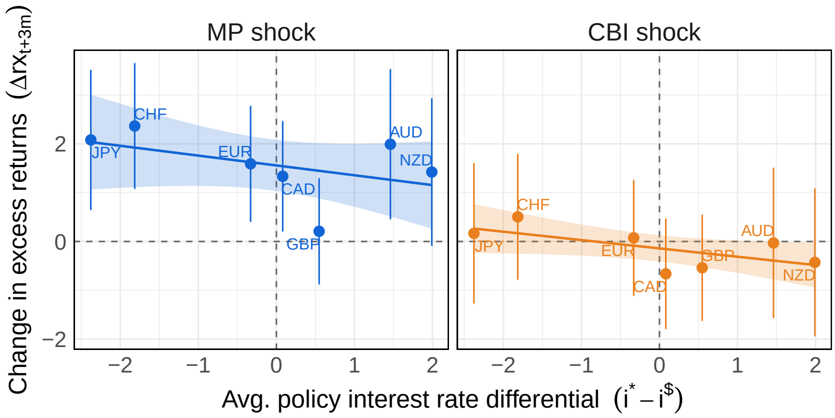

Notes: This figure shows the cross-sectional relationship between the average policy interest rate differential ($\overline{pird} = \bar{i}^* - \bar{i}^\$$) and the effect sizes of the change in realized currency excess returns associated with the monetary policy shock (left panel, blue color) and with the central bank information shock (right panel, orange color) for each currency. The shocks are standardized. The change in currency excess returns is defined as $\Delta rx_{t+3} = rx_t^{3m} - rx_{t-1}^{3m}$. The vertical bars denote 90% confidence intervals around the estimated coefficient. The solid line in each panel represents the fitted cross-sectional regression, and the shaded area its 90% confidence interval.

Table C2: Regression output of cross-sectional relationships depicted in figures.

	Figure 1		*Figure 2*				*Figure C1*
	$\overline{rx_{t+3m}}$	$\overline{NOI}$	$\beta_j^{s_t}$	$\beta_j^{\Delta s_{t+3}}$	$\beta_j^{ird_t^{3m}}$	$\beta_j^{rx_{t+3m}}$	$\beta_j^{\Delta rx_{t+3m}}$
$\overline{pird}$	1.022***	5.405***					
	(0.231)	(0.892)					
			Monetary policy shock ($j = MP$)				
$\overline{pird}$			−0.042	0.161***	0.014	−0.628***	−0.201
			(0.065)	(0.039)	(0.015)	(0.141)	(0.176)
			Central bank information shock ($j = CBI$)				
$\overline{pird}$			−0.129	0.033	−0.066*	−0.197	−0.171
			(0.441)	(0.029)	(0.027)	(0.133)	(0.090)

Notes: Cross-sectional regressions using variables (*Figure* 1) or estimated coefficients (Figures 2 and C1) as dependent variables and the average policy interest differential ($\overline{pird}$) as the independent variable. Number of observations is $N = 7$. *, **, and *** indicate statistical significance at the 10%, 5%, and 1% levels, respectively.

Table C3: Tests of equal responses to monetary policy and central bank information shocks.

Outcome	Currency	$\hat{\beta}_{MP}$	$\hat{\beta}_{CBI}$	$\hat{\beta}_{MP} - \hat{\beta}_{CBI}$	SE	p-value
Spot rate	AUD	0.673	−2.640	3.313***	(1.140)	0.004
	CAD	0.546	−1.500	2.045**	(0.898)	0.023
	CHF	0.743	−3.588	4.331***	(1.343)	0.001
	EUR	0.971	−1.011	1.982**	(0.845)	0.020
	GBP	0.217	0.981	−0.764	(0.896)	0.395
	JPY	0.836	−0.638	1.474	(1.000)	0.141
	NZD	0.781	−3.104	3.885***	(1.135)	0.001
Spot rate change	AUD	0.046	0.071	−0.026	(0.395)	0.948
	CAD	−0.001	−0.084	0.083	(0.260)	0.751
	CHF	−0.378	−0.036	−0.342	(0.311)	0.273
	EUR	−0.261	0.131	−0.392	(0.311)	0.208
	GBP	0.121	−0.167	0.288	(0.285)	0.313
	JPY	−0.691	−0.166	−0.525	(0.369)	0.155
	NZD	0.001	0.048	−0.047	(0.401)	0.907
Interest rate differential	AUD	−0.102	−0.212	0.109	(0.120)	0.364
	CAD	−0.015	−0.069	0.054	(0.055)	0.327
	CHF	−0.117	−0.126	0.009	(0.098)	0.928
	EUR	−0.118	−0.297	0.179**	(0.090)	0.047
	GBP	−0.012	−0.257	0.244***	(0.079)	0.002
	JPY	−0.167	0.092	−0.259*	(0.135)	0.057
	NZD	−0.114	−0.299	0.185*	(0.107)	0.084
Excess returns	AUD	−0.276	−0.494	0.218	(1.593)	0.891
	CAD	−0.001	0.269	−0.270	(1.043)	0.796
	CHF	1.412	0.024	1.388	(1.260)	0.271
	EUR	0.932	−0.820	1.752	(1.249)	0.162
	GBP	−0.495	0.411	−0.906	(1.139)	0.427
	JPY	2.609	0.760	1.849	(1.490)	0.215
	NZD	−0.102	−0.485	0.384	(1.608)	0.812
Change in excess returns	AUD	1.991	−0.030	2.022	(1.245)	0.105
	CAD	1.336	−0.663	1.998**	(0.915)	0.030
	CHF	2.365	0.505	1.860*	(1.042)	0.075
	EUR	1.591	0.074	1.517	(0.960)	0.115
	GBP	0.208	−0.539	0.747	(0.878)	0.396
	JPY	2.081	0.165	1.916	(1.162)	0.100
	NZD	1.422	−0.428	1.850	(1.224)	0.132

Notes: The table reports tests of the null hypothesis $H_0 : \beta_{MP} = \beta_{CBI}$ for the currency-specific regressions in Eq. (3.1). $\hat{\beta}_{MP}$ and $\hat{\beta}_{CBI}$ denote the estimated responses to the monetary policy and central bank information shocks, respectively. The fourth numerical column reports $\hat{\beta}_{MP} - \hat{\beta}_{CBI}$. The standard error accounts for the covariance between the two jointly estimated coefficients. The p-value refers to the two-sided Wald test of equality. *, **, and *** indicate statistical significance at the 10%, 5%, and 1% levels, respectively.

Figure C2: Cross-sectional variation of the reaction to monetary policy and central bank information shocks (excluding the GFC episode).

(a) Dependent variable: spot rates.

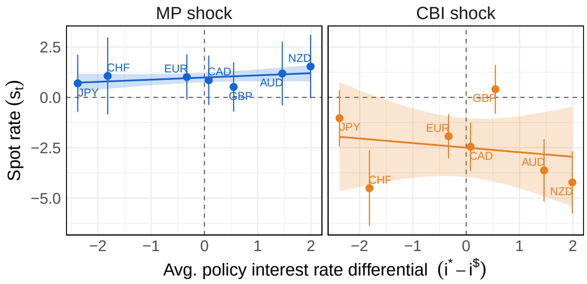

(b) Dependent variable: change in spot rates.

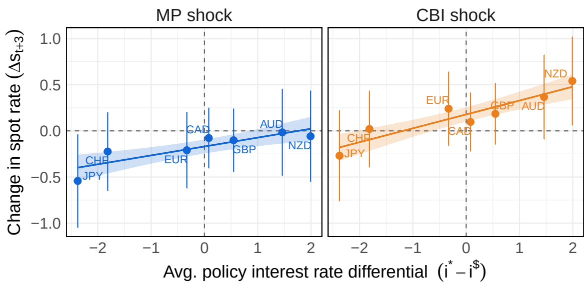

(c) Dependent variable: interest rate differentials.

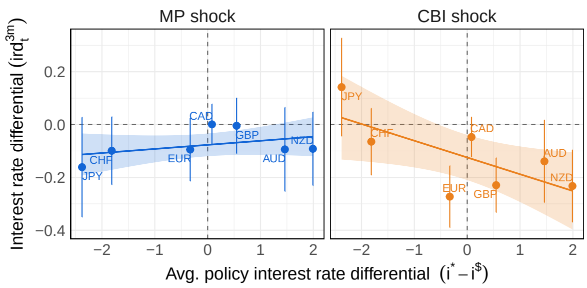

(d) Dependent variable: currency excess returns.

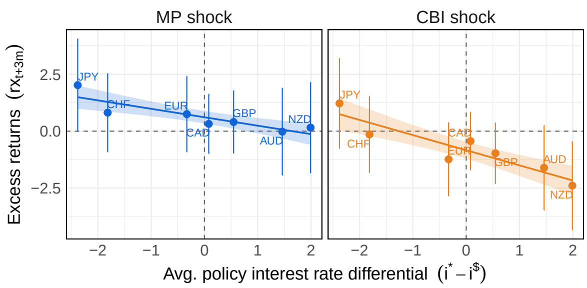

Notes: This figure shows the cross-sectional relationship between the average policy interest rate differential ($\overline{pird} = \bar{i}^* - \bar{i}^\$$) and the effect sizes of the spot rates (panel a), changes in spot rates (panel b), interest rate differentials (panel c), and currency excess returns (panel d) associated with the monetary policy shock (left panel, blue color) and with the central bank information shock (right panel, orange color) for each currency. We drop the observations in the Global Financial Crisis episode (2007M12-2009M6). The shocks are standardized. Definitions of the change in the spot rate, $\Delta s_{t+3} = s_{t+3} - s_t$, the interest rate differential, $ird_t^{3m} = i_t^{*,3m} - i_t^{\$,3m}$, and the currency excess returns, $rx_{t+3} = ird_t^{3m} - 4\Delta s_{t+3}$. The vertical bars denote 90% confidence intervals around the estimated coefficient. The solid line in each panel represents the fitted cross-sectional regression, and the shaded area its 90% confidence interval.

Figure C3: Cross-sectional variation of the reaction to monetary policy and central bank information shocks (excluding the COVID episode).

(a) Dependent variable: spot rates.

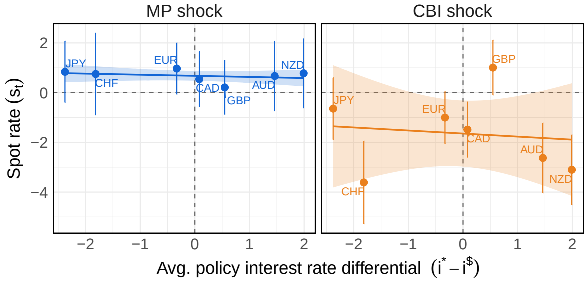

(b) Dependent variable: change in spot rates.

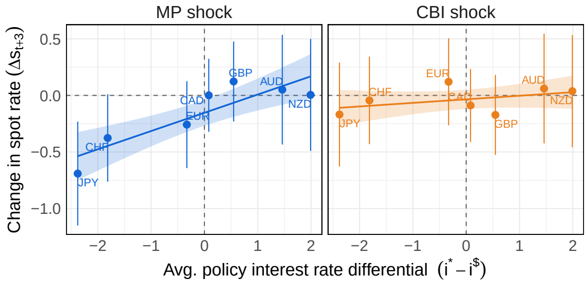

(c) Dependent variable: interest rate differentials.

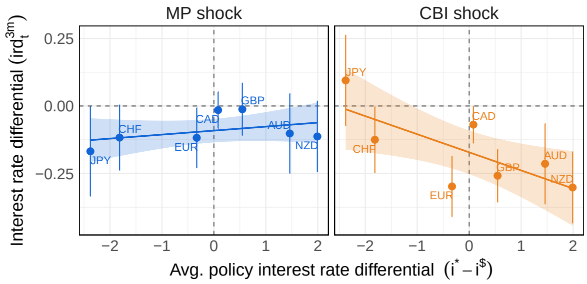

(d) Dependent variable: currency excess returns.

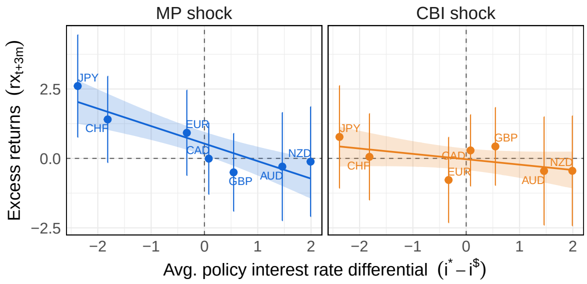

Notes: This figure shows the cross-sectional relationship between the average policy interest rate differential ($\overline{pird} = \bar{i}^* - \bar{i}^\$$) and the effect sizes of the spot rates (panel a), changes in spot rates (panel b), interest rate differentials (panel c), and currency excess returns (panel d) associated with the monetary policy shock (left panel, blue color) and with the central bank information shock (right panel, orange color) for each currency. We drop the observations in the COVID episode (2020M3-2020M5). The shocks are standardized. Definitions of the change in the spot rate, $\Delta s_{t+3} = s_{t+3} - s_t$, the interest rate differential, $ird_t^{3m} = i_t^{*,3m} - i_t^{\$,3m}$, and the currency excess returns, $rx_{t+3} = ird_t^{3m} - 4\Delta s_{t+3}$. The vertical bars denote 90% confidence intervals around the estimated coefficient. The solid line in each panel represents the fitted cross-sectional regression, and the shaded area its 90% confidence interval.

Table C4: Regression output of cross-sectional relationships depicted in figures (excluding the GFC and COVID episodes).

	Monetary policy shock ($j = MP$)				*Central bank information shock* ($j = CBI$)			
	$\beta_{MP}^{s_t}$	$\beta_{MP}^{\Delta s_{t+3}}$	$\beta_{MP}^{ird_t^{3m}}$	$\beta_{MP}^{rx_{t+3m}}$	$\beta_{CBI}^{s_t}$	$\beta_{CBI}^{\Delta s_{t+3}}$	$\beta_{CBI}^{ird_t^{3m}}$	$\beta_{CBI}^{rx_{t+3m}}$
Figure 2: Baseline								
$\overline{pird}$	−0.042	0.161***	0.014	−0.628***	−0.129	0.033	−0.066*	−0.197
	(0.065)	(0.039)	(0.015)	(0.141)	(0.441)	(0.029)	(0.027)	(0.133)
Figure C2: Exclusion of GFC episode								
$\overline{pird}$	0.107	0.096**	0.015	−0.371**	−0.227	0.150***	−0.063*	−0.665***
	(0.080)	(0.025)	(0.014)	(0.092)	(0.488)	(0.026)	(0.029)	(0.126)
Figure C3: Exclusion of COVID episode								
$\overline{pird}$	−0.044	0.161***	0.015	−0.631***	−0.123	0.032	−0.067*	−0.193
	(0.066)	(0.038)	(0.015)	(0.141)	(0.444)	(0.029)	(0.027)	(0.130)

Notes: Cross-sectional regressions using estimated coefficients (Figures 2, C2, and C3) as dependent variables and the average policy interest differential ($\overline{pird}$) as the independent variable. GFC episode: 2007M12-2009M6. COVID episode: 2020M3-2020M5. Number of observations is $N = 7$. *, **, and *** indicate statistical significance at the 10%, 5%, and 1% levels, respectively.

C.2 Additional results of the trading exercise

Tables C5 and C6 show that the main trading results are robust to alternative ways of conditioning on FOMC announcement information. Table C5 considers the interest rate derivative and stock market surprises separately and shows that both surprise-based strategies deliver higher Sharpe ratios and positive, statistically significant alphas relative to the conventional carry benchmark and the FOMC-day carry strategy. Table C6 yields similar results when portfolio allocation is conditioned on the identified shocks: the monetary-policy-based and joint shock-based strategies deliver positive and statistically significant alphas, whereas the central-bank-information-based strategy does not significantly outperform the benchmarks.

Table C7 shows that the main trading results remain robust after excluding the GFC episode. Although the average returns of the surprise-based strategies remain strong and are somewhat higher than in the full sample, these strategies continue to deliver higher Sharpe ratios than the conventional end-of-month and announcement-day carry portfolios. Moreover, their alphas relative to both benchmark strategies remain positive and statistically significant, somewhat larger than in the full sample. Hence, the superior performance of portfolios conditioned on FOMC announcement surprises is not driven by the GFC period.

Table C8 shows that the main trading results remain robust after excluding the COVID period. The surprise-based strategies continue to deliver higher Sharpe ratios than the conventional end-of-month and announcement-day carry portfolios. Moreover, their alphas relative to both benchmark strategies remain positive and statistically significant, with only a modest reduction in magnitude. Hence, the superior performance of portfolios conditioned on FOMC announcement surprises is not driven by the COVID episode.

Table C5: Currency portfolio returns (1-week holding period) with risk-adjusted alphas.

	$\text{HML}^{\texttt{eom}}$	$\text{HML}^{\texttt{fomc}}$	$\text{HML}^{\texttt{fff}}$	$\text{HML}^{\texttt{sp500}}$	$\text{HML}^{\texttt{surprises}}$
Panel A: Summary statistics					
Mean (bps)	14.430	13.277	24.077	20.339	21.681
SD (%)	1.653	1.356	1.203	1.105	1.096
Skewness	−1.601	−0.588	−0.247	−0.583	−0.626
Excess Kurtosis	12.554	5.759	6.383	5.197	5.361
Sharpe ratio	0.087	0.098	0.200	0.184	0.198
N	240	240	240	240	240
Panel B: Alpha relative to HML^{eom}					
$\alpha^{\text{HML}^{\text{eom}}}$ (bps)		10.823	22.626***	17.819**	19.182***
$\alpha^{\text{HML}^{\text{eom}}}$ SE		(8.274)	(7.105)	(6.990)	(6.975)
Panel C: Alpha relative to HML^{fomc}					
$\alpha^{\text{HML}^{\text{fomc}}}$ (bps)			17.592**	14.868**	16.179**
$\alpha^{\text{HML}^{\text{fomc}}}$ SE			(7.107)	(6.525)	(6.433)

Notes: This table reports the performance of five carry trade strategies constructed from one-week forward exchange rates for the period from January 1995 to December 2024. The currency universe comprises seven developed market currencies against the U.S. dollar. The sample is restricted to months containing scheduled FOMC announcements. $HML^{\texttt{eom}}$ sorts currencies by forward discounts at the end of the month. $\text{HML}^{\texttt{fomc}}$ applies sorting on the FOMC announcement day. $\text{HML}^{\texttt{fff}}$ and $\text{HML}^{\texttt{sp500}}$ condition portfolio allocation on the interest rate derivative and stock market high-frequency surprises. $\text{HML}^{\texttt{surprises}}$ conditions portfolio allocation on both surprises. Mean returns are weekly and expressed in basis points. Standard deviation is in percent. The Sharpe ratio is the mean excess return divided by its standard deviation. The risk-adjusted alpha is obtained from time-series regressions in Eq. (3.6) relative to $\text{HML}^{\texttt{eom}}$ and $\text{HML}^{\texttt{fomc}}$, with Newey-West standard errors (four lags) in parentheses. *, **, and *** indicate statistical significance at the 10%, 5%, and 1% levels, respectively.

Table C6: Currency portfolio returns (1-week holding period) with risk-adjusted alphas.

	$\text{HML}^{\texttt{eom}}$	$\text{HML}^{\texttt{fomc}}$	$\text{HML}^{\texttt{MP}}$	$\text{HML}^{\texttt{CBI}}$	$\text{HML}^{\texttt{shocks}}$
Panel A: Summary statistics					
Mean (bps)	14.430	13.277	24.018	10.996	19.371
SD (%)	1.653	1.356	1.123	1.085	1.043
Skewness	−1.601	−0.588	−0.895	−0.465	−0.800
Excess Kurtosis	12.554	5.759	6.487	4.931	5.605
Sharpe ratio	0.087	0.098	0.214	0.101	0.186
N	240	240	240	240	240
Panel B: Alpha relative to HML^{eom}					
$\alpha^{\text{HML}^{\text{eom}}}$ (bps)		10.823	21.786***	9.673	16.967**
$\alpha^{\text{HML}^{\text{eom}}}$ SE		(8.274)	(7.239)	(7.851)	(6.552)
Panel C: Alpha relative to HML^{fomc}					
$\alpha^{\text{HML}^{\text{fomc}}}$ (bps)			18.189***	5.944	14.082**
$\alpha^{\text{HML}^{\text{fomc}}}$ SE			(6.761)	(7.196)	(6.129)

Notes: This table reports the performance of five currency strategies constructed from one-week forward exchange rates for the period from January 1995 to December 2024. The currency universe comprises seven developed market currencies against the U.S. dollar. The sample is restricted to months containing scheduled FOMC announcements. $HML^{\texttt{eom}}$ sorts currencies by forward discounts at the end of the month. $\text{HML}^{\texttt{fomc}}$ applies sorting on the FOMC announcement day. $\text{HML}^{\texttt{MP}}$ and $\text{HML}^{\texttt{CBI}}$ condition portfolio allocation on the monetary policy and central bank information shocks. $\text{HML}^{\texttt{shocks}}$ conditions portfolio allocation on both shocks jointly. Mean returns are weekly and expressed in basis points. Standard deviation is in percent. The Sharpe ratio is the mean excess return divided by its standard deviation. The risk-adjusted alpha is obtained from time-series regressions in Eq. (3.6) relative to $\text{HML}^{\texttt{eom}}$ and $\text{HML}^{\texttt{fomc}}$, with Newey-West standard errors (four lags) in parentheses. *, **, and *** indicate statistical significance at the 10%, 5%, and 1% levels, respectively.

Table C7: Currency portfolio returns (1-week holding period) with risk-adjusted alphas (excluding the GFC).

	$\text{HML}^{\texttt{eom}}$	$\text{HML}^{\texttt{fomc}}$	$\text{HML}^{\texttt{fff}}$	$\text{HML}^{\texttt{sp500}}$	$\text{HML}^{\texttt{surprises}}$
Panel A: Summary statistics					
Mean (bps)	10.735	12.120	27.006	21.267	22.682
SD (%)	1.370	1.275	1.091	1.033	1.024
Skewness	−2.064	−0.820	−0.298	−0.651	−0.701
Excess Kurtosis	13.565	6.486	7.433	5.771	5.989
Sharpe ratio	0.078	0.095	0.247	0.206	0.222
N	227	227	227	227	227
Panel B: Alpha relative to HML^{eom}					
$\alpha^{\text{HML}^{\texttt{eom}}}$ (bps)		9.140	26.012**	19.983***	21.418***
$\alpha^{\text{HML}^{\texttt{eom}}}$ SE		(8.547)	(6.874)	(6.438)	(6.401)
Panel C: Alpha relative to HML^{fomc}					
$\alpha^{\text{HML}^{\texttt{fomc}}}$ (bps)			21.580***	16.103***	17.488***
$\alpha^{\text{HML}^{\texttt{fomc}}}$ SE			(6.656)	(5.968)	(5.852)

Notes: This table reports the performance of five carry trade strategies constructed from one-week forward exchange rates for the period from January 1995 to December 2024, excluding the Global Financial Crisis (GFC) period from December 2007 to June 2009. The currency universe comprises seven developed market currencies against the U.S. dollar. The sample is restricted to months containing scheduled FOMC announcements. $HML^{\texttt{eom}}$ sorts currencies by forward discounts at the end of the month. $\text{HML}^{\texttt{fomc}}$ applies sorting on the FOMC announcement day. $\text{HML}^{\texttt{fff}}$ and $\text{HML}^{\texttt{sp500}}$ condition portfolio allocation on the interest rate derivative and stock market high-frequency surprises. $\text{HML}^{\texttt{surprises}}$ conditions portfolio allocation on both surprises. Mean returns are weekly and expressed in basis points. Standard deviation is in percent. The Sharpe ratio is the mean excess return divided by its standard deviation. The risk-adjusted alpha is obtained from time-series regressions in Eq. (3.6) relative to $\text{HML}^{\texttt{eom}}$ and $\text{HML}^{\texttt{fomc}}$, with Newey-West standard errors (four lags) in parentheses. *, **, and *** indicate statistical significance at the 10%, 5%, and 1% levels, respectively.

Table C8: Currency portfolio returns (1-week holding period) with risk-adjusted alphas (excluding COVID).

	$\text{HML}^{\texttt{eom}}$	$\text{HML}^{\texttt{fomc}}$	$\text{HML}^{\texttt{fff}}$	$\text{HML}^{\texttt{sp500}}$	$\text{HML}^{\texttt{surprises}}$
Panel A: Summary statistics					
Mean (bps)	14.192	13.388	24.278	19.626	20.984
SD (%)	1.660	1.358	1.204	1.107	1.098
Skewness	−1.592	−0.590	−0.250	−0.569	−0.612
Excess Kurtosis	12.452	5.762	6.402	5.188	5.350
Sharpe ratio	0.085	0.099	0.202	0.177	0.191
N	238	238	238	238	238
Panel B: Alpha relative to HML^{eom}					
$\alpha^{\text{HML}^{\texttt{eom}}}$ (bps)		10.982	17.771**	14.074**	15.401**
$\alpha^{\text{HML}^{\texttt{eom}}}$ SE		(8.328)	(7.159)	(6.541)	(6.450)
Panel C: Alpha relative to HML^{fomc}					
$\alpha^{\text{HML}^{\texttt{fomc}}}$ (bps)			17.771**	14.074**	16.103**
$\alpha^{\text{HML}^{\texttt{fomc}}}$ SE			(7.159)	(6.541)	(6.450)

Notes: This table reports the performance of five carry trade strategies constructed from one-week forward exchange rates for the period from January 1995 to December 2024, excluding the COVID period from March 2020 to May 2020. The currency universe comprises seven developed market currencies against the U.S. dollar. The sample is restricted to months containing scheduled FOMC announcements. $HML^{\texttt{eom}}$ sorts currencies by forward discounts at the end of the month. $\text{HML}^{\texttt{fomc}}$ applies sorting on the FOMC announcement day. $\text{HML}^{\texttt{fff}}$ and $\text{HML}^{\texttt{sp500}}$ condition portfolio allocation on the interest rate derivative and stock market high-frequency surprises. $\text{HML}^{\texttt{surprises}}$ conditions portfolio allocation on both surprises. Mean returns are weekly and expressed in basis points. Standard deviation is in percent. The Sharpe ratio is the mean excess return divided by its standard deviation. The risk-adjusted alpha is obtained from time-series regressions in Eq. (3.6) relative to $\text{HML}^{\texttt{eom}}$ and $\text{HML}^{\texttt{fomc}}$, with Newey-West standard errors (four lags) in parentheses. *, **, and *** indicate statistical significance at the 10%, 5%, and 1% levels, respectively.

D. Additional results of the time-series analysis

In this appendix, we present additional results from the linear and nonlinear VAR analyses. For the linear VAR results, we additionally show the impulse responses of the individual country models, extend the model to inspect transmission mechanisms, and provide additional results regarding the term structure.

For the nonlinear VAR results, we show additional findings regarding the regime allocation, the relationship of the effects in both regimes to the cross-sectional distribution of the interest rate differential, and the regime-dependent results on the term structure.

D.1 Additional results of the linear VAR analysis

In Figure D1, we report the impulse responses of the extensions. In these extensions, we append one variable at a time to the baseline model, which allows us to examine the underlying transmission mechanisms. We extend the baseline model with measures for economic growth, such as the global industrial production index from the database of global economic indicators by the Federal Reserve Bank of Dallas and the world industrial production index of Baumeister and Hamilton (2019). To proxy for market participants' appetite for risk and intermediaries' risk-bearing capacity, we use the Chicago Board Options Exchange Volatility (VIX) index of implied volatility from S&P 500 options (Pan and Singleton, 2008; Adrian and Shin, 2010), the global financial cycle factor of Miranda-Agrippino and Rey (2020), and the risk aversion and uncertainty indicators provided by Bekaert et al. (2022).

A conventional contractionary monetary policy shock leads to a deterioration in the outlook for economic activity; investors engage in a flight to quality and shift toward safer assets during times of high uncertainty. This is supported by the strong increases in the risk aversion and uncertainty indices, while the global financial cycle contracts. The increase in the VIX is associated with a "risk-off" episode and, following Forbes and Warnock (2012), is strongly associated with retrenchment and sudden stops in capital flows.

The central bank information shock causes a clear increase in economic activity and decreases the VIX, risk aversion, and uncertainty, while the global financial cycle factor increases. Together, these responses characterize a "risk-on" episode in which investors' risk appetite increases. As the VIX is generally negatively correlated with speculative carry positions (see, e.g., Brunnermeier et al., 2008), the decrease in the VIX sets in motion a reallocation away from low-yielding funding currencies toward high-yielding investment currencies.

As a plausibility check, we also report the responses of the remaining baseline variables in these extended models in Figure D2. We report the median response and the credible sets of the baseline model, together with the median responses of each of the extended models as dashed lines. For both shocks, the responses are qualitatively and quantitatively similar. They do not strongly deviate from those of the baseline model. While the responses of the interest rates fluctuate more strongly (given the implied responses of the interest rate differential and the excess return), the responses of the Treasury basis and the spot rate are remarkably close to the baseline model.

Figure D1: Impulse responses of the extension variables.

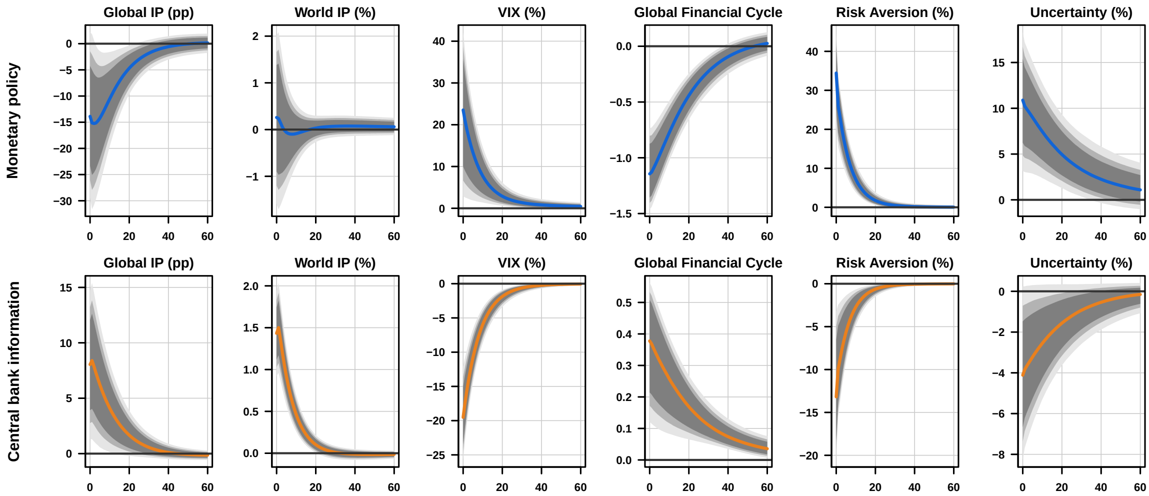

Notes: The figure shows the impulse responses to the U.S. monetary policy shock (upper panel, blue color) and to the central bank information shock (lower panel, orange color). Estimation is based on the group-mean estimator of the linear VAR model. Solid lines represent posterior median estimates and shaded areas indicate the 68%, 80%, and 90% credible sets. The horizontal axes measure time in months. The vertical axes measure deviations from the pre-shock level in percent (%) or percentage points (pp).

Figure D2: Impulse responses of baseline variables of extensions.

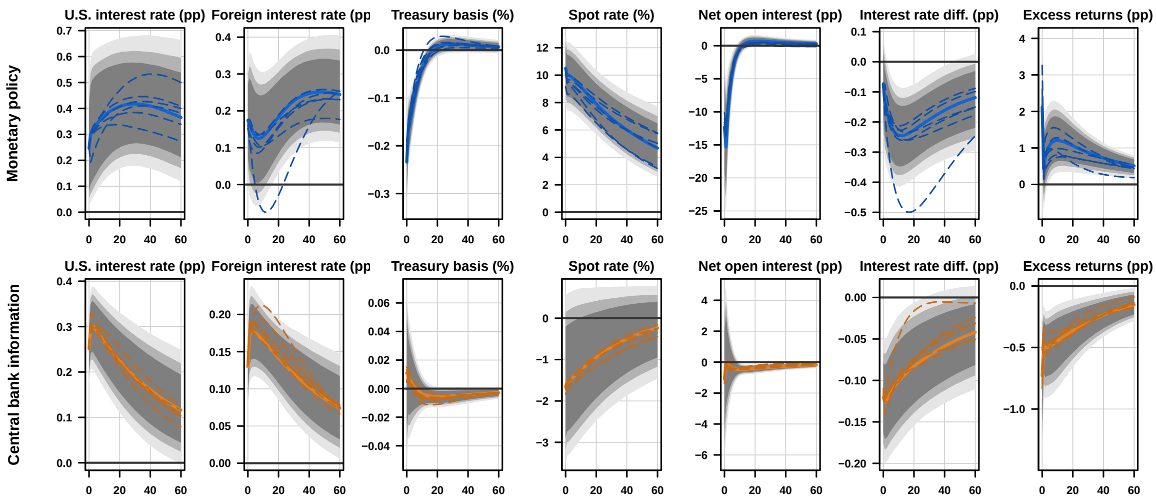

Notes: The figure shows the impulse responses to the U.S. monetary policy shock (upper panel, blue color) and to the central bank information shock (lower panel, orange color). Estimation is based on the group-mean estimator of the linear VAR model. Definitions of the constructed responses for the interest rate differential, $ird_t^m = i_t^{*,m} - i_t^{\$,m}$, and the currency excess returns, $rx_{t+m} = ird_t^m - \frac{12}{m}\mathbb{E}_t[\Delta s_{t+m}]$. Solid lines represent posterior median estimates of the baseline model and dashed lines represent the responses of the models extended with one variable. Shaded areas indicate the 68%, 80%, and 90% credible sets in the baseline model. The horizontal axes measure time in months. The vertical axes measure deviations from the pre-shock level in percent (%) or percentage points (pp).

Figure D3: Baseline responses with country-specific responses.

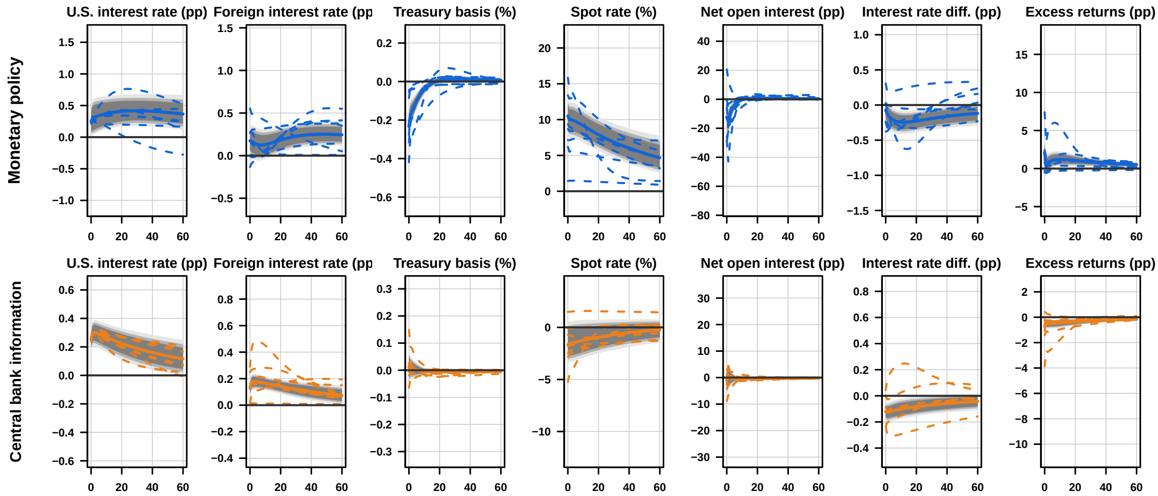

Notes: The figure shows the impulse responses to the U.S. monetary policy shock (upper panel, blue color) and to the central bank information shock (lower panel, orange color). Estimation is based on the group-mean estimator of the linear VAR model. Definitions of the constructed responses for the interest rate differential, $ird_t^m = i_t^{*,m} - i_t^{\$,m}$, and the currency excess returns, $rx_{t+m} = ird_t^m - \frac{12}{m}\mathbb{E}_t[\Delta s_{t+m}]$. Solid lines represent posterior median estimates of the baseline model, while the dashed lines represent the country-specific impulse response functions. The shaded areas indicate the 68%, 80%, and 90% credible sets of the baseline model. The horizontal axes measure time in months. The vertical axes measure deviations from the pre-shock level in percent (%) or percentage points (pp).

In Figure D3, we report the country-specific responses together with the equally weighted group-mean estimator. The figure reveals strong similarities for most responses across different currencies. The strongest differences arise in the response of the spot rate to the monetary policy shock, which also affects excess returns. Furthermore, foreign interest rates behave more heterogeneously in response to the central bank information shock, affecting the interest rate differential and subsequently the implied ex ante excess returns. Overall, we conclude that there are differences across currencies regarding their spot rate elasticities. Hence, we provide a more thorough discussion of the cross-sectional implications of the dynamic model in our discussion of Figure 4.

In order to examine the effects on the term structure of excess returns, we extend the baseline model in which we only use interest rates with a 3-month maturity. The extended model includes interest rates (U.S. and foreign) with 1-, 6-, and 12-month maturities. This yields the following vector of endogenous variables: $\boldsymbol{y}_t = (i_t^{\$,3m}, i_t^{*,3m}, x_t^{Treas}, s_t, noi_t, i_t^{\$,1m}, i_t^{*,1m}, i_t^{\$,6m}, i_t^{*,6m}, i_t^{\$,12m}, i_t^{*,12m})'$. Hence, the number of endogenous variables increases to $n_y = 11$. Furthermore, we provide two alternative specifications. In the first specification, we replace the 3-month U.S. and foreign interest rates with each alternative maturity one at a time to keep the number of endogenous variables at $n_y = 5$. Here, the vector of endogenous variables is as follows: $\boldsymbol{y}_t = (i_t^{\$,m}, i_t^{*,m}, x_t^{Treas}, s_t, noi_t)'$ where $m \in \{1, 3, 6, 12\}$. In the second alternative specification, we add either the 1-, 6-, or 12-month maturity to the 3-month rates, increasing the number of endogenous variables only to $n_y = 7$. Hence, the vector of endogenous variables reads as follows: $\boldsymbol{y}_t = (i_t^{\$,3m}, i_t^{*,3m}, x_t^{Treas}, s_t, noi_t, i_t^{\$,m}, i_t^{*,m})'$ where $m \in \{1, 6, 12\}$. To have the same shock scaling across all models, we use a 10% appreciation of the U.S. dollar for the monetary

Figure D4: Term structure effects using alternative models.

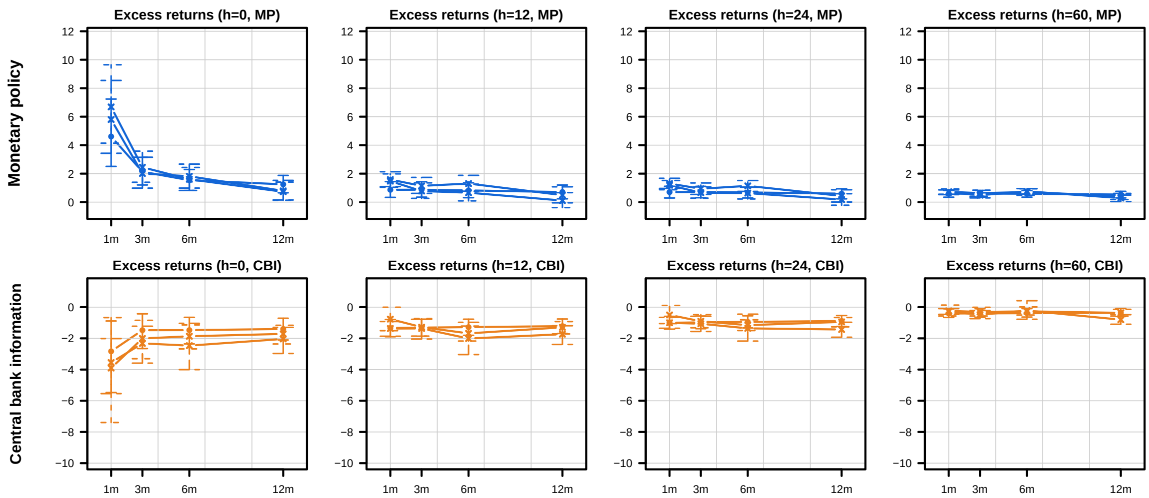

Notes: This figure shows the effects on the term structure for the U.S. monetary policy shock (upper panel, blue color) and for the central bank information shock (lower panel, orange color) using the baseline and alternative models. Estimation is based on the group-mean estimator of the linear VAR model. Definitions of the constructed responses for the currency excess returns, $rx_{t+m} = (i_t^{*,m} - i_t^{\$,m}) - \frac{12}{m}\mathbb{E}_t[\Delta s_{t+m}]$. Points represent posterior median estimates and the whiskers indicate 68% credible sets. Alternative models are indicated with dashed lines. The horizontal axes measure maturity in months. The vertical axes measure deviations from the pre-shock level in percentage points (pp).

policy shock and a 5% depreciation of the U.S. dollar for the central bank information shock as normalization.

In Figure D4, we report the outcomes across these three different specifications. The results are robust to these different specifications. We report the dynamic effects on the term structure at horizons $h \in \{0, 12, 24, 60\}$. We find that the term structure of ex ante excess returns is strongly downward sloping for both shocks. The strongest excess returns arise when using interest rates with a 1-month maturity, while the lowest occur for higher maturities. In terms of dynamics, the effects dissipate relatively quickly. Still, we observe across all three specifications positive (negative) excess returns for the monetary policy (central bank information) shock after one and two years for almost all maturities.

In Figure D5 and Figure D6, we report two robustness checks with alternative specifications. First, we use different weights for constructing the average coefficients $\overline{\boldsymbol{\theta}} = \sum_{i=1}^{N} w_i \boldsymbol{\theta}_i$, where we use equal weights $w_i = 1/N$ in the baseline. We use the following alternative weights: trade weights used by the BIS to construct narrow exchange rate indices, renormalized to reflect U.S. trade exposure. We also use two weighting schemes derived from the U.S. Commodity Futures Trading Commission (CFTC) data provided by Brunnermeier et al. (2008). Here, we construct two weighting schemes based on the net open interest and the number of speculative investors in the dataset.

The results are robust to using different weights, as shown in Figure D5. For the monetary policy shock, there are some smaller differences arising from the reaction of the foreign interest rate and the spot rate, which subsequently feed into the interest rate differential and excess returns. However, the responses are mostly within the credible sets of the baseline model, with some minor exceptions. The qualitative picture remains similar.

Figure D5: Robustness: different weighting schemes.

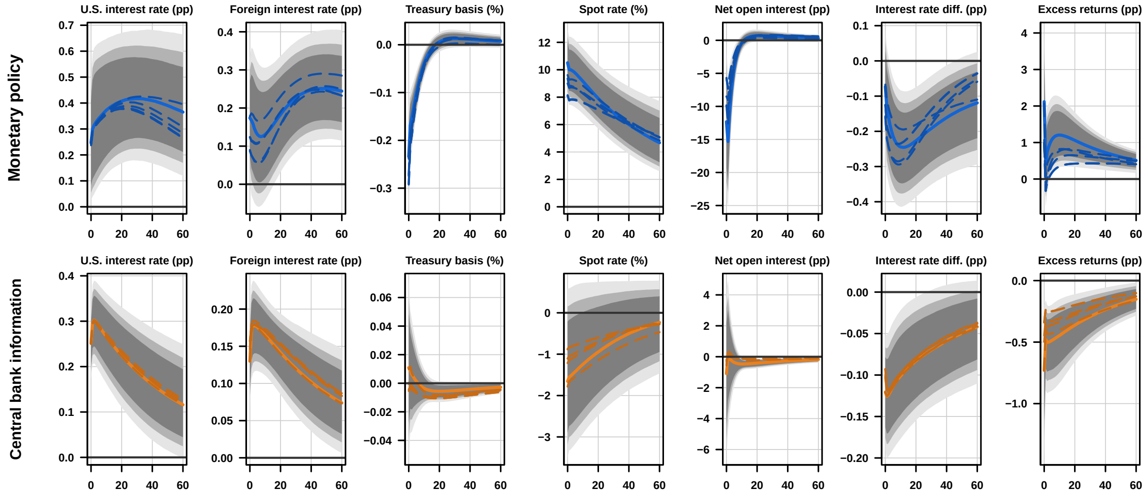

Notes: The figure shows the impulse responses to the U.S. monetary policy shock (upper panel, blue color) and to the central bank information shock (lower panel, orange color). Estimation is based on the group-mean estimator of the linear VAR model. Definitions of the constructed responses for the interest rate differential, $ird_t^m = i_t^{*,m} - i_t^{\$,m}$, and the currency excess returns, $rx_{t+m} = ird_t^m - \frac{12}{m}\mathbb{E}_t[\Delta s_{t+m}]$. Solid lines represent posterior median estimates of the baseline model and the dashed lines refer to alternative specifications with different weighting schemes. Shaded areas indicate the 68%, 80%, and 90% credible sets of the baseline model. The horizontal axes measure time in months. The vertical axes measure deviations from the pre-shock level in percent (%) or percentage points (pp).

Figure D6: Robustness: different numbers of lags and dummies for certain episodes.

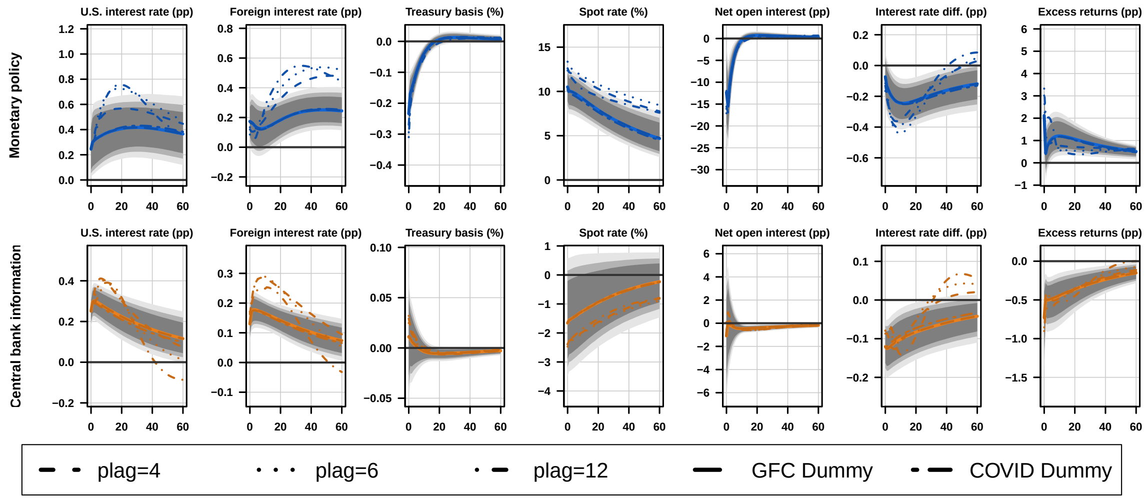

Notes: The figure shows the impulse responses to the U.S. monetary policy shock (upper panel, blue color) and to the central bank information shock (lower panel, orange color). Estimation is based on the group-mean estimator of the linear VAR model. Definitions of the constructed responses for the interest rate differential, $ird_t^m = i_t^{*,m} - i_t^{\$,m}$, and the currency excess returns, $rx_{t+m} = ird_t^m - \frac{12}{m}\mathbb{E}_t[\Delta s_{t+m}]$. Solid lines represent posterior median estimates of the baseline model and the dashed lines refer to alternative specifications with $p \in \{4, 6, 12\}$ lags and the inclusion of dummy variables for the GFC episode (2007M12-2009M6) and the COVID episode (2020M3-2020M5). Shaded areas indicate the 68%, 80%, and 90% credible sets of the baseline model. The horizontal axes measure time in months. The vertical axes measure deviations from the pre-shock level in percent (%) or percentage points (pp).

The second robustness check concerns specification choices in the VAR, where we assess robustness to the number of lags in the VAR and add dummies for certain historical episodes, specifically the Global Financial Crisis (GFC) and the COVID episode. We define the GFC episode as occurring from December 2007 to June 2009, aligning with the NBER recession dates. The COVID episode ranges from March 2020 to May 2020. We report the outcomes in Figure D6. Overall, the results are also robust to using a higher number of lags. Some notable changes arise, which we briefly discuss. The reaction of interest rates (both U.S. and foreign) shows a more hump-shaped response to both shocks. Hence, the interest rate differential also shows a stronger hump shape. Furthermore, both shocks elicit stronger spot rate reactions. However, the reaction of the excess returns is close to the baseline model. It seems that the stronger hump-shaped response of the interest rate differential offsets the slightly stronger spot rate reaction. When adding the dummy for the GFC or the COVID episode to the model, the estimates are very close to those of the original model.

In Figure D7, we compare the baseline linear VAR model to an alternative specification by replacing the spot rate variable. Instead of using the spot rate at the end of the month (eom), we use the average spot rate for each month. This attenuates the spot reaction to the monetary policy shock quite strongly, showing less than half of the effect size on impact. For the central bank information shock, the reaction is somewhat attenuated as well, but less striking. However, the uncertainty bands clearly narrow in both cases. Consequently, currency risk premia are lower for the monetary policy shock, but they are still positive and statistically significant. We observe one interesting finding: the impact effect is not the strongest effect in absolute value. This could point to delayed overshooting. However, we argue that this is due to the variable definition. When using average spot rates, it can happen that at the time of the FOMC announcement (often in the middle of the month), about half of the observations influencing the arithmetic mean have already occurred. Hence, we observe a more gradual response on impact. The responses of the remaining endogenous variables are remarkably close to the baseline responses.

Figure D7: Robustness: using the average spot rate.

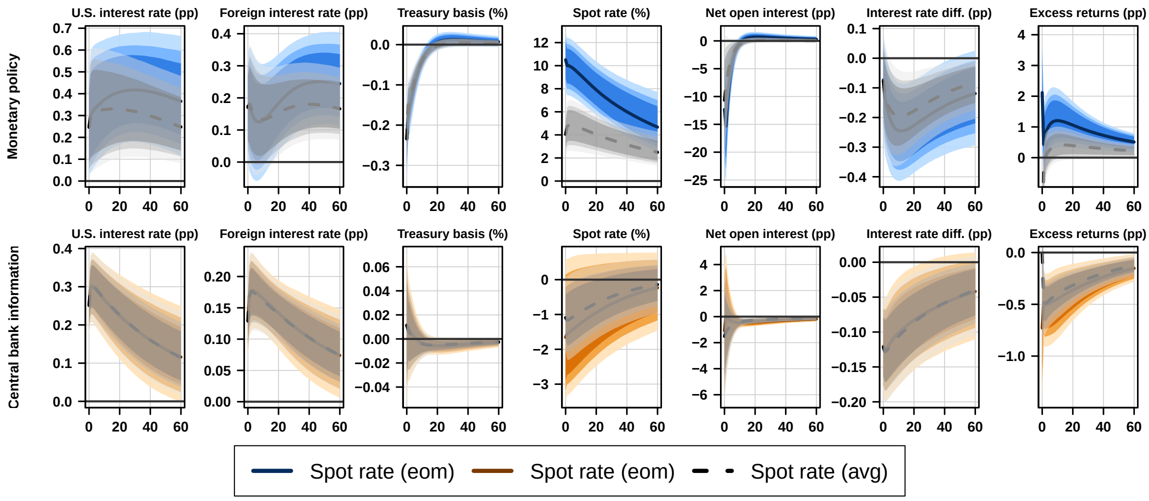

Notes: The figure shows the impulse responses to the U.S. monetary policy shock (upper panel, blue colors) and to the central bank information shock (lower panel, orange colors) in the baseline specification using end-of-month (eom) spot rates and in an alternative specification using average (avg) spot rates. Estimation is based on the group-mean estimator of the linear VAR model. Definitions of the constructed responses for the interest rate differential, $ird_t^m = i_t^{*,m} - i_t^{\$,m}$, and the currency excess returns, $rx_{t+m} = ird_t^m - \frac{12}{m}\mathbb{E}_t[\Delta s_{t+m}]$. Solid (dashed) lines represent posterior median estimates of the baseline (alternative) model. Shaded areas indicate the 68%, 80%, and 90% credible sets of the baseline model. The horizontal axes measure time in months. The vertical axes measure deviations from the pre-shock level in percent (%) or percentage points (pp).

D.2 Additional results of nonlinear VAR analysis

In Figures D8 and D9, we report the regime allocation for each currency, together with the spot rate and the carry trade intensity indicator, respectively. The estimates of the threshold parameters, γ_1 and γ_2, are reported in Table 5 in the main text and are shown as solid black lines in Figure D9, together with their credible sets (dashed lines). As already indicated in Table 5, the second regime is seldom visited—each model spends most of the sample in the first and third regimes. We classify the lower regime as the regime with a low value of the carry trade intensity indicator, and the third regime, or upper regime, as the regime with a high value of the carry trade intensity indicator. This regime classification implies that carry trade activity is elevated in the third regime, as we reverse the sign of the net open interest for currencies with average policy interest rate differentials that are negative. Those currencies, which have negative policy interest rate differentials on average, are mostly used as borrowing currencies, while the U.S. dollar constitutes the investment currency in this trade. This means going long in the U.S. dollar. For currencies with a positive average policy interest rate differential, investors favor short positions in the U.S. dollar, meaning that the U.S. dollar is the borrowing currency in this trade. To align these different trading positions, we reverse the sign in the carry trade intensity indicator.

In Figure D10, we report the relationship between the average policy interest rate differential and the regime-dependent effects on the spot rates, the interest rate differential, and currency excess returns. Across the three variables, we do not find strong differences in the cross-sectional slopes. In Figure D11, we report the term-structure results. We can only estimate the model specification in which we replace the 3-month U.S. and foreign interest rates one at a time to keep the number of endogenous variables at $n_y = 5$. The model using 6-month interest rates is not particularly stable in one of the regimes, but it nevertheless shows no strong differences across regimes. We conclude that no strong regime differences appear with respect to the term structure. As in the linear model, the term structure shows a downward-sloping profile, albeit with large statistical uncertainty.

Figure D8: Regime allocation: spot rates.

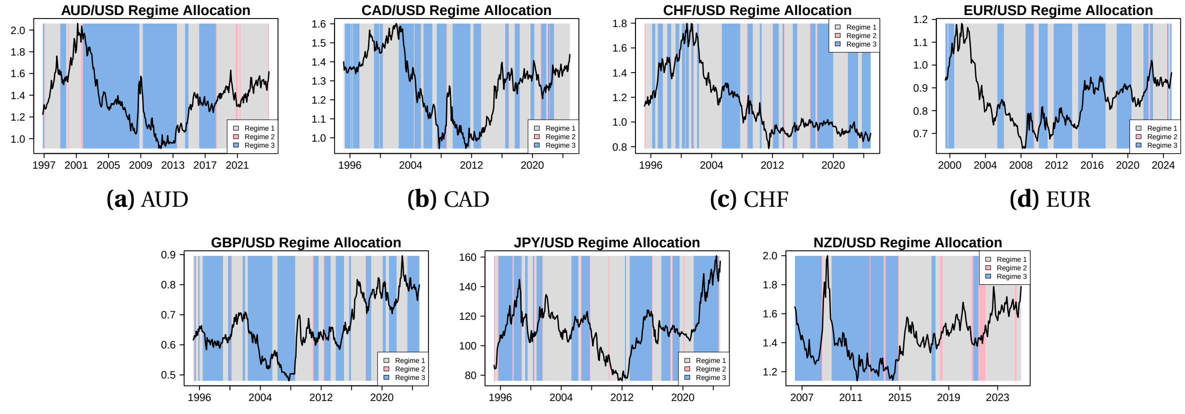

(a) AUD **(b)** CAD **(c)** CHF **(d)** EUR

(e) GBP **(f)** JPY **(g)** NZD

Notes: Each panel shows the spot rate, s_t, together with the regime allocation estimated from the threshold vector autoregressive model. The black solid line denotes the spot rate. The vertical axis denotes the spot rate in units of foreign currency per U.S. dollar. The horizontal axis denotes the sample period. Currencies: Australian dollar (AUD), Canadian dollar (CAD), Swiss franc (CHF), euro (EUR), British pound (GBP), Japanese yen (JPY), and New Zealand dollar (NZD). Colors indicate the regime allocation with the first regime denoted in gray, the second regime in light pink, and the third regime in blue, respectively.

Figure D9: Regime allocation: carry trade intensity indicator.

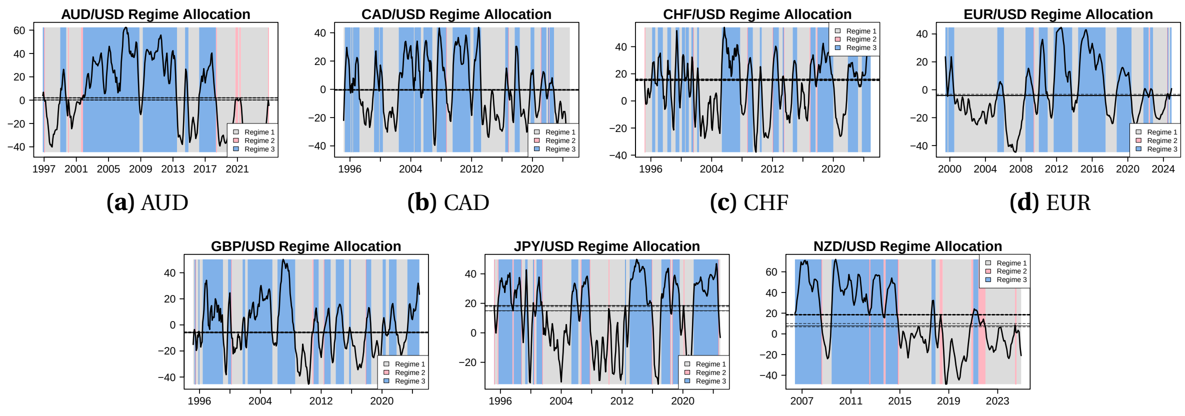

(a) AUD **(b)** CAD **(c)** CHF **(d)** EUR

(e) GBP **(f)** JPY **(g)** NZD

Notes: Each panel shows the carry trade intensity indicator, CTI_t, together with the regime allocation estimated from the threshold vector autoregressive model. The solid horizontal lines depict the thresholds together with their credible sets (dashed lines). The black solid line denotes the carry trade intensity indicator. The vertical axis denotes the size of the carry trade intensity. The horizontal axis denotes the sample period. Currencies: Australian dollar (AUD), Canadian dollar (CAD), Swiss franc (CHF), euro (EUR), British pound (GBP), Japanese yen (JPY), and New Zealand dollar (NZD). Colors indicate the regime allocation with the first regime denoted in gray, the second regime in light pink, and the third regime in blue, respectively.

Figure D10: Cross-sectional results in the nonlinear baseline model.

(a) Spot rates.

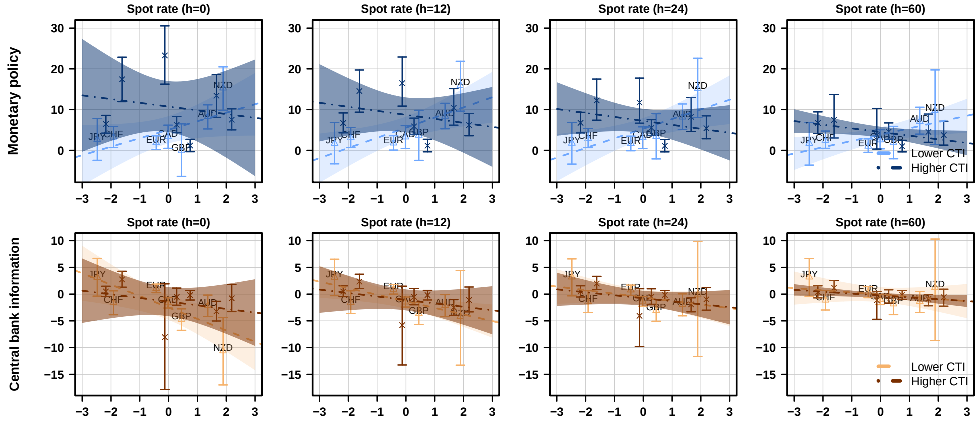

(b) Interest rate differentials.

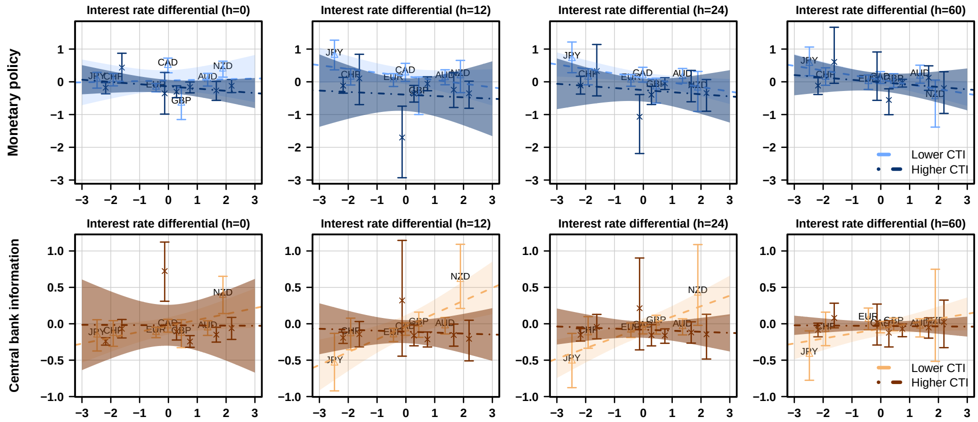

(c) Currency excess returns.

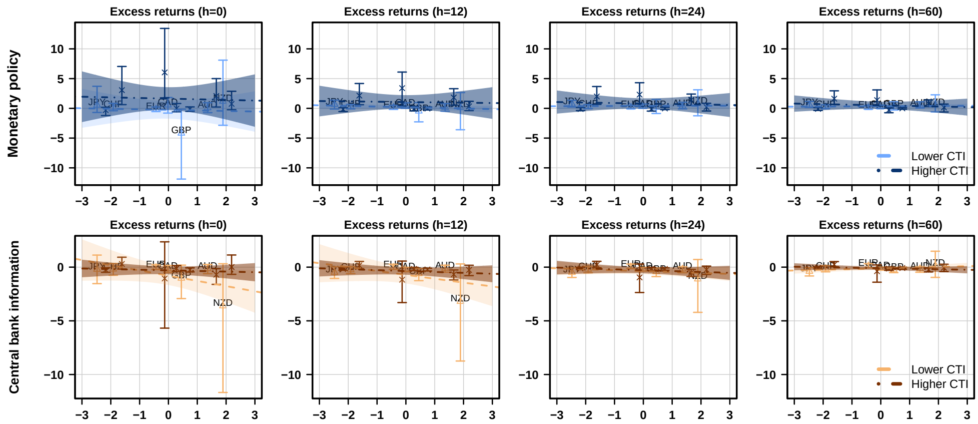

Notes: This figure shows the relationship between the average policy interest rate differential $\overline{pird} = \overline{i}_t^* - \overline{ir}^{\$}$ and the cross-sectional reaction of the spot rate (panel a), interest rate differentials (panel b), and currency excess returns (panel c) for selected horizons ($h \in \{0, 12, 24, 60\}$) to the monetary policy shock (upper panel, blue) and central bank information shock (lower panel, orange) for each currency and for the lower (brighter color) and higher (darker color) carry trade intensity regimes. Definitions of the constructed responses for the interest rate differential, $ird_t^m = i_t^{*,m} - i_t^{\$,m}$, and the currency excess returns, $rx_{t+m} = ird_t^m - \frac{12}{m}\mathbb{E}_t[\Delta s_{t+m}]$. The vertical bars denote 68% credible sets around the estimated reaction. The dashed line in each panel represents the fitted cross-sectional regression, and the shaded area its 90% confidence band.

Figure D11: Term structure effects in the nonlinear baseline model.

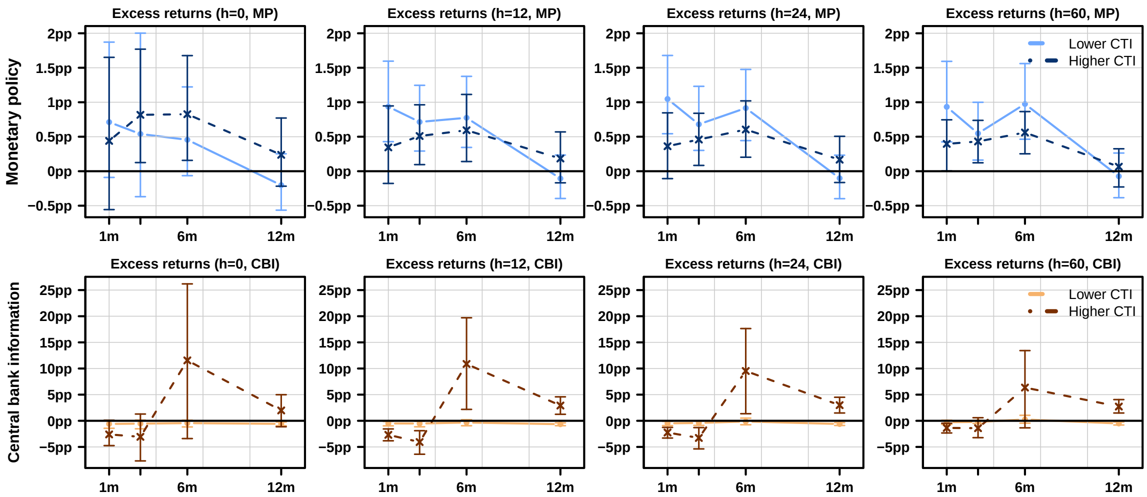

Notes: This figure shows the effects on the term structure for the U.S. monetary policy shock (upper panel, blue colors) and for the central bank information shock (lower panel, orange colors). Estimation is based on the group-mean estimator of the nonlinear threshold VAR model. Definitions of the constructed responses for the currency excess returns, $rx_{t+m} = (i_t^{*,m} - i_t^{\$,m}) - \frac{12}{m}\mathbb{E}_t[\Delta s_{t+m}]$. Points represent posterior median estimates and the whiskers indicate 68% and 80% credible sets. The horizontal axes measure maturity in months. The vertical axes measure deviations from the pre-shock level in percentage points (pp).